Master of Science Thesis

Improved Waterflooding Performance Using Model Predictive Control

Amin Rezapour

December 10, 2009

Delft Center for Systems and Control

Delft University of Technology

Improved Waterflooding Performance Using Model Predictive Control

MASTER OF SCIENCE THESIS

For obtaining the degree of Master of Science in Systems & Control at Delft University of Technology

Amin Rezapour

December 10, 2009

Faculty of Mechanical, Maritime and Materials Engineering · Delft University of Technology

TUDelft

Delft University of Technology

Delft University Of Technology
Delft Center for Systems and Control

The undersigned hereby certify that they have read and recommend to the Faculty of Mechanical, Maritime and Materials Engineering for acceptance a thesis entitled **"Improved Waterflooding Performance Using Model Predictive Control"** by **Amin Rezapour** in partial fulfillment of the requirements for the degree of **Master of Science**.

Dated: December 10, 2009

Supervisor:

____
prof.dr.ir. P.M.J. Van den Hof

Readers:

____
prof.dr.ir. J.D. Jansen

____
ir. G.M. van Essen

To My Parents

Abstract

Hydrocarbon resources around the world are limited, and to satisfy future energy demands more efficient recovery solutions are needed. In oil production, a common method to bring the oil to the surface is to flood a reservoir by injecting water. After properly locating the injection and production wells, injection continues as long as it is profitable, and the wells are shut in afterwards (refer to as reactive control). In order to increase the recovery factor, this task has been cast into an integrated and more structured approach called Closed Loop Reservoir Management (CloReM). In this methodology, optimal production settings are determined based on reservoir models in a feedback loop. These models are highly non-linear and have large number of parameters and states, which are usually expressed with a great deal of uncertainties. Therefore the performance of CloReM is highly dependant on quality of the models, that are not updated quite often.

To circumvent the unwanted effects of uncertainties and disturbances, a reference tracking framework using Model Predictive Control (MPC) is investigated, in order to provide more rapid corrective responses. This framework acts like a secondary loop (in addition to the original feedback loop) that has a supervisory task, and reoptimizes the settings based on low order linear models. Validity (i.e. the prediction horizon) of such models is relatively short, but they can get updated rapidly in several working points. In this assignment we have studied the possibility of using system identification methods using Prediction Error Identification (PEI) and Subspace Identification (SubID) to derive Linear Time Invariant (LTI) reservoir models to be implemented later in MPC. Furthermore, the benefits of the proposed loop are examined in an open loop life-cycle optimization of the reservoir, i.e. with fixed optimal references during the whole production life. The MPC has been implemented on a 5-spot homogeneous, and a 3D multi layered heterogeneous reservoirs. It has been shown that manipulating the injection rates and Bottom Hole Pressure (BHP) according to an MPC controller, can increase the profit up to 6.3% in heterogeneous reservoir and up to 18% in the homogeneous case, in compare to the conventional control scheme.

Acknowledgements

I am sincerely thankful to my supervisor, Ir. Gijs Van Essen, for all of his support, encouragement and guidance throughout this whole time. From the initial to the final level of this project he enabled me to develop an understanding of the subject. I would also like to thank Prof. P.M.J. Van den Hof for his undeniable role, because this project would never shaped without his support and supervision. It was also an honor for me to had a chance to take two related courses with Prof. J.D. Jansen, who helped me have better understanding of the problem.

Lastly, I offer my regards and blessings to all of those who supported me in any respect during the completion of my project.

Delft, University of Technology — Amin Rezapour
December 10, 2009

Table of Contents

Abstract **i**

Acknowledgements **v**

1 Introduction **1**

Hydrocarbon Origin 1
Energy Demand 1
Production of Oil 2
Future of Oil 3
1-1 Exploration and Production of Oil and Gas 3
Reservoir Management 4
1-2 Problem Setting 5
1-3 Closed Loop Reservoir Management 6
Background 6
1-3-1 Life Cycle Production Optimization 6
1-3-2 Updating Models and State Estimation 7
1-3-3 Research Gap 7
1-4 Project Goal 8
1-5 Report Outline 8

2 Methodology **9**

2-1 Introduction 9
2-2 Reference Tracking Using Model Predictive Control 10
2-3 Linear Models of Reservoirs 11
2-4 Two Level Control of Waterflooding 13
2-4-1 Open-Loop Dynamic Optimization 15
2-4-2 Estimating the States and Receding Horizon of MPC 16
2-4-3 Importance of y_{ref} 16
2-5 Using Reservoir Simulator (MoReS) 17

3 Data Driven Linear Model of Oil Reservoir 19
3-1 Introduction . . . 19
3-2 Reservoir Models and Properties . . . 19
Sources of Nonlinearity and Uncertainties . . . 20
3-2-1 Low Order Linear Models . . . 21
3-2-2 Inputs, Outputs and States of Downscaled Models . . . 21
3-3 System Identification . . . 22
System Identification Procedure . . . 23
3-3-1 Experiment Design and Data Preprocessing . . . 23
Preparatory Experiments . . . 24
Sampling Time and Aliasing . . . 25
Persistency of Excitation . . . 25
Data Preprocessing . . . 26
3-3-2 Model Set Selection . . . 26
Prediction Error Identification . . . 26
Subspace Identification . . . 28
3-4 Chapter Conclusion . . . 28

4 Model Predictive Control 31
4-1 Introduction . . . 31
4-2 The Model . . . 32
4-3 Optimal Control . . . 32
4-4 Receding Horizon Principle . . . 33

5 Reservoir Modeling with System Identification 35
5-1 Introduction . . . 35
5-2 2D Homogenous Reservoir . . . 36
5-2-1 Step Response Analysis . . . 37
5-2-2 Input Design . . . 38
5-2-3 Model Identification . . . 39
5-2-4 Discussion of Results . . . 42
5-3 2D Heterogeneous Reservoir . . . 44
5-3-1 Step Response Analysis . . . 44
5-3-2 Model Identification . . . 44
5-4 3D Heterogeneous Reservoir . . . 48
5-4-1 Step Response Analysis . . . 48
5-4-2 Model Identification . . . 48
5-5 Reservoir with 6 Wells . . . 51
5-5-1 Step Response Analysis . . . 51
5-5-2 Model Identification . . . 51
5-6 VanEssen Reservoir Model . . . 56
5-6-1 Introduction . . . 56
5-6-2 Model Dynamics . . . 56
5-6-3 Model Identification . . . 57
5-7 Chapter Conclusion . . . 58

6 Waterflooding Using Model Predictive Control 63

6-1 Introduction . . . 63
6-2 2D Homogeneous Reservoir . . . 63
6-2-1 Model Identification . . . 65
Input Signal Design . . . 66
Data Pre-Processing . . . 67
Model Quality . . . 69
6-2-2 Model Predictive Control . . . 69
Formulation . . . 70
Primary Results . . . 71
Results After Water Break-Through . . . 73
6-3 Heterogeneous Reservoir, VanEssen Model . . . 82
6-3-1 Early Production Stage . . . 86
6-3-2 Mid Production Stage . . . 86
6-3-3 Final Production Stage . . . 87
6-3-4 Life Cycle MPC Controlled VanEssen Model . . . 89
6-4 Chapter Conclusion . . . 90

7 Conclusions and Recommendations 93

7-1 Review of Results . . . 94
Reservoir Modeling with System Identification . . . 94
Waterflooding Using Model Predictive Control . . . 95
7-2 Recommendations for Future Work . . . 96
Input Design . . . 96
Model Structure . . . 96
Inputs and Outputs . . . 96
Validating Models . . . 97
Moving Horizon MPC . . . 97
Adding Measurement Noise and Disturbances . . . 97
Integrating with CloReM . . . 97

Bibliography 99

A Discrete Time Signals and Systems 103

A-1 Discrete Time Signals . . . 103
A-2 Discrete Time SISO Systems . . . 104
A-3 Discrete Time MIMO Systems . . . 105
A-4 Linear Process with Disturbances . . . 106

B Prediction Error Identification Methods **107**
B-1 Least Squares Methods 107
B-1-1 Finite Impulse Response 107
B-1-2 ARX Models 108
B-2 Extension of Least Squares Methods 108
B-2-1 Output Error Methods 109
B-2-2 Prediction Error Methods 109
B-2-3 (1)ARMAX 109
B-2-4 (2)Box-Jenkins 110
B-2-5 Output Error vs. Prediction Error 111

C Subspace Identification **113**
C-1 Subspace Identification for Deterministic Systems 113
C-2 RQ Factorization to Improve Numerical Efficiency 115
C-3 Subspace Identification with Process and Measurement Noise 116
C-4 Estimating the Kalman Gain K_T 119

D Relative Permeability Effects on Multiphase Flow **121**

Acronyms **125**

Chapter 1

Introduction

Hydrocarbon Origin

Origin of oil and gas is mainly the decomposed body of the prehistoric animals and plants. These organic substances were deposited on top of each other, mixed with sands and rocks, and formed several layers, usually on the sea beds. Under the pressure of the top layers and sea water from above, and influence of earth heat from below, currently known ”petroleum” has been created over millions of years. Oil is often located next to the shores or places that used to be seas or oceans, since it was a perfect place where every requirements of forming oil were present. Simply because it is lighter than water, oil migrated towards the surface of the earth. During the migration, reservoirs have been formed when oil encountered a rock layer that was impossible to penetrate. Figure 1-1 shows a simple example of a reservoir, that oil has been trapped between an aquifer and a non-permeable rock. A common depth at which a reservoir can be found is between a hundred meters to a few kilometers. It must be noted that reservoir is not like a pond, and oil is in fact inside the rock pores (like a sponge full of water).

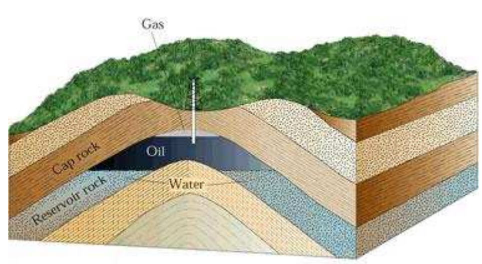

Figure 1-1: Example of an Oil Reservoir, from Lite Oil Investment Co..

Energy Demand

BP Statistical Review of World Energy in June 2009 [BP, 2009], shows that about 80% to 90% of the whole energy consumed worldwide is provided by the combustion of the fossil fuels; charcoal, oil and gas. As it is shown in Figure 1-2, the demand for energy is predicted to be rising in the coming years, and oil and gas take the major portion of the energy supply.

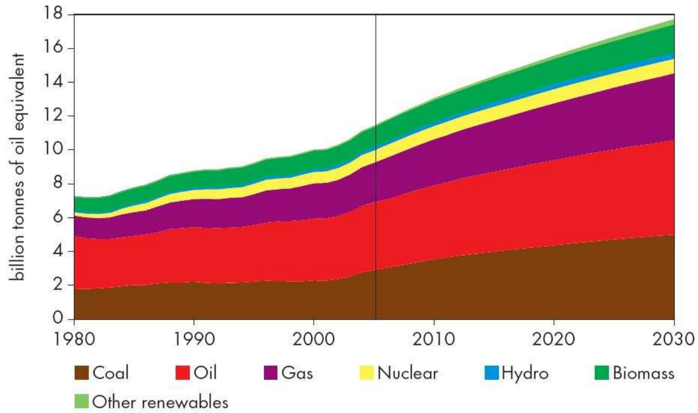

Figure 1-2: World Primary Energy Demand in Reference Scenario, after [IEA-WEO, 2008].

Production of Oil

Unfortunately hydrocarbon resources are limited. It means that, in one hand the current production rates of oil and gas cannot satisfy future global energy demands, and on the other hand the discovered reserves are depleting, and hope of discovering new reservoirs are getting dimmer. Global aggregate rate of petroleum production has been growing exponentially in past years, until it peaks to its highest point. Afterwards, the production rate will decline and ultimately we will reach a point with no oil at all, as depicted in Figure 1-3. Considering the fact that this figure may not take into account all the factors, it can be seen that we are currently in the peak period and heading towards producing less and less.

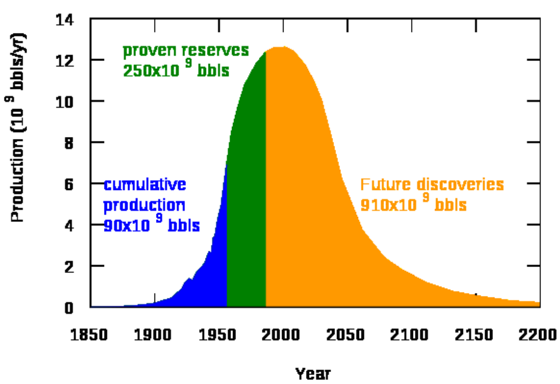

Figure 1-3: A Bell-Shaped Production Curve, as Originally Suggested by [Hubbert, 1956] in 1956.

Some experts believe that, the high dependence of most modern industrial transport, agricultural, and industrial systems on the relative low cost and high availability of oil, will cause even more rapid post-peak production decline. Therefore the oil price will increase severely that may have negative implications for the global economy [1]. This concern can be conceived clearly nowadays, with economical crisis followed by an expensive oil period in $2008-2009$. After more than 150 years of production, it is believed that all the easy oil and gas has been pretty much found, and from now on it takes harder work to *find* and *produce* oil, from more challenging environments [2].

Future of Oil

It is not exactly possible to predict the date when we are running out of oil. The initial estimates of newly discovered oil fields are usually too low and as years pass, successive estimates of the ultimate recovery tend to increase. On the other hand new oil reservoirs are still being discovered, although they are mostly of unconventional oil types. It is said that in 40 years, the world will face an oil crisis, a threat that was anticipated 40 years ago. It is obvious that oil is getting more scarce and more expensive, and in the future companies need to employ new technology in order to recover oil more efficiently.

1-1 Exploration and Production of Oil and Gas

The hydrocarbon recovery process can be divided into two major phases called *Exploration & Production*. Based on geological tests and surveys on certain areas, a map of subsurface rock layers is constructed. Appraisal wells are drilled and rock samples are extracted and studied, to increase the reliability of this map. An example of a 3D map is presented in Figure 1-4. If the results of the first stage seem promising, it leads to field development and then oil production begins. More efficient production demands better understanding of rock properties that leads to more informed *well placement* and *reserves estimation*. To this end, future production is planned by a team of experienced inter-disciplinary experts in large visualization rooms. During the production phase, new tests are conducted and field data are logged, and geologist, geophysicist and engineers who are able to interpret and integrate the data, are continuously busy with improving the models and production plannings.

The production lifecycle of a reservoir is in the order of decades. There are basically three stages in the whole period; a primary stage in which the reservoir has a naturally high pressure that provides enough driving force to bring only 10% of the oil to the surface. The secondary stage consists of injecting fluids into the porous medium from one side (injection side) to push the oil towards the other side (production side), or in other words inundate the whole reservoir. Depending on the configuration, number of the injecting wells, flooding strategy and reservoir type, around $15-40\%$ of the oil can be recovered. The final stage consists of number of techniques that alter the original properties of oil, e.g. using chemicals, injecting CO_2 or steam. It is quite obvious that easily reachable portion of the oil in complex geological structure is surprisingly very low, and as more oil is recovered the production becomes harder. This is due both to the uncertainty in assessing hydraulic continuity between wells, and the trapped oil in some unswept layers or areas of the field. This portion could be largely enhanced if clearer knowledge of oil bearing geological layers were achieved. Such

[1] The quotation was extracted from Wikipedia, on page "Peak Oil", which originally stated by Kenneth S. Deffeyes and Matthew Simmons

[2] William J. Cummings, Exxon-Mobil company spokesman, December 2005

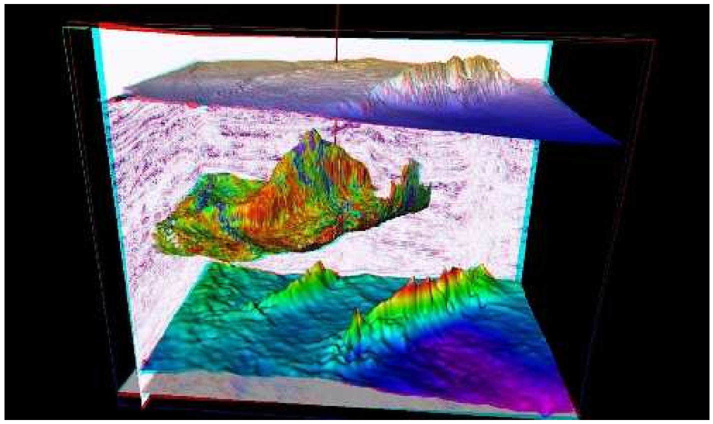

Figure 1-4: 3D Map of a Reservoir from Seismic Tests.

knowledge can help to propose some modifications in injection schemes to design profile control operations [Renard et al., 1998].

Reservoir Management

Reservoir management is a term that refers to an iterative task of reservoir surveillance and field (re)development, in order to increase reservoir profitability. Technically it requires mathematical modeling, field data assimilation and expert knowledge. In real life however, reservoir management is still being done by production engineers in a manual ad hoc fashion on the basis of long and short term plans.

The basic challenges that they face, are limitations of current infrastructures, oil price, available capital for expenditures, physical properties of subsurface and surface systems, and confidence in reservoir models upon which the decisions must be made [Saputelli et al., 2003].

In past decades, new technologies have brought more possibilities;

- New software packages for simulating fluid flow.
- 3D and 4D seismic tests.
- Horizontal and multilateral wells.
- Inflow Control Valves (ICV) to have servo control over the rates.
- Vast use of sensors and measurement devices all over the oil field.
- New recovery techniques.

Many oil companies have started to equip the newly developed fields with all these devices and techniques (so called smart wells or smart oil fields). Despite all the possibilities and improvements achieved by new technologies, production operations that are solely based on these techniques may cause more complexity and less reliability. Unexpected costs during the process, early water breakthrough and production rates lower than expected, are only some of the few challenges rooted in lack of knowledge about the dynamics of oil bearing layers of rock.

On the other hand, an optimal decision making process must take into account several factors. These factors are not necessarily in the same level of hierarchy, which makes it hard to integrate all of them into a single objective function. Resource scheduling, facility design, well locations and trajectories(for horizontal wells), production parameter settings and recovery factor, to name a few. Therefore, devising new techniques must be well integrated with expert knowledge, in a feedback loop, and with the advantage of enormous field data, available models can be updated more often.

For that reason, it is not surprising that hydrocarbon recovery has found a common ground with systems and control recently, in search for better parameter estimation and optimized solutions. Therefore, still there is more room to improve if these methods are better realized and more efficiently integrated with expertise.

1-2 Problem Setting

As the thesis title implies, we are only focusing on the secondary production phase, i.e. to improve the waterflooding performance. In this stage, the reservoir does not have enough pressure and looks like a big balloon that has lost its pressure and yet some air is trapped inside. Therefore, a number of wells to inject water are drilled in certain areas of the reservoir. Injection continues until it generates enough pressure to force the oil to start moving again. Everything goes on just like before, until the time that injected water reaches the producer wells. This means that water has found a channel towards the producers, and inevitably oil and water are produced together. Therefore, oil must be separated in large separators that are constructed next to the wells, and the recovered water can be used for injection again. The injection and separation processes, of course cost money and thus the waterflooding continues, until the costs can be compensated by selling the produced oil.

Such a control scheme is called reactive control, which does not seem efficient enough (only about 35% of oil is recovered). Imagine that a perfect model of reality was available (i.e. a perfect reservoir map with exact rock properties of each point, and a perfect mathematical model that can describe all fluid dynamics phenomena around everywhere in the field). Then it would be possible to perfectly analyze the waterflooding by simulating the effects of various decisions, and find a solution that can maximize the recovery factor. This type of control that considers the process dynamics for better performance is referred to as model based control that is more efficient than reactive control.

Unfortunately, the perfect process models never exist in reality, and implementing any optimal solution based on approximate models, will not guarantee the highest profit because;

- Geological realization of reservoirs that are meant to characterize rock properties are not fully reliable, and they are far from being certain.
- Mathematical models that are used in order to describe fluid flow in reservoir, in wells and in other equipments are obtained with simplifying assumptions that increase chances of undermodeling.

- Disturbances available in models and measurements cannot be well quantified and represented.

1-3 Closed Loop Reservoir Management

Background

An advanced method of controlling a reservoir is proposed by [Jansen et al., 2008] that is called Closed-loop Reservoir Management (CloReM), and is depicted in Figure 1-5. The loop is in fact a model based optimizing algorithm to maximize the reservoir profitability. Usually more than one realization of the reservoir is employed as the "system models", in order to reduce the undesired effects of model uncertainties. These models are primarily constructed from well logs, well tests and seismic test and are updated during the production life of the field. Two blocks of "data assimilation" and "optimization" seem to carry out most of the job, and are described in more details in the following sub-sections. The main advantage of this method is that, it systematizes the reservoir management by getting the most out of data, provided by "sensors" all over the field. Unlike the conventional method, CloReM provides optimized control schemes in a closed loop based on updated models.

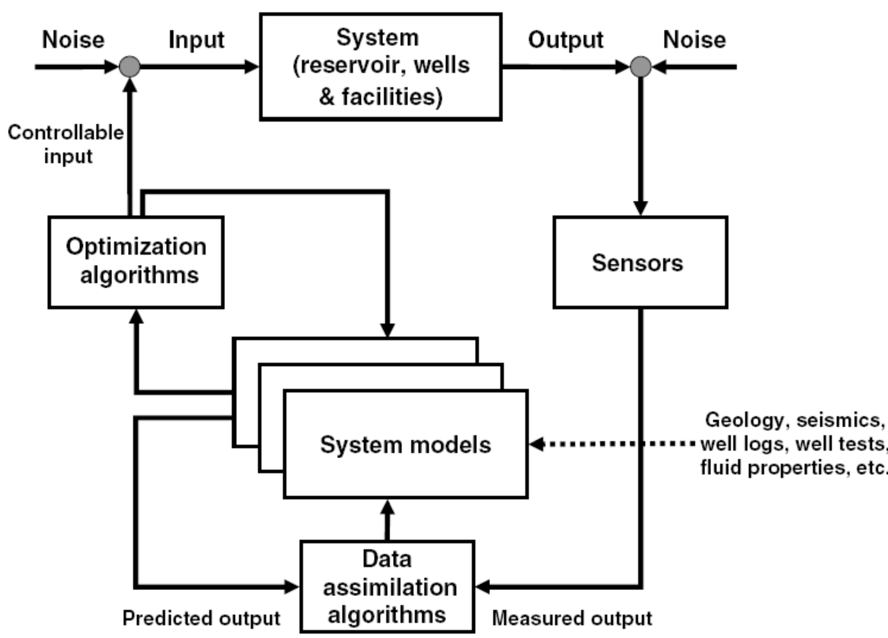

Figure 1-5: CloReM Block Diagram [Jansen et al., 2008].

1-3-1 Life Cycle Production Optimization

Knowing the system boundaries and equipments, a performance measure in form of an economical cost function can be defined to maximize the reachable profit (more detailed information about the cost function can be found in Section 2-4). Injection rates, production rates and well operations, are the inputs that must be optimized. For example, for an oil field with certain configuration of injector and producer wells, it must be analyzed how much water and for how long should be injected in order to sweep more oil. In the meantime, for the sake of higher oil production, it could happen that for some reasons, a production well needs to be shut down while it is still producing oil. This is obviously an odd decision which cannot be verified at all, and considering model discrepancies, we can see that optimal solutions are somewhat questionable. Moreover, translating the future effect of a decision into an economical measures is not always possible. For instance addition of a new well may cost something between $1 - 100 Million\$$, and due to the volatile oil price it may not be possible to fully analyze the beneficial aspects of drilling one or few wells in the mid-life of an oil field.

Optimization is based on the future behavior of the reservoir, predicted by the models. Since the models are of large scales, and simulating each effect requires very long time, an adjoint model is used in order to reduce the computational burden. In the meantime, large scale multivariable optimization problem solving is required, because of the large number of inputs and outputs. It can be seen that although exploiting new technologies gives more freedom and potential increase of oil recovery factor, basically they bring more expenses and complexity to the system boundaries. Life cycle optimization of reservoir is beyond the scope of this assignment, and for more details the reader is referred to [Zandvliet, 2008] and [Jansen and Currie, 2008].

1-3-2 Updating Models and State Estimation

It has previously been mentioned that the role of the models is to predict (or simulate) reservoir behavior in the future. The models and system boundaries of the wells and facilities can generally be defined reasonably accurate, but they are much more uncertain for the reservoirs. Consequently, the parameters of the subsurface models contain many uncertainties, and usually multiple subsurface models are used to simulate the fluid flows for different geological realizations [Jansen et al., 2008]. These models and parameters are primarily determined based on seismic and core samples. Every once in a few years, parameters are updated by geologists and experts. To this end all models' properties are adjusted in such a way that they match field data and well logs that are collected in the past (History Matching).

During the period that models are not updated, system outputs and states are estimated in CloReM using systems and control methods. In every loop, the measured system output is assimilated with the predicted output from the models to determine the values of system states. For state estimation of nonlinear systems, there exist several methods that are mostly a version of Kalman filtering. In CloReM, Ensemble Kalman Filter (EnKF) has been successfully used with history matching. In this method an ensemble of prior estimates of reservoir models is incorporated to compute the the error covariance of estimated states [Jansen et al., 2008].

1-3-3 Research Gap

The above presented CloReM is well studied on different models with promising results. Many authors have shown that, using EnKF to estimate and predict the future states and parameters of the system, in combination with adjoint based optimization, can improve the loop efficiency [Zandvliet, 2008]. In fact CloReM is able to satisfy two needs; 1) Reducing the existing uncertainties (and their effects on the results). 2) Rejecting the disturbances (and their effects on the results).

However, a complete loop is not run continuously in practice for one reason because it is very time consuming. History matching and model updating is also carried out very rarely, roughly speaking every 5 years during the time that the field is under *re-development*, which gives enough time. Negative effects of low frequency loop execution are,

1. Slow (or delayed) response to undesired effects of uncertainties.
2. Slow (or delayed) disturbance rejection.

More clearly, this means that sometimes due to the differences between the model and the reality, production does not proceed as expected. This possible drift may have some negative effects on the overall profit that cannot be fixable anymore. Hopefully, these effects can be avoided if we can provide appropriate control action in time. Furthermore, the large reservoir models contain quite a few number of simplifying assumptions that can possibly affect the quality of the short-term predictions. In other words, undermodeling effects influence CloReM short-term performance quality, and loop efficiency is confined due to its large time scale.

1-4 Project Goal

Apparently there are a lot of undiscovered areas to reach to the ultimate point of maximized hydrocarbon recovery. This thesis however, is about devising an idea that can be later on integrated into CloReM. In fact the performance of the CloReM can be improved by addressing undermodeling effects, more frequent response to uncertainty effects, and faster disturbance rejection. In this project, firstly we are going to investigate the data based modeling methods, that can provide better short term predictions. Secondly, a proper control scheme must be studied, in order to reject the undesired effects of uncertainties and disturbances. Therefore, the main research objective is;

Investigating the application of System Identification methods, to provide linear low order reservoir models, and using Model Predictive Control technique to improve optimal reference tracking of CloReM.

1-5 Report Outline

In the following chapter the proposed methodology is presented. Chapter 3 deals with low order linear modeling of reservoir. A brief introduction to Model Predictive Control is provided in Chapter 4. To investigate the applications of system identification in a reservoir, 5 different tentative reservoir models are studied in Chapter 5, and the whole idea of implementing MPC into waterflooding is treated in Chapter 6. Finally we included some remarks and suggestions for future works in Chapter 7.

Chapter 2

Methodology

There are specific factors that influence directly the profitability of a reservoir. These factors are generally connected to a number of decisions and control techniques that must be taken into account before and during the production life of the reservoir. In this chapter, a two level control strategy of reference generating and trajectory tracking using MPC is introduced. Then the idea is more elaborated by introducing a faster secondary loop to CloReM in order to improve its performance. This chapter will be concluded with a few discussions about the issues concerning fast model updating and use of reservoir simulators.

2-1 Introduction

It was discussed in the previous chapter that low frequency of executing a complete loop, causes a few negative effects on the performance of CloReM. Model discrepancies and existing disturbances bring about unwanted matters which sometimes are not fixable if we have to wait for the next loop run. Although decreasing the time scale of CloReM would improve the ”response time”, unfortunately loop frequency is limited due to the high computational burden of model updating and re-optimization procedure. Reservoir models are of large scales with complex structures, which require experienced people and huge computers to get updated. On the other hand, as long as model structures are kept almost constant, they are not able to deal with undermodeling issues. Moreover, re-optimization is also cumbersome and is dependant on simulations that indeed take a long time.

Alternatively, the system can be forced to track specific trajectories that are assuming to be the aftermath of the true optimal production settings. Thanks to the available measuring devices for monitoring the reservoir, any deviation from optimal trajectories can be indicated immediately. Therefore, a proper corrective control action may be applied to keep the system on the references. Just because this control action can have short time scale, it is expected to attenuate the effects of model uncertainties, disturbances and undermodeling more effectively. However, keeping the reservoir on a certain optimal track does not necessarily lead to the highest recovered oil percentage, unless the track represents *The Optimal* output, which is not easy to get verified, but at least it increases the reliability of the proposed optimal solution. Additionally, because of the model discrepancies, tracking a certain reference might be completely impossible in the case that the output lies on an infeasible region. It must be noted that sometimes these differences between models and reality result in better performance in comparison with the optimal output.

In this work we investigate the reference tracking alternative while the following assumptions are adopted (the validity of the assumptions will be discussed later in more details, in Chapter 5 and 6);

1. Uncertainties, undermodeling and disturbances have negative effects on CloReM performance in terms of achievable profit.

2. Input constraints are relaxed to enable reference tracking.

2-2 Reference Tracking Using Model Predictive Control

Choosing a control method in practice depends on the underlying system characteristics and the control purpose. PID and PID based controllers are the most popular control methods in every branch of industry. A well tuned PID is able to meet most of the required specifications, without having a perfect model of the system. For Multi-Input Multi-Output (MIMO) processes however, implementing and tuning PID is difficult, if not impossible. Furthermore, for a reservoir as a system with the dynamics that are changing continuously in a nonlinear behavior, applying PID control demands frequent re-tuning.

Alternatively, in process industry a control scheme that is well suited with the process characteristics is employed. Model Predictive Control (MPC) is a model based control method that can be implemented easily for MIMO systems. Popularity of MPC also rooted in its ability to handle any signal or state constraints in the system very easily. Since the control action is optimized based on the process model, it can take into account all the short term and long term phenomena in the process. Meanwhile, dependency of MPC to a model could also be its major disadvantage; because firstly there should be a modeling or a system identification step beforehand, and secondly the control quality is then highly dependent on model quality. While only linear models can be implemented in MPC, it must be noted that some processes have large nonlinear effects that cannot be captured by linear approximations. Nonlinear MPC, or NMPC is a variant of model predictive control that is characterized by the use of nonlinear system models for prediction. While optimization problem is convex in linear MPC, in NMPC it is not convex anymore and requires numerical solutions, which poses challenges like stability and computational issues. Principals of MPC will be described in more details in Chapter 4, and for further readings regarded NMPC refer to [Allgower et al., 2000] and for NMPC application to reservoir management refer to [Meum et al., 2008].

Regarding the discussion above, we propose a secondary loop to CloReM as shown in Figure 2-1. This loop is in fact a supervisory control loop that provides corrective control actions, based on the updated model. Using linear models in an MPC framework can potentially decrease the time scale of the loop. The idea of integrating a supervisory loop into CloReM will be explained in more details in Section 2-4.

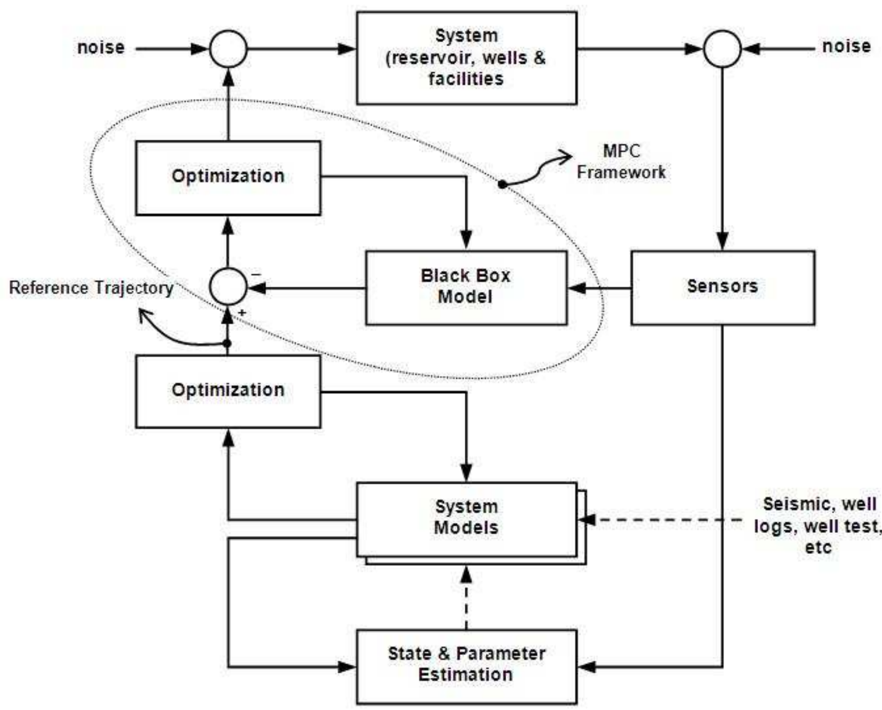

Figure 2-1: CloReM Block Diagram with Proposed Secondary Loop.

2-3 Linear Models of Reservoirs

Generally, there are three possible approaches towards fluid flow modeling. One way is using mathematical models that are based on first principle laws, such as conservation of mass and momentum. These principles are usually non-linear and contain high order derivatives and become more complex when they are coupled together. Another way is to use empirical relationships to explain inter-well connectivity. These empirical relations are based on lab experiments under various conditions. Alternatively under some assumptions, a combination of both might be employed, it means that having a structure of the first principle models with some simplifications using empirical laws, e.g. Darcy's law.

In practice, models of the latter type are used most often for describing the fluid flow in the reservoirs, wells and other equipments. These models are updated through data-assimilation, referred to as History Matching in reservoir engineering, using all the logged data collected during the production life of the reservoir. In this method, model parameters are adjusted in such a way that they match the production history. The complexity of model updating stems from the fact that, these models have a very large number of parameters and different combinations of values for each parameter may have the same matching error of the *past* data, while they predict a totally different *future*. In other words, estimating reservoir parameters in this scale is an ill conditioned problem and they are not uniquely identifiable.

For the proposed MPC controller, we need to have a linear model of the reservoir. The first option is the linearization of the existing nonlinear models using mathematical methods. In this way instead of modeling, we can linearize and downscale the reservoir models around any desired working point (for more details see [van Doren et al., 2005]). Although such techniques will reduce the computational burden of simulation and optimization, they are not good candidate for MPC because; firstly the original models have undermodeling issues, and the linearized versions will also suffer from this problem., and secondly these models are not updated but just replaced in different working points.

In recent publications there are some attempts to replace large scale reservoir models with simplified proxy models such as Capacitance Resistive Models, see [Yousef et al., 2006a], [Yousef et al., 2006b], [Liu and Mendel, 2007]. These models have a simplified structure of fluid flow based on the empirical laws, and their parameters are simply the coefficients of those equations, which obtained by multiple linear regression to match the field data. In the mentioned publications, these models have shown promising results for simple reservoirs and also been used for optimizing oil production, also see [Liang et al., 2007], [Saputelli et al., 2003], [Sayarpour et al., 2007], [Awashti et al., 2008]. The name ”capacitance resistive” is chosen because the differential equations of the models resemble relationships in electrical circuits. CRM has some great advantages such as;

1. It is very simple and straightforward.
2. It is based on physical laws, which means it accounts for physical phenomena potentially.
3. Model parameters are rapidly identifiable, and they can be verified readily, since they have physical interpretations.

On the other hand these models have major disadvantages too;

1. Simplified model structure prevents a proper prediction of unforeseen phenomena (undermodeling).
2. They cannot be extended further to cope with undermodeling issues, because then the structure becomes complex.
3. Comparing the results against 3D reservoir simulators, it has been shown that CRM fails to estimate well with presence of noise and disturbances, [Yousef et al., 2006a].

Fully data driven black box approach has also been studied in recent publications such as, neural network structure [Demiryurek et al., 2008], rate fluctuation analysis [Albertoni and Lake, 2003], [Yousef, 2005], [Kuchuk et al., 2005], [Lee et al., 2008], and subspace identification [T.Heijn et al., 2004]. These models do not take into account any physics of the reality and their quality is dependant on the ”training” dataset. Therefore, they can be easily misleading for unforseen reservoir phenomena such as water break-through. Also model and parameter validation are not trivial, because they don’t have any specific physical meanings.

Black box models that are identified based only on the measured data may not have good predictions for long horizon, but they can get updated rapidly. System identification methods with linear model structures are therefore the main focus of this assignment. Locally identified downscaled models are believed to be good candidates for the proposed MPC framework, since they can describe the dynamics around that working point and provide good short term predictions for a certain period of time. Linear reservoir modeling using system identification and their prediction quality will be studied in more details in Chapter 5 and 6.

2-4 Two Level Control of Waterflooding

The (optimal) decisions referred to so far, naturally belong to different levels of operational hierarchy and therefore different time-scales are involved; e.g. corporate planing and portfolio management in years or decades, reservoir management and history matching in months or years, and production operation and field adjusting in days. Each upper level determines strategic goals and objectives in addition to defining certain constraints for the lower levels, and each lower level provides new forecasting outlook and historical data for the upper level. The idea of improving CloReM using a MPC framework can be seen in a two hierarchial control levels, presented in Figure 2-2. Optimal trajectories are generated in the upper level, and the required control action is determined in the lower level to keep the system on these trajectories.

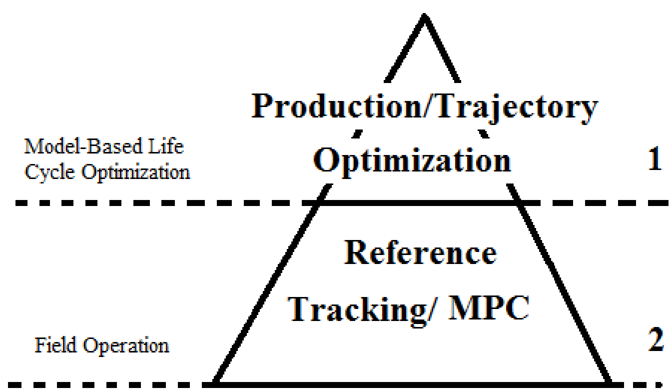

Figure 2-2: Hierarchial Two Level Control of Oil Reservoir to Maximize Profitability.

Translating the effects of well locations, well trajectories, appraisal wells, and extensive available field data into one optimization problem with a single objective function is very complicated. Therefore, in this project we only focus on the best injection and production strategy that can maximize the reachable profit. For a certain configuration of wells and field equipments, an optimal strategy is equivalent to maximize the volume of the produced oil by the end of a certain time horizon. However, oil companies are interested in representing the results in terms of a monetary measure of Net Present Value. NPV has an advantage of taking into account the time value of the profit that is gained by selling oil. From project economics point of view, money loses its value in time if it is not used for any investment[1]. This effect must not be confused with inflation, and is taken care of through *discounting* the project cash flow. Therefore, using NPV measure does not necessarily imply the highest recovery factor. NPV of oil production using waterflooding is presented by

[1]For instance if somebody has 100$ now and saves his money in bank, in one year he will have 105$ (if rate of interest is 5% per year). But if instead he does nothing and just keeps his money at home he will have the same 100$.

$$J_{NPV}(u) = \int_t^{t+T} \Bigg\{ \underbrace{\sum_{j \in \mathcal{N}_{prod}} r_{oil}(\tau)[1 - f_w^j(\tau)]q^j(\tau)}_{\text{oil revenue}} - \underbrace{\sum_{j \in \mathcal{N}_{prod}} r_{prod}(\tau) f_w^j(\tau) q^j(\tau)}_{\text{production cost}} + \underbrace{\sum_{j \in \mathcal{N}_{inj}} r_{inj}(\tau) q^j(\tau)}_{\text{injection cost}} \Bigg\} \underbrace{\frac{1}{(1 + d(\tau))^\tau}}_{\text{discount factor}} d\tau \tag{2-1}$$

Where r_{oil}, r_{prod} and r_{inj} are oil revenue, water production cost and injection cost per unit volume respectively. $d(t)$ is called the discounting factor that represents the devaluation of the money over time. $\mathcal{N}_{prod}$ and $\mathcal{N}_{inj}$ are the numbers of the production and injection wells, and $q(t)$ refers the total production rate (water and oil in combination), which is also assumed to be equal to the injection rate. The fractional flow rate is denoted by f_w, and is defined as the fraction of the water flow rate over the total flow rate, namely sum of oil and water flow rate, and of course $f_o = 1 - f_w$. The above formula indeed considers the time dependency of the variables, such as the oil price and the varying rate of interest [Zandvliet, 2008].

Considering the objective function above, for the time horizon of $[t^j, t_f^j]$ with the sampling time of Δt, the corresponding optimization problem is[2] [Kadam and Marquardt, 2007];

$$\begin{aligned} &\min_{u^j(t)} \Phi(x(t_f)) \\ s.t. \quad &\dot{x}(t) = f(x(t), y(t), u^j(t), \hat{d}^j(t)), \qquad x(t^j) = \hat{x}^j \\ 0 \geq\ &h(x(t), y(t), u^j(t)), \quad t \in [t^j, t_f^j], \quad t_f^j := t_f^{j-1} + \Delta t \\ &0 \geq e(x(t_f^j)) \end{aligned} \tag{2-2}$$

Where $x(t)$ are the state variables with the initial condition $\hat{x}^j$, and $y(t)$ are the outputs. Process dynamics is described by $f(\cdot)$, and time dependant $u(t)$ are the control variables for optimization. $h(\cdot)$ and $e(\cdot)$ are given for input and state constraint and end constraint respectively. Uncertainties such as unknown model parameters, measurement disturbances and possible changing economical (or market) condition is then treated in $\hat{d}^j(t)$ [3].

Due to large number of states, inputs and output, the optimization is very complex and computationally demanding. Therefore it is required to have large sampling time of Δt, at the cost of more uncertainties. In order to maximize the obtainable profit, the problem decomposed into two levels of an *economical dynamic optimization*, and a *tracking control problem*. Integration of these two levels is in fact proposed by [Kadam et al., 2003], for industrial processes such as polymerization, and is depicted in Figure 2-3. This Figure can be compared with CloReM with fast loop presented in Figure 2-1. We see that y_{ref} and u_{ref} are updated

[2] It must be noted that in order to prevent any confusion, the notation in this formulae is kept the same as in the reference. It means that the presented objective function is an economical NMPC criteria calculated every $\Delta\bar{t}$, with j being the loop counter.

[3] Disturbances d and states x do not have a fixed value, and are presented with a hat on the top as $\hat{d}$ and $\hat{x}$.

by re-optimizing the economical objective function, using data feedback in the upper level. In every re-optimization, all the measurable and unmeasurable economical effects (e.g. price of product or unexpected expenditures), are taken into account by d_E. Obtaining the references indeed requires models, that are able to predict longer future of the process. For this reason dynamic optimization is based on fundamental models that contain process dynamics and can foresee all the phenomena. Consequently, model uncertainties are treated in "tracking control" box, in a lower level.

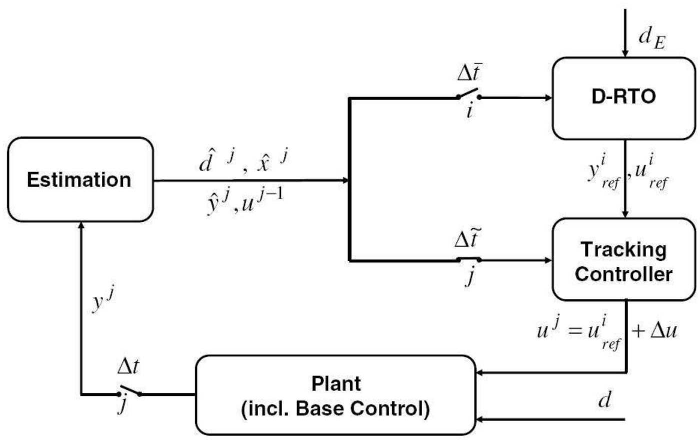

Figure 2-3: Two-Level Dynamic Real Time Optimization(D-RTO) and Control Strategies, after [Kadam et al., 2003].

Referring again to Figure 2-3, this decomposition has two different time-scales, a slow time-scale denoted by $\bar{t}$ on the optimization level and a fast tim-scale denoted by $\tilde{t}$ on the control level with the corresponding sampling times $\Delta\bar{t}$ and $\Delta\tilde{t}$ respectively. Practically $\Delta\tilde{t} < \Delta\bar{t}$ and this means that during the time $[t^j, t^j + \Delta\bar{t}]$ the control input $u^j = u^j_{ref} + \Delta u$ is updated to keep the system output on the reference and to minimize the deviation from y^j_{ref}. The output drift is basically a result of model uncertainties, which can be attenuated using a local updated model. The sampling time $\Delta\bar{t}$ (i.e. the time interval between two successive re-optimizations) has to be sufficiently large to capture the process dynamics, yet small enough to make flexible economic optimization possible. Also, sampling interval $\Delta\tilde{t}$ must be reasonably small to handle the fast control-relevant process dynamics. Note that the superscripts i and j are only representing the loop iterations, to distinguish between the time intervals.

2-4-1 Open-Loop Dynamic Optimization

Dynamic (re)optimization is surely very time consuming and must be done intuitively. In this assignment, we are only focusing on the controller performance. This means that reference trajectories are generated in the beginning of the reservoir life, and further measurements are not fed back to re-optimize the references. This is equivalent to have $\Delta\bar{t} = \infty$ as depicted in Figure 2-4. Instead, as it can be seen in the Figure, only the control action is updated to keep the system on the track. The new inputs are calculated with the MPC controller based on the output feedback from the system.

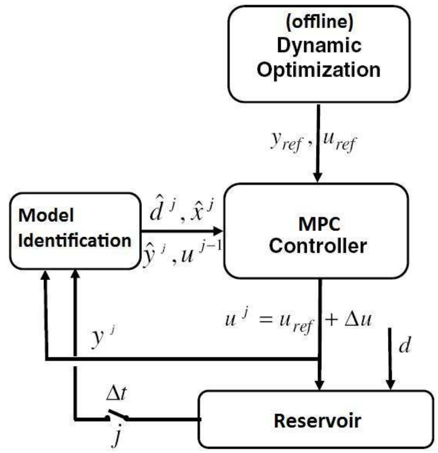

Figure 2-4: Open Loop Dynamic Optimization(D-RTO) with MPC Controller.

2-4-2 Estimating the States and Receding Horizon of MPC

In the proposed integrated two level approach, the values of initial condition and disturbances for control problem are estimated from measurements with a suitable estimation procedure such as Kalman filtering methods or moving horizon estimator. However, as it has been shown in Figure 2-4 estimation box is replaced with the system identification, i.e. system states and outputs are not estimated, but are predicted with the locally identified models.

It will be explained later in Chapter 4 that in conventional MPC framework, the input is re-optimized in every time-step after feeding back the output measurements. Unfortunately integrating the MPC controller box with the simulator required a more extensive programming which was beyond the scope of this thesis. Therefore, in order to simplify the controller implementation linked to the simulator, instead of designing an observer we use the prediction provided by locally updated model for the time $[t^j, t^j + \Delta\tilde{t}]$, while the noise is disregarded. Additionally in the same period the measurements are not fed back to the controller to update the control output. That means the solution of the optimization problem at time t^j will be applied to the reservoir in the corresponding time window, without re-optimization.

As a result, the MPC controller has a fixed prediction and control horizon. The length of this window is then selected with trial and error, that will be further motivated in Chapter 6.

2-4-3 Importance of y_{ref}

It must be noted that the performance of the lower control level is dependant on the upper optimization level to a great extent. It means that the degree of optimality achieved by employing the two level approach depends upon the reference trajectories provided by the dynamic optimization. The choice of the to be followed output is important, in a sense that it must be selected from the most important output variable of the system. On the other hand, the availability of such output must be considered. For instance although fractional flow of each producer may give more insight about the reservoir situation and also be easier in terms of reference tracking control, practically it is not economically feasible to measure oil and water production rate of each well separately in a real time manner. Therefore, we must choose from other choices like liquid rates or cumulative rates instead. Furthermore, according to the model uncertainties and ill-posed optimization problem of finding the optimal y_{ref}, there is always a chance of sub-optimality. In such a large scale multivariable system, the uniqueness of the optimal input and output reference is questionable. This issue may increase the production risks or limitations for infeasible references.

2-5 Using Reservoir Simulator (MoReS)

To simulate the reservoir behavior, there are several software packages for exclusive purposes, and also a few commercial packages developed by oil and service companies. These software use finite difference methods to solve material and energy balance equations to model a subsurface petroleum reservoir. Future effects of different input schemes are considered using simulators to come up with the optimal references (in the upper level). The obtained optimal inputs are then applied to the real reservoir and the corresponding outputs are measured with sensors (in the lower level).

Using real oil field data seems infeasible for three reasons;

1. Oil companies are not willing to publish their production data to prevent disclosing company's strategic records on the market.
2. A typical reservoir life is at least 5 years.
3. Different control approaches cannot be compared, since it is not possible to repeat the experiments in reality.

Therefore we must create reservoir models as a replacement for the reality and use the computer software to simulate their performances. A good advantage of employing simulator is that by synthesizing more simplified models, we are able to interpret the effects and issues more easily before we jump into the complex real reservoir models. Therefore, we use imaginary reservoir models in simulator not only for optimization, but also for implementation. This means that the input and output references are optimized using a model with certain properties (we call it "Model-Model"). Thereafter, the inputs are applied to another model that is developed in the simulator (and we call this one the "Real-Model"). In order to imitate the differences between the model and reality, geological properties of the Real-Model are selected to be slightly different from the Model-Model, e.g. by using another permeability realization. Additionally in order to have better approximation of the reality, more modifications must be done for Real-Model. For instance pressure has larger gradients around the wells, and to avoid numerical difficulties for simulating fluid flow, more grid blocks are needed around the wells (grid block refinement). Also to have more data available from injection and production rates shorter, time step for simulation is required. Inevitably the simulation time of Real-Model will increase in compare to the Model-Model, because of the numerical and computational issues.

Chapter 3

Data Driven Linear Model of Oil Reservoir

3-1 Introduction

The process of waterflooding a reservoir can be described primarily by principal laws such as conservation of mass, momentum and energy. For example, we can imagine a reservoir in the shape of a homogenous block that contains only oil, with one injection and one production well on two sides. Then, it is possible to build up a model based on above mentioned laws that can describe fluid flow in the reservoir. Block's pressure and saturation, and fluid and geological (rock) properties would be the corresponding states and parameters respectively. The amount of injected water is the system input, and the produced oil is the output.

However, reservoirs are not uniform masses and geological properties are not likely distributed spatially. Figure 3-1 shows water injection into a single block reservoir that contains heterogeneities. We can see that because of non-similar rock properties in the block, oil-water front will have an irregular shape. While it was expected to sweep the whole oil, due to the existing heterogeneities water will find a channel and reach the production well before the whole oil is recovered.

3-2 Reservoir Models and Properties

To construct a complete reservoir model, finite element techniques are used. The whole field is partitioned into the separate blocks, each of them is assumed to have a similar property in the entire block. In order to capture all the heterogeneities adequately, the number of these blocks must be high (usually in order of $10^4 - 10^6$). Consequently the models will have gigantic number of states (at least one pressure and one saturation for each block) and parameters. These parameters are fluid properties such as density ρ, compressibility c and viscosity μ of each phase (water, oil and gas), and rock properties such as permeability k, porosity ϕ and

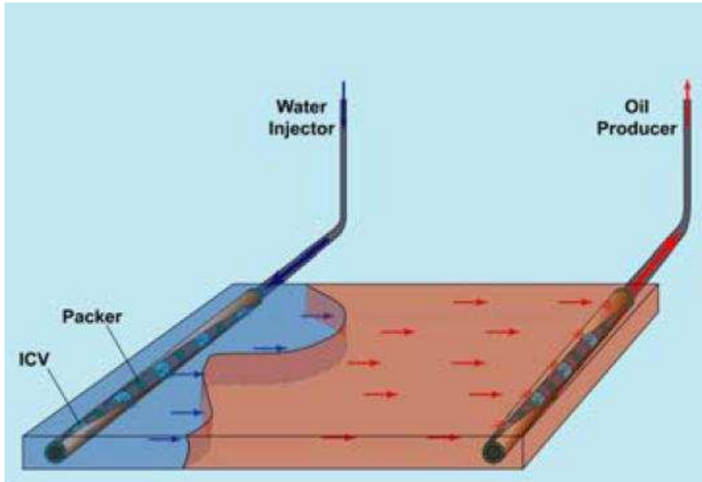

Figure 3-1: Process of water flooding using a horizontal injection and production well. The irregular-shaped oil-water front is a result of the reservoir heterogeneities, after [Brouwer and Jansen, 2004].

rock compressibility c_r. The governing equations for multi-phase flow through porous media are a set of mildly nonlinear parabolic (diffusion) equations, describing the rate of change of "pressures", coupled to a set of strongly nonlinear parabolic-hyperbolic (diffusion-convection) equations, describing the rate of change of fluid "saturations" [Jansen, 2007]. Under some assumptions and using a number of empirical laws for fluid flow, these equations are decoupled and simplified.

In reservoir management, behavior of the oil reservoir during production is simulated by the numerical study of these models. Simulation in many practical cases is the only way one can describe quantitatively such multi-phase flow. Nowadays simulators are important tools, which are used daily by many reservoir engineers.

Sources of Nonlinearity and Uncertainties

In reality, geological properties are conceivable using seismic tests and core samples. Usually the seismic measurements contain a lot of noises, and core samples are very sparse. Therefore, main source of uncertainty is the limited knowledge of the system parameters. Moreover, values of the parameters do not remain constant during the life of the reservoir. These changes are due to the fact that parameters are not only dependent on the values of states, but also sometimes they are dependent on each other. This brings a great deal of non-linearity to the system equations.

To summarize, reservoir as a system and water flooding as a process, have the following properties [Renard et al., 1998];

- Dynamics of the system are highly non-linear, described by complicated equations.
- Oil Recovery is similar to a single batch process, that happens only in one long period of time.

- System has several inputs, and several outputs with different natures.
- Reservoir dynamics have states of different and very large time constant.
- Available field data are usually very uncertain and contaminated by measurement noises.
- The observation time period used for identification is very short related to frequency range. It cannot be expanded unless to disable the stationarity hypothesis of the studied system, especially concerning the saturation constancy.
- The huge number of combinations between potential inputs and possible model structures. Too large number of unknowns would have to be determined, leading to unreliable results.

3-2-1 Low Order Linear Models

Dynamics of high order reservoir models are usually captured in a smaller degree space than the models initially may apply [T.Heijn et al., 2004]. Therefore, low order models that are obtained by either direct or indirect approach, are often sufficiently accurate to describe reservoir dynamics. Based on these low order models, low order controllers can be constructed. It must be noted that in this work, downscaled models are not a replacement for reservoir simulation in order to reduce computational burden (simply because they do not contain sufficient knowledge), but on the other side they are very good alternatives for low order control algorithms.

In the previous chapter, two possible approaches of identifying a lower order model were discussed in Section 2-3. Ideally model reduction of a high order model captures only the most important and dominant features of the system. However, the neglected dynamics may play a major role for predicting the short term reservoir behavior. From reference trajectory point of view, we must note that undermodeling issue is very important and should not be underestimated.

3-2-2 Inputs, Outputs and States of Downscaled Models

Low order models indeed have lower number of states and these new state variables do not have any direct physical meanings necessarily. This issue implies that low order models are hard to validate. However, if these models are obtained by projecting the high order non linear model into a lower order subspace, then it is possible to have an estimate of the real system states by applying some mathematical methods. Black box models that are directly identified with a low order must have the desired inputs and outputs, because constructing the output predictions from the states is impossible.

In the proposed reference trajectory scheme, it is important to keep track of production rates, because the estimated profit is calculated from the amount of produced oil. Therefore, production rates must be selected to be the outputs of the identified models. From control point of view, inputs must be chosen from the elements that have the most influence on the outputs. Injection rates and total amount of injected water has a direct impact on the total amount of produced oil (or oil and water). Moreover individual production rates of each well can be controlled more directly with valve settings.

Flowing Bottom Hole Pressure or simply BHP[1] is used as input because it can be easily manipulated by valve openness [2]. In practice the difference between BHP and pressure of the block that contains producer well, determines the flow rate q as suggested in

$$q = J(p_{wf} - p_R), \tag{3-1}$$

where J is called *well index* or *productivity index*, p_R is the grid block pressure or simply reservoir pressure around the well and p_{wf} is BHP (the subscript wf refers to *well flow*), see [Jansen, 2008].

Therefore system inputs will be the BHP of the producer wells, the injection rates of the injector wells, and system outputs will be the production rates (or to be more precise, the liquid rates, whether it is only oil or a mixture of oil and water) of the producer wells. It should be noted that inputs have different physical natures and system responses to individual inputs might have different properties.

3-3 System Identification

System identification is basically about data based modeling, and is successfully used in wide range of technical areas such as chemical or mechanical engineering. Following issues make system identification a powerful tool for modeling:

- Using principle laws to construct a model always have lots of assumption. Additionally, there are always so many unknown physical parameters in reality, and sometimes it is not possible to find any value for them. Therefore either with or without assumptions these models generally have uncertainty.
- Models that are obtained by physical laws are usually very complex (high order). With system identification one can end up with more simplified models that can describe the dynamics of the real system with acceptable accuracy margins (reduced order models). This depends on some issues which will be discussed in the following sections.
- With system identification, one can also have a model for the disturbances, which always exist in practice.
- Modeling of a system using principal laws has a risk of losing sensors and actuators dynamics.

Models that are obtained by system identification methods are independent, i.e. regardless of existing large scale nonlinear models, system identification can directly provide low order models if it is necessary. On the other hand employing these methods has two major drawbacks; firstly a set of sufficiently informative data must be provided before modeling, and

[1]The adjective "flowing" is used to distinguish the pressures from the closed-in values (also referred to as the static values) for BHP which occur when the well is closed-in at surface. But here we simply use BHP and it refers to pressure at the bottom of the well, i.e. the tubing.

[2]It must be noted that in practice BHP is controlled by manipulating the Chokes on top of the wells.

secondly model quality and validity range is highly dependent on the training data specially for processes with changing dynamics. Although oil production is done with certain constraints on inputs and outputs, abundant data is available thanks to vastly use of sensors. However, second drawback is more significant pertaining to reservoir modeling, just because the underlying dynamics are changing during the production life cycle. This implies that models might only be valid locally around certain working points and under certain assumptions, and it might be required to identify several models instead of using a single model for the whole process.

According to the reservoir characteristics and also model properties, around each working point these assumptions must be hold; (validity of the assumptions will be more studied in Chapter 5)

1. The process remains near a certain working point for a long time in compare to the largest time constant.
2. At each working point the process dynamics are time invariant or at least the change is very slow.
3. At each working point the disturbances are considered to be stationary.
4. At each working point the process behavior can be described sufficiently accurate by a linear model.
5. Input is sufficiently rich to excite all the relevant dynamics.

System Identification Procedure

Major steps of system identification are depicted in a flowchart in Figure 3-2. In the first place, a set of data is required for identification. This data might be available from normal operating records, or a specific experiment must be designed to gather the required data, for instance a step or a sinusoidal response. Also a certain structure of the model must be specified, i.e. a model set within which the most accurate parameters are to be identified. Properties of the real system is in fact plays a major role in determining the model set. Lastly an identification criterion must be constructed from the measurement data and the model set. In this sense several methods are available such as minimization of Prediction Error with transfer function model sets, or Singular Value Decomposition with subspace system representation.

After determining the above mentioned aspects, the identified model needs to be validated to see if it meets the user requirements. If not, this process must be repeated with some modifications in one or more of the above aspects. It can be seen that a proper treatment of each aspect can influence the results and proper or improper selection of each aspect can increase or decrease the model quality. Experiment design is studied in Section 3-3-1, and model set selection and identification criterion are discussed in Section 3-3-2.

3-3-1 Experiment Design and Data Preprocessing

Experiment design is one of the most important steps of system identification. In the literature, much more attention has been paid to identification algorithms than to the design of

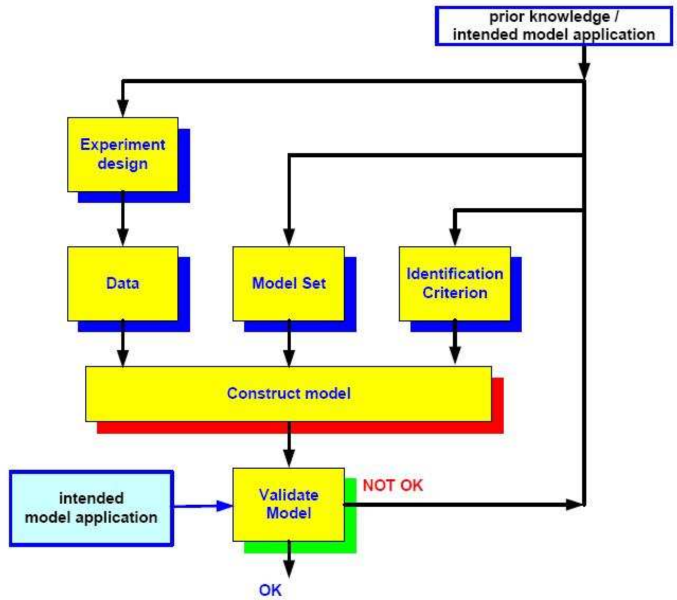

Figure 3-2: Identification Procedure, after [Van den Hof, 2006]

the experiments. Sometimes with a well designed experiment and well collected input/output data, a good model can be determined with the simplest least square criterion. Generally this step consists of a few preparatory experiments in order to realize the features of the system and disturbances and to come up with a suitable input signal.

Usually the designed input and the recorded output from the reservoir (or any system in general) cannot be readily used. The measured data on site are often of erratic nature for various reasons. For instance the properties of the produced fluid are changing continuously or lifting methods may change from time to time, in addition to the errors that may exist according to the measurement techniques and sensors' failure, etc. Therefore, before these data can be used for identification, they require some preprocessing operations such as data smoothing, resampling and filtering.

Preparatory Experiments

To find the characteristics of the disturbances on the process output, free-run experiments are applied, i.e. a normal inspection of the output. Another important test is the staircase experiment, which is applied to determine the linearity range of the process. With the same test, one can also obtain another three important properties; static gain, estimation of the time constant and possibly the time delay. The importance of the time constant is that one can determine the duration of the experiment ($5-10$ times longer than the largest time constant). For the cases that the staircase experiments seem impossible for economical and/or technical restrictions, a step input can be employed. A third set of experiments which is called white noise experiments, are applied to determine the bandwidth. The bandwidth of the open loop process can be useful to decide the right sampling frequency of the identification experiment (working frequency).

Sampling Time and Aliasing

Generally, measurements are not picked up at a regular time spacing. Moreover, there can be a lack of measurements during several weeks or months. The goal of resampling is to get a regular data set, with identical time spacing between consecutive data values [Renard et al., 1998]. Sampling frequency f_s is the frequency at which the data samples are recorded (or similarly the sampling time T_s is the time between two consecutive samples). Also, since the identified models are presented in the discrete time format, there exists another sampling time for the models. Usually sampling time of the data acquisition is high in order not to lose any information. Reservoirs however have typically very slow dynamics and it is not desired to have a high sampling frequency because;

- Discrete time models built with high sampling frequency in relation to the process's time constant, is numerically sensitive, because all poles cluster around (1,0) in z-plane.
- If the model is biased, the fit might be better in high frequency band, which is not desirable for most of the model application.
- A fast sampled model will often be non-minimum phase even if the original continuous time process is minimum phase (instability issue).
- Process with time delays may be modeled with many delay samples. Such effect will cause difficulties in control design.

A fine rule of thumb for the sampling frequency f_s is

$$f_s = \frac{3}{2\pi\tau_{min}}, \tag{3-2}$$

where τ_{min} is the smallest process time constant of interest. This means that if data set has high sampling rate, then it must be resampled before using it for identification. To prevent the interesting data get distorted or lost by the aliasing effect, an anti-aliasing filter is applied for all the input and output data before sampling. Therefore data is filtered offline using an analog filter with a cut-off frequency equal to Nyquist frequency[3].

Another benefit of the anti-aliasing filter is noise reduction. In reservoir simulation, the disturbances have low frequency content, while measurement noises are more broadbanded than that of the useful signal. Thus the sampling time is usually chosen, so that most of the spectrum of useful part is below Nyquist frequency. The anti aliasing filter also removes the high frequency noise content.

Persistency of Excitation

To make sure that the recorded data have sufficient information about the dynamics of the process, the input signal should have enough power to excite the modes of the system. It can be shown that, a necessary condition for consistent estimation of a n-*th* order linear process

[3]Nyquist frequency is the half sampling frequency of a discrete signal.

is that the test signal is persistently exciting of order $2n$. When there is no prior knowledge about the system, it is recommended to use a signal with an infinite order, e.g. PRBS with an small clock time. In addition to this, in case of significant measurement noises, higher degrees are suggested in order to have better noise reduction. However, for identifying a reduced order reservoir model it doesn't seem necessary to have high order of escitation, since not so many parameters are intended to be identified (further discussion can be found in Chapter 5). On the other hand in MPC controlled reservoir, not much freedom exists to design the input signal, as the optimal inputs are already fixed. In other words, it is a dual problem to have an optimized input signal for control purposes and in the meantime using the same set of data for identification purposes. Therefore it is the matter of consistency, in which the persistency order of the input signal should be checked in order to be at least twice as the order of the desired model.

The degree of persistent exciting of a signal can be recognized either by building the symmetric Toeplitz matrix of auto correlation of the signal, or by checking the spectrum of the signal over its frequency range. It must be noted that due to the nature of the reservoirs, sometimes the expected effects on the outputs cannot be observed even for a persistently exciting input.

Data Preprocessing

Before starting the identification, some pretreatment should be done on the datasets such as peak shaving, detrending, scaling and offset correction, delay correction and resampling. Data preprocessing or smoothing consists in sweeping the data using a sliding window to reject non appropriate data according to the statistical median estimator given a rejection percentage. Care must be taken in this step to keep the maximum of relevant information pertained to the initial measurements. The width of the sliding window is chosen to take shut-ins of the wells into accounts. Smoothing deals mainly with watercut or flowrates of producing wells. The injection rates are usually known beforehand, and consequently do not need any smoothing step [Renard et al., 1998].

3-3-2 Model Set Selection

A model can be represented in several ways, which is determined by the its application. As for example non parametric model representations such as Bode diagrams or step responses, is not sufficient if the model is intended to predict or simulate the output. Additionally efficient control methods are available based on dynamical models.

Prediction Error Identification

A common method to develop data-driven parametric models is Prediction Error Identification (PEI) that in fact identifies parameters of a transfer function between input and output, represented in discrete time as follows

$$y(k) = G(q)u(k) + \upsilon(k), \tag{3-3}$$

where $G(q)$ is a Linear Time-Invariant (LTI) stable transfer function that represents input/output relation, and $v(k)$ is a nonmeasurable disturbance term. $G(q)$ is in fact an abstraction of the reality (with limited order), and for identification of a low order model $G(q)$ would be an approximate of the real system. Practically no system exhibits LTI properties, but with some assumptions they have only small deviations. A stable transfer function $G(q)$ is a fraction of two polynomials as in

$$G(q) = \frac{B(q)}{A(q)} = \frac{b_1 q^{-1} + \ldots + b_n q^{-n}}{1 + a_1 q^{-1} + \ldots + a_n q^{-n}}, \tag{3-4}$$

Additionally the term $v(k)$ accounts for all the disturbances in the system. These disturbances contain

- Measurement noise.
- Process disturbance.
- Effects of nonmeasurable input signals.
- Effects of linearization.

Therefore structure of $v(k)$ must be determined properly to be able to reflect all the disturbance terms available in the identification procedure. In PEI, $v(k)$ is modeled as a zero mean stationary stochastic process with a rational spectral density[4].

$$v(k) = H(q)e(k) \tag{3-5}$$

where $H(q)$ is a proper rational stable transfer function, and $e(t)$ is a sequence of zero mean white noise. PEI has several variations depending on the structure of $G(q)$ and $H(q)$, and are briefly studied and compared in Appendix B.

Although PEI is a very widely used identification technique and a lot of user-friendly software are available for it, parametrization of MIMO processes with PEI model sets is not computationally efficient. Additionally, optimization of the PEI algorithm [5] boils down to a linear regression scheme only if the identification criterion is linea with respect to the to be identified parameters, i.e. ARX and FIR. For other structures however it requires nonlinear optimization methods that become even more complex for MIMO systems. From computational point of view, to find the optimal parameters an iterative search method must be applied. Generally in such methods instead of global minimum, the optimization algorithm get stuck in a local minima. This basic issue in nonlinear optimization problems can only be treated by starting the iterative search in several points of the parameter space, and thus by scanning this space for convergence to the global minimum [Van den Hof, 2006]. Therefore, those software packages do not provide tools to identify a MIMO model directly with model structures of ARMAX, OE or BJ.

[4]For Definition of spectral density $\Phi_v(\omega)$ refer to Appendix A-1

[5]For clarifying the term "optimization" here, note that identification can be defined as finding the optimal parameters of the chosen structure that minimize the error between the measured and predicted output.

Therefore ARX and FIR are potentially the best candidates to start with. Approximating the real system with a low order model directly in these structures does not necessarily have a good fit. This issue becomes more severe especially when the process involves one or more of the above mentioned disturbances. Generally lower order identified models are less accurate and more biased to account for the existing disturbances. Therefore, in order to have an accurate simulation, the order must be increased, and yet no accurate models can be obtained for the disturbance. Unfortunately, this is not desirable because the variance of the models is dependant on the number of the identified parameters. As it was previously mentioned, this is not desirable from controller design point of view either. A possible solution is to downscale the high order models beforehand by employing a mathematical method. We will see in Chapter 6 that this issue will cause some problems for implementing the MPC controller.

Subspace Identification

In mid 90's a so-called Subspace IDentification (SubID) for approximate realization of the real system (direct downscaled model identification) has been introduced. This popular area connects with realization theory and essentially encompasses projections of signal spaces onto subspaces that represent limited-dimensional linear systems (i.e. the identification criterion is not expressed explicitly). A principal tool in these operations is the singular value decomposition. One of the advantages of the approach is that handling of multivariable systems is practically as simple as handling scalar systems. More detailed study related to SubID can be found in Appendix C.

3-4 Chapter Conclusion

Waterflooding process can be modeled using principle laws, such as conservation of mass and momentum. The obtained models with this method are highly nonlinear and have large number of states and parameters. High order models require high order controllers that are not favorable since it is not easy to analyze their performance. Moreover high order controllers are harder to (re)tune both computationally and intuitively. Low order data driven models can be used for control purposes instead. It must be noted that according to the properties of reservoirs, identified models are only valid under certain assumptions.

Tracking optimal production rates obtained from lifecycle optimization of a reservoir, indeed requires models that can describe the relation between production rates (outputs) and all the elements in the system that has influence on them, such as injection rates and BHP (inputs). With system identification methods, linear low order models can be built directly from input/output data.

Since the quality of the model is dependant on the data set, a proper input signal must be designed. A suitable input is determined according to the characteristics of the system, and therefore input design is preceded by a number of experiments in order to get rudimentary knowledge about the underlying dynamics.

Usually different methods are combined to get the most confident results and it was motivated that PEI and SubID are good candidates to be used for the model structure. PEI can provide a disturbance model and also there are useful software packages available to identify and validate the models. On the other hand SubID has a simple structure that is well suited for MIMO systems, and more importantly it is computationally efficient, since the model parameters are obtained by matrix algebra instead of minimization.

Chapter 4

Model Predictive Control

4-1 Introduction

Among all the available model based control techniques, MPC is the most popular method in process industry since early 80's. MPC can easily handle processes with large time-delays and even unstable systems. This success is indeed inherited from properties of this method; firstly is the explicit use of process model in control calculation in contrast with PID like methods. This can be seen both as an advantage and a disadvantage in the same time [Tyagunov, 2004]. This means that either one should have an insight over the underlying dynamics to construct a model or, identification methods have to be applied preceding the controller implementation. This allows the controller to deal with process phenomena directly. Therefore the controller performance will be dependant on model quality to great extent. Secondly MPC considers inputs, outputs and states of the system in control calculation step by step, which enables the controller to take into account any signal constraint, or even system changes by adapting the control strategy. That is why in industry for "supervisory" optimizing control of MIMO processes, MPC is often preferred over robust control techniques such as LQ or H_∞.

Limitations of MPC are closely related to prediction qualities of the models used inside the model predictive control system. Almost all manufacturing processes are nonlinear, and majority of MPC application are based on linear models. Therefore linear approximation of non-linear process behavior restricts the dynamical range of the model and limits the prediction accuracy. In most cases however, a carefully identified linear model around a working point is sufficiently accurate, since the process is not changing rapidly from one point to another. On the other hand, implementing a linear model and a quadratic objective function, the MPC algorithm will provide a reliable solution by using a convex Quadratic Programming (QP).

In general MPC is rather a methodology than a single technique, and refers to a wide range of controllers depending on mathematical translation of the problem. Basically any MPC controller has 5 items in design procedure

- Modeling of process and disturbances.

- Defining a performance index.
- Introducing constraints.
- Control calculation using optimization.
- Implementation.

4-2 The Model

Role of the model is to make an estimation of the behavior of the system, and also make predictions of the states and output signals. State space representation is commonly used to describe the system, since it is well suited for MIMO processes, more compact and easier to implement the MPC algorithms.

$$\begin{aligned} x(k+1) &= Ax(k) + B_1 e(k) + B_2 w(k) + B_3 v(k) \\ y(k) &= Cx(k) + D_{11} e(k) + D_{12} w(k), \end{aligned} \tag{4-1}$$

with $e(k)$ being a zero mean white noise of measurements, and $w(k)$ is any known disturbance signal. Models given in impulse response or transfer function structure can be converted to state space models easily using the following equations,

$$\begin{aligned} G(q) &= C(qI - A)^{-1} B_3 \\ F(q) &= C(qI - A)^{-1} B_2 + D_{12} \\ H(q) &= C(qI - A)^{-1} B_1 + D_{11}, \end{aligned} \tag{4-2}$$

where $G(q)$ is the process model, $F(q)$ is the disturbance model and $H(q)$ is the noise model. While the performance of the controller is not highly dependant on model structure, choice of model type may influence the accuracy and computational effort of the predictive control algorithm. Finite response and step response models are preferred in process manufacturing because they don't need any advanced process knowledge, but on the other hand they require a large number of parameters. This results in larger parameter variance in contrast to the parametric models such as state space models. While structuring the predicted values are compact and easy to implement for parametric models, it becomes much more complex and cumbersome for FIR models [van den Boom and Backs, 2007].

4-3 Optimal Control

A control action that can minimize the tracking error needs a performance index or a cost function formulation. For a MPC with linear model the standard predictive control performance index is defined as

$$\begin{aligned} \min_{u(k)} J(\upsilon, k) &= \sum_{j=0}^{N-1} \hat{z}^T(k+j|k)\Gamma(j)\hat{z}(k+j|k) \\ \text{subjected to } & \; h(x(k), u(k)) = 0 \\ & g(x(k), u(k)) \leq 0 \end{aligned} \tag{4-3}$$

In which N is the prediction horizon, $z(k)$ is a measurable signal that must be controlled, $\hat{z}(k+j|k)$ is the prediction of $z(k+j)$ at time k and $\Gamma(j)$ is just a diagonal selection matrix with ones and zeros on the diagonal. The entries of $\Gamma(j)$ are determined based on the selection of the signal $z(k)$. $h(\cdot)$ and $g(\cdot)$ are linear equality and inequality constraints of inputs and states respectively. $z(k)$ is defined according to the output and control signal such as

$$z(k) = \begin{bmatrix} y(k+1) - r(k+1) \\ R^{1/2}u(k) \end{bmatrix} \tag{4-4}$$

Substituting Equation 4-4 into Equation 4-3 yields in a quadratic cost function with a weighting matrix R between control action and tracking error. The relation between the predictions of $\hat{z}(k)$ and the inputs are defined by the process model 4-1, and thus the solution of 4-3 can be found using QP.

4-4 Receding Horizon Principle

Predictive control uses the receding horizon principle. This means that after computation of the optimal control sequence, only the first control sample will be implemented, and subsequently the horizon is shifted one sample ahead and the optimization is restarted with new information from the feedback measurements.

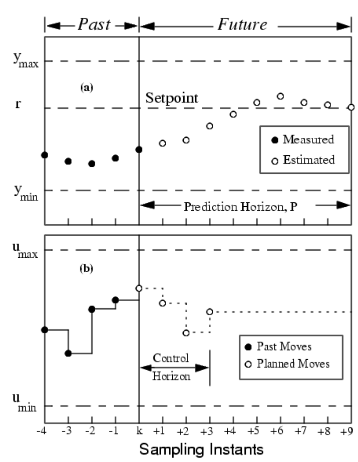

Figure 4-1: Moving Horizon MPC

Chapter 5

Reservoir Modeling with System Identification

5-1 Introduction

Having a model that can describe the relation between inputs and outputs, is the first step in any control relevant problem. Regardless of the control method that is chosen, the results will improve if a more accurate model is at hand. Although robust control techniques has developed significantly in past years, still modeling is considered as an important stage of almost every project.

System identification is basically about data based modeling. This means that a model is identified from the information included in the measurements that has been obtained from a real system. Therefore, model accuracy can be improved when measured data have enough information about the system dynamics. Proper design of the input signal based on the characteristics of the system can improve the quality of the data to a great extent. Experiments such as step response analysis, impulse response analysis, free run analysis and etc. are designed to carry out for specific purposes, and are commonly used in the process industry to obtain the basic knowledge about an unknown system.

Although there are several techniques of system identification available, it was motivated in Chapter 3 that linear PEI and SubID are good candidates for reservoir modeling. This chapter aims to investigate the issues pertaining to model identification of reservoirs and also to systematize identification procedure, based on experiment on 5 synthetic reservoirs.

System identification of each reservoir follows a certain procedure. The first step consists of a number of experiments that leads to design of a proper input signal. A step response test is applied between each input/output pair to realize three important attributes; first the possible delay samples in the signals, second the time constant of the response of each pair, and third the frequency range of the system. From this information it can be determined what length and what frequency content should the inputs have, and whether it is necessary to resample the measured data. Input signal amplitudes can be chosen by applying a staircase experiment.

For approximating highly nonlinear systems with LTI models, it is very important to know the range of the inputs amplitude that only excite the system dynamics linearly. To this end, a number of consecutive step-like increases and decreases of an input are applied, and output responses are inspected to follow the same pattern. If the system remains linear, this means that the superposition rule is hold and the measured output must have the same proportional increase and decrease.

In the next step, 3 linear models of FIR, ARX and SubID are identified, and the model orders are determined based on the highest simulation fit. Finally for validating the models, we look into their step responses and also the predicted outputs compared to simulator the results. It must be noted that most of the experiments and proper model selections are based on rules of thumb in several simulations.

Range of the models are from a simple 2D homogeneous to a 3D heterogeneous reservoir.The first reservoir model is a very simple example that we are looking into identifying a model between injector and producer rates. In "2D heterogeneous reservoir" the effects of adding more complexity to the geological properties are studied. An extra complexity is added to the reservoir models by introducing 3 rock layers in "3D heterogeneous reservoir". The hardship of identifying directly a multi input multi output system is investigated in a 2D reservoir with "6 wells". Finally a reservoir with all the complexities and also two physically different inputs, is studied in "VanEssen reservoir" model.

5-2 2D Homogenous Reservoir

As it is shown in Figure 5-1, this reservoir looks like a single block with with similar rock properties in everywhere. The term "2D" stems from the discretization method of the field and construction of the corresponding dynamical equations in the simulator. This reservoir has been meshed with only one layer, and it is assumed that the fluid does not move vertically. Moreover, there are four injectors located in the corners and one producer in the center.

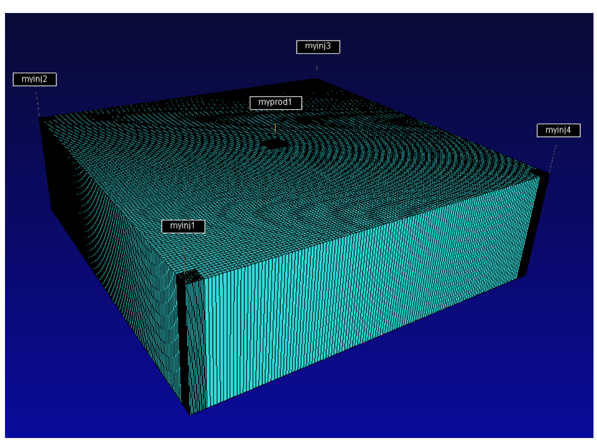

Figure 5-1: 5-spot Homogeneous 2D Reservoir

5-2-1 Step Response Analysis

Response of a system with an initial condition to a sudden change of an input is referred to *step response*. Before applying a step response test two main characteristics of reservoir dynamics must be reminded; they are slow and they are not stationary. For instance, shutting in an injection valve may need up to one month of logging of decreasing production rates, to have a complete test result. Therefore it should be investigated whether the acquired knowledge, economically motivates such tests or not. Moreover, during this period whether the reservoir produces or is entirely in shut-in phase, the dynamics of the system does not remain the same. The question that needs to be answered is that for how long after the test, it is valid to assume system properties are unchanged.

Figure 5-2 shows the step response, resulted from the sudden injection rate of $100BBL/day$ in one injector and due to the existing symmetry, it is not necessary to repeat this test for each injection well. Since the reservoir starts producing from the *rest* condition [1], we do see a smooth increase of the oil production rate. The difference between the steady state production rate and the injection rate in this figure should not be confused with any kind of error. In fact injectors 2, 3 and 4 are not entirely shut down and injecting the small rate of $1BBL/day$, to avoid numerical issues of the simulator. Therefore, according to the conservation of mass, the amount of the total production rate must be equal to the total injected water.

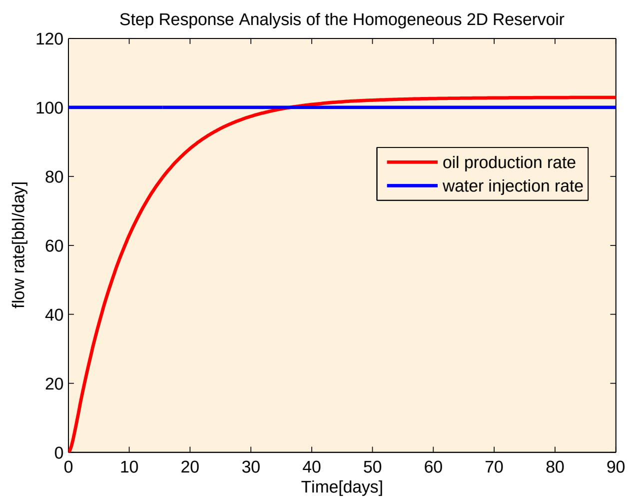

Figure 5-2: Step Response Analysis of Homogeneous 2D Reservoir

Obviously the behavior is indeed a sign of a simple dynamic and of course in such simplified version of reality, we do not expect significant changes of the system over the reservoir life. This means that the realized information from this step response is assumed to remain valid in reasonably long enough period.

Figure 5-3 shows the staircase experiment of injecting various rates in the same reservoir. It can be inferred that as long as the injection rates remain under $300BBL/day$, the system outputs change linearly.

[1] The initial pressure of the reservoir is assumed to be zero, or alternatively reservoir has lost its initial pressure already

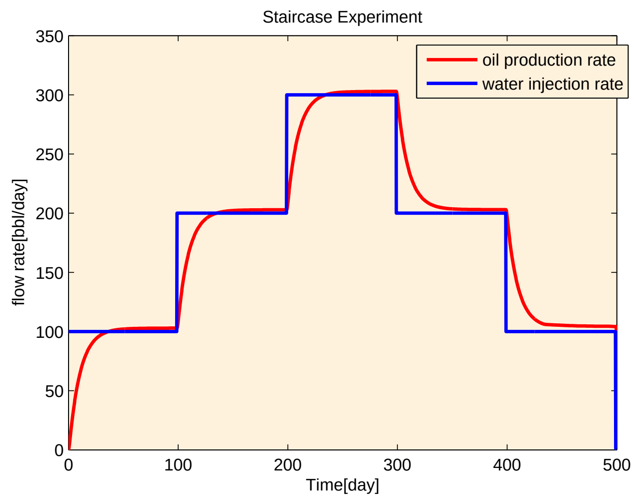

Figure 5-3: Staircase Experiment of Homogeneous 2D Reservoir

5-2-2 Input Design

Before designing the input, it needs to be reminded that the time scale upon which we run the experiments could be normalized from days to seconds, due to the slowness of the reservoirs.

Length of the experiment is determined based on the longest time constant of the whole system. The time that takes for the system to reach 63% of its final value in step response is referred to as *time constant*, and is represented by τ. In linear systems, $\frac{1}{\tau}$ gives an estimate of the system bandwidth frequency(Hz). According to a rule of thumb, experiment length T_N of 5 to 10 times of τ is enough to capture the most important dynamics.

Amplitude of the input signal is limited by two factors; signal to noise ratio and the linearity range. For the time being that we use simulator and all the measurements are generated by computer, it should be noted that nothing such as noise or noise model exist [2]. Therefore, increasing the signal amplitude seems unnecessary. On the other hand, referring to Figure 5-3, the linearity can be assured by injection rate of under $300BBL/day$.

Another important aspect of the input signal is indeed *sampling frequency*, $\omega_s(Hz)$, or *sampling time*, $T_s(s)$. As we have already fixed T_s in the simulator, (i.e. data acquisition frequency), here we need to decide sampling frequency that is used in the identification procedure, (i.e. the sampling frequency for which the discrete-time model is built). Information that obtained from step response, suggest a system with a bandwidth, ω_b, around $0.1rad/sec$ (being equal to $1/\tau$). A rule of thumb proposes to have a sampling frequency of $10\omega_b < \omega_s < 30\omega_b$. This way, the constructed discrete model from the continuous system, can be prevented from aliasing effect. The upper limit also prevent clustering of the poles near the unit circle, and other numerical issues. (more info could be added). Thus the measured data is resampled by factor 12, since T_s is decided as $3s$.

Moreover, based on the estimated ω_b, to have more emphasize on frequencies near to the bandwidth (and also band of interest), the input signal is generated in a way that it has higher energy in the low frequency, up to half of the *Nyquist frequency*.

[2]However, we still have $H(z)$ that represents model disturbances. Refer to Section 3-4 for more details

5-2-3 Model Identification

After deciding on the appropriate input signal, we need to choose for the appropriate model structure and eventually identify a model. Figure 5-4(a) shows the RBS input signal of length 100 days.

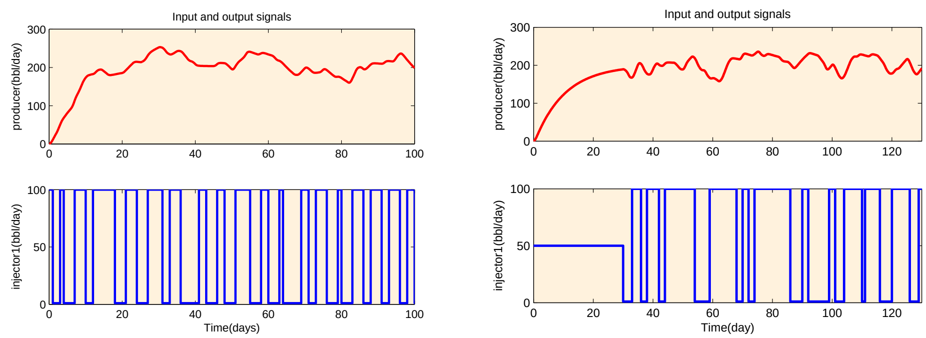

(a) (b)

Figure 5-4: RBS Input Signal Applied on Homogeneous 2D Reservoir

Since the reservoir has no initial pressure, after starting the injection at time zero it takes almost 10 to 15 days for the reservoir to reach to a new working point. To investigate whether the information that has been captured during that period is useful or not, another set of input signal could be applied with slightly different properties. This time, we apply a constant rate of $50 bbl/day$ (almost equal to the mean of the previous input) for 30 days to bring the reservoir close to the desired condition first, and then applying the previously generated RBS. Figure 5-4(b) presents the input-output measurements of the second data set.

Identification results with the first signal input are shown in Figure 5-5. The simplest structure of FIR can be reached in two ways in MATLAB toolbox of identification. One way is to select zero order for polynomial A in ARX structure, and another way is to select zero order for polynomial F in OE. There is a fundamental difference between these two structures, and that is ARX has a linear regressor in terms of the to be estimated parameters, which gives computational advantages. These two models are validated against a first order SubID model, which shows better simulation fit. The second set of input signal has been treated the same and the results are presented in Figure 5-6.

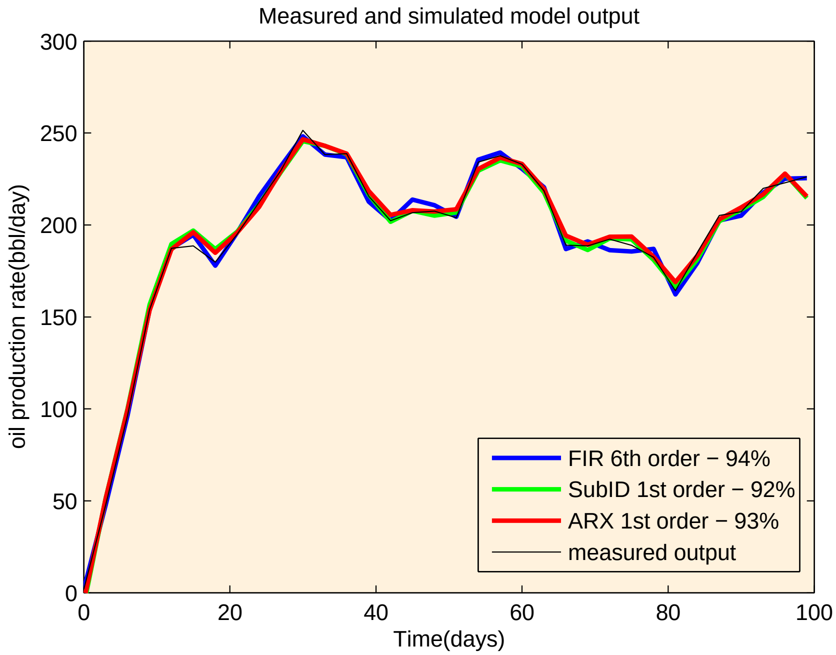

(a) Simulation Fit of Different Model Structures

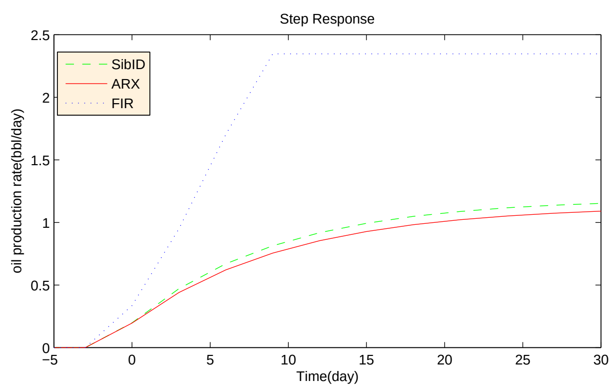

(b) Step Response of Identified Models

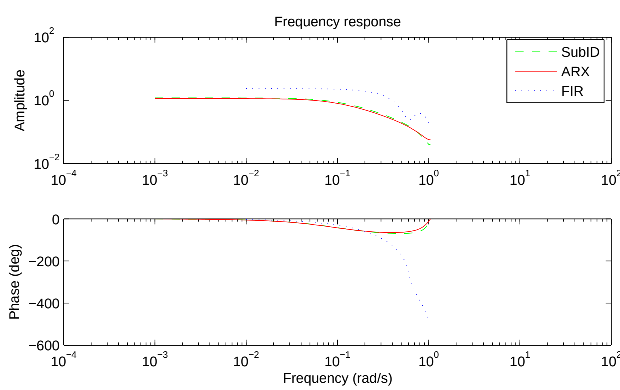

(c) Bode Diagram of Identified Models

Figure 5-5: Model Identification of Homogeneous 2D Reservoir with 1st Set of RBS Input Signal (including the transition period)

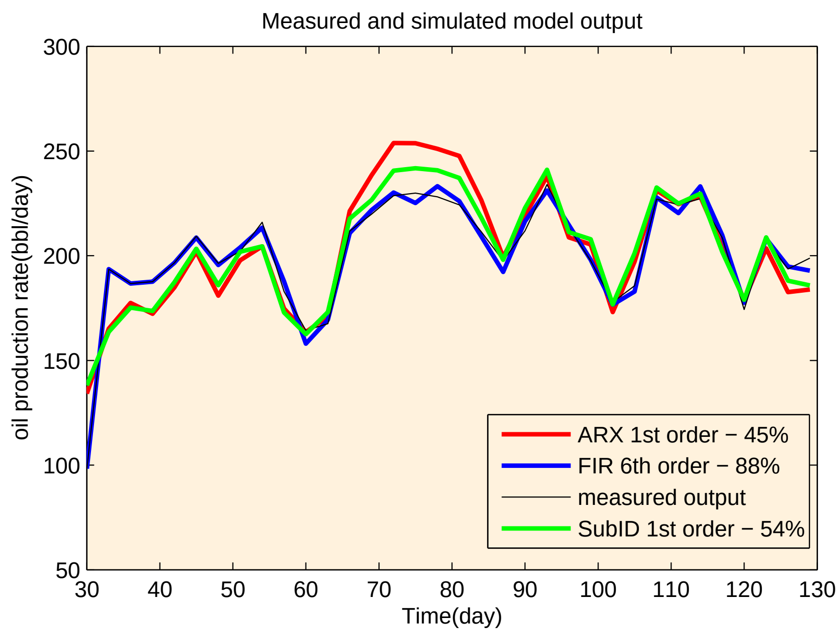

(a) Simulation Fit of Different Model Structures

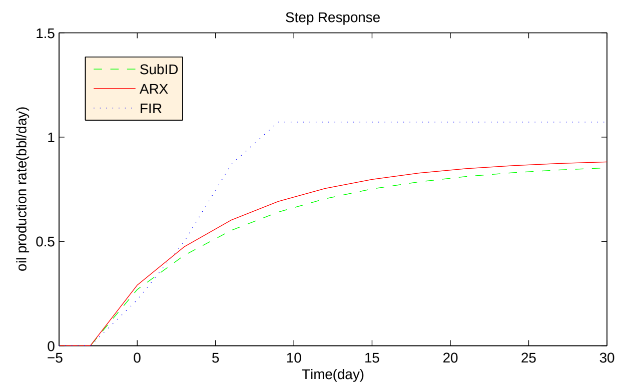

(b) Transient Response of Identified Models

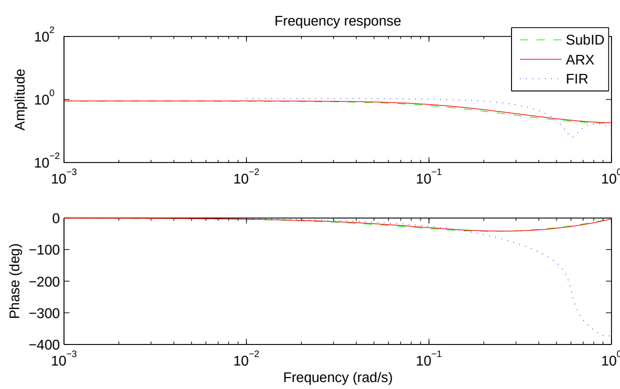

(c) Bode Diagram of Identified Models

Figure 5-6: Model Identification of Homogeneous 2D Reservoir with 2nd Set of RBS Input Signal (excluding the transition period)

5-2-4 Discussion of Results

Although increasing the model order in FIR structure increases the fit of the output, order selection is indeed limited by the number of samples in the dataset. A FIR model of order n without noise model can be presented by:

$$y(k) = a_1 u(k) + a_2 u(k-1) + \ldots + a_n u(k-n+1) \quad (5\text{-}1)$$

Here it should be noted that the values of $y(0)$ to $y(n-1)$ is inevitably fixed to be equal to the available output values measured from the system (i.e. the initial condition), and the parameters a_1 to a_n are estimated based on the data from n to N. On the other hand, the maximum number of parameters that can be identified from a certain dataset cannot exceed the number of the samples. Therefore the FIR model order is limited due to the length of the dataset.

In the identification toolbox, for SubID model structure, the initial states of the system are estimated as an extra set of parameters. For polynomial models, there is no such thing as initial states, and therefore it is not estimated. In these structures, depending on the model order, the required initial output values are taken from the available measured outputs. To be able to calculate the values of the states, we need to design an observer for the model. However, a property can be assigned to the models before identification to estimate the initial values to improve the simulation fit.

According to the Figures 5-5 and 5-6, it can be seen that the models show better behavior when the first input signal is applied. The unexpectedly low accurate results from the second input signal can be explained by the problem that is caused by numerical issues. Resampling the data by factor 12 corrupts the data set, as it gives negative values for the inputs. Moreover, using the function `resample` on a non-zero mean data-set causes an odd pattern specially in the first few samples. Identifying a model based on the negative measurements for injection rates may not be realistic. Therefore, the estimated parameters might be significantly misleading. As it can also be seen in Figure 5-6, we have better simulation fit as the time passes. This issue can be investigated by identifying new models with the same data set, but after removing the mean of the signal. Figure 5-7 shows the simulated output from the models with the same orders as before, and it can be seen that fits have significantly improved. Identification using this dataset has a drawback, which is shown in Figure 5-8. This plot presents the same models that have been validated by the same dataset with nonzero mean, i.e. the level of the measured input values are real. Here we can see that the simulated output from these models are following the pattern, but in a wrong level.

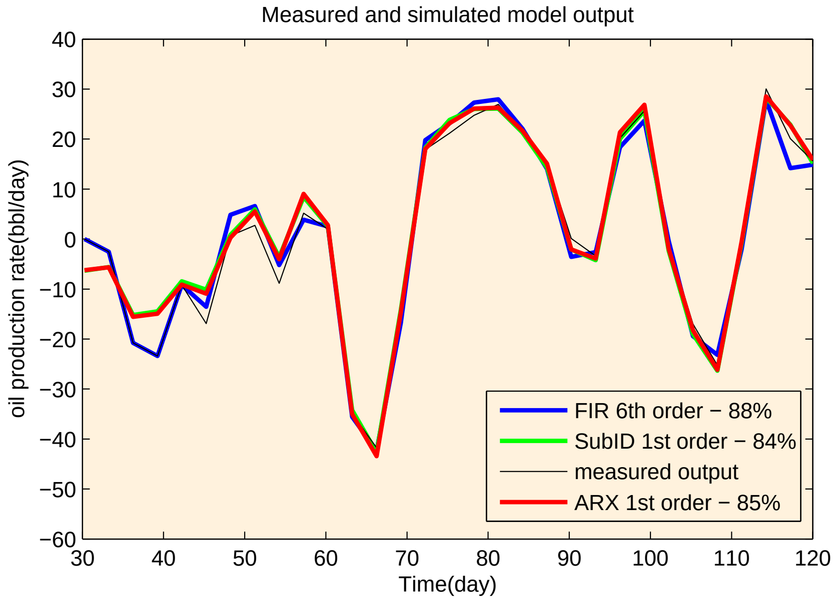

Figure 5-7: Simulation Fit of Identified Models from the 2nd Set of RBS Signal After Removing the Mean, in Homogeneous 2D Reservoir

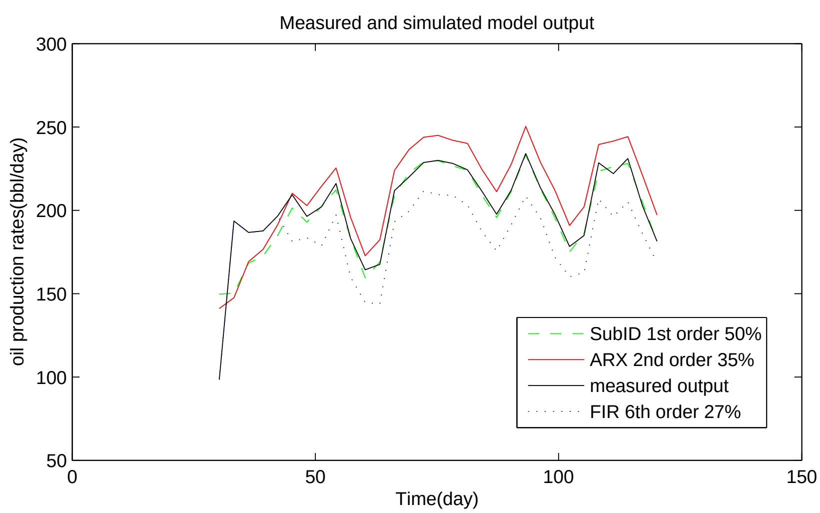

Figure 5-8: Validation of the Identified Models from the 2nd Set of RBS Signal After Removing the Mean, with the Same Data Set Before Removing the Mean, in Homogeneous 2D Reservoir

5-3 2D Heterogeneous Reservoir

We have seen in the previous section that the identified models of homogeneous reservoir had reasonably accurate simulations. In this section we would like to investigate the effect of adding more complexities on the quality of these models. To this end, as it is presented in Figure 5-9, we added two more-permeable streak line to the 2D reservoir.

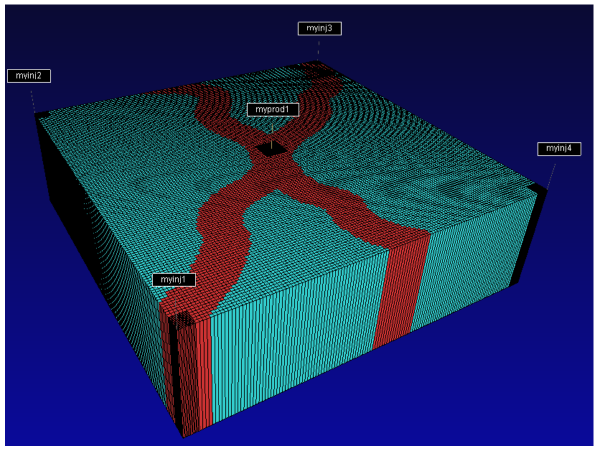

Figure 5-9: 5-spot Heterogeneous 2D Reservoir

5-3-1 Step Response Analysis

The response from the second injector 2 that is located in the less permeable area is slower than the response from the injector 1, as they are depicted in Figure 5-10(b). This means that the length of the experiment must be determined based on the time constant of the injector 2 and producer. Also, the pattern of this response suggests a higher order dynamics for the models. It should be noted that due to the symmetry of the reservoir, the step responses from 3rd and 4th injectors are not presented here.

Figure 5-11 shows another step response with a higher level of injection. Here it can be seen that although the pattern of the first injector has remained the same, the second injector's step response has changed. This means that the dynamics is no longer linear with higher injection level (whether it is because of numerical difficulties in the simulator or not). For this reason, the amplitude of injection rates are kept less than $500BBL/day$.

5-3-2 Model Identification

Considering the information gathered from the step responses, the applied input signal is presented in Figure 5-12. Length of the input must be around 70 days, and as it can be seen it contains a 10 day constant injection phase in order to bring the reservoir to a new condition. Data set is then resampled by the factor 4, since the sampling time of the identified models decided to be equal to 1.

The simulation fit of the FIR model is shown in Figure 5-13 and is validated against a $3rd$ order SubID model. The order of the models from the injectors 2 and 4 are larger than

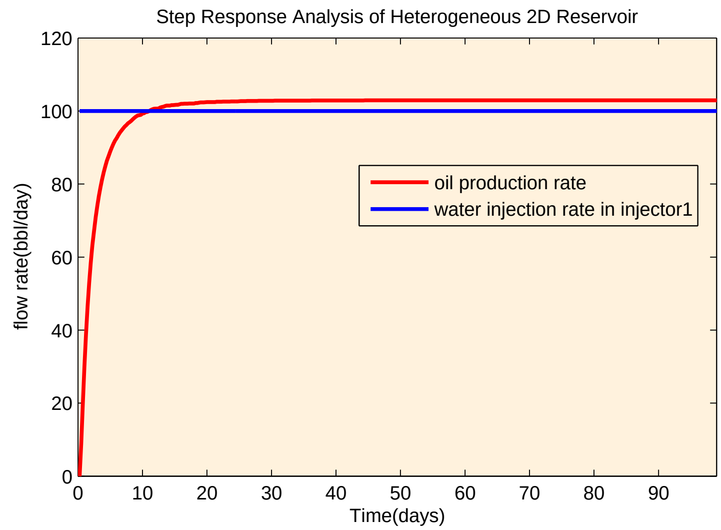

(a) Step Response of Injector1, $100 bbl/day$ injection

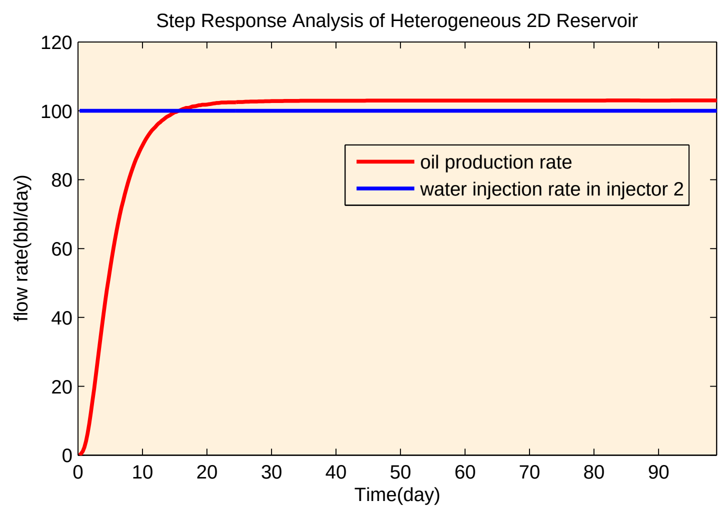

(b) Step Response of Injector2, $100 bbl/day$ injection

Figure 5-10: Step Response Analysis of Heterogeneous 2D Reservoir

injectors 1 and 3. In this section we also present the prediction quality of the two identified models in Figure 5-14. This Figure shows 10 step ahead predictions of the FIR and SubID from the last 10 samples of the same RBS signal.

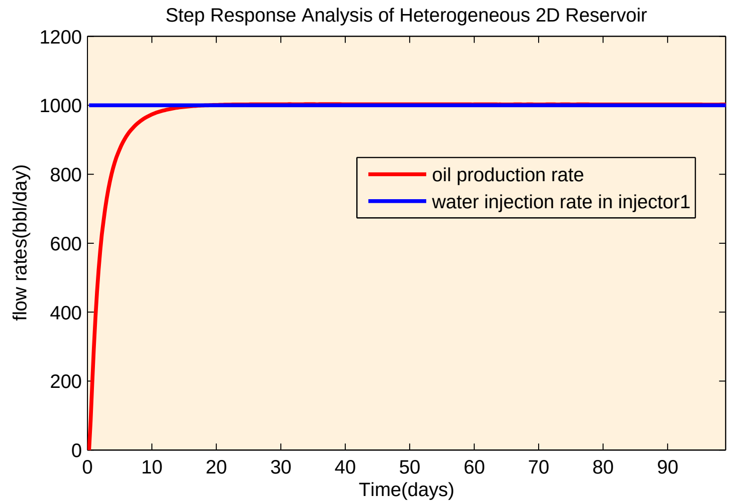

(a) Step Response of Injector1, $1000bbl/day$ injection

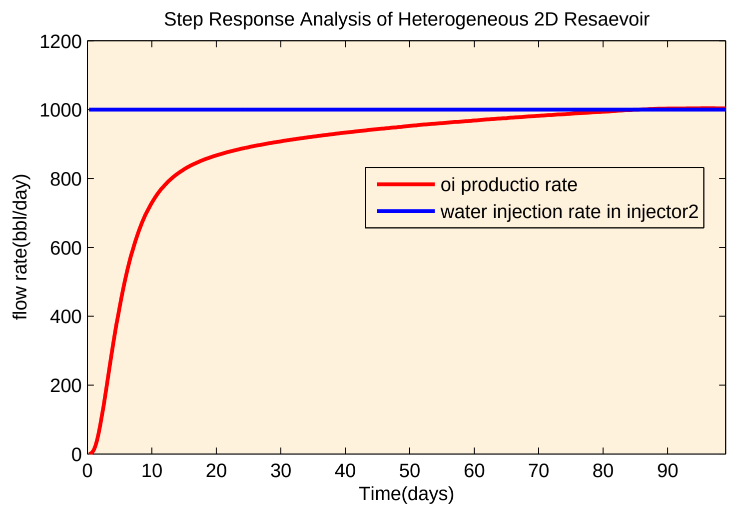

(b) Step Response of Injector2, $1000bbl/day$ injection

Figure 5-11: Step Response Analysis of Heterogeneous 2D Reservoir, Higher Injection Rates

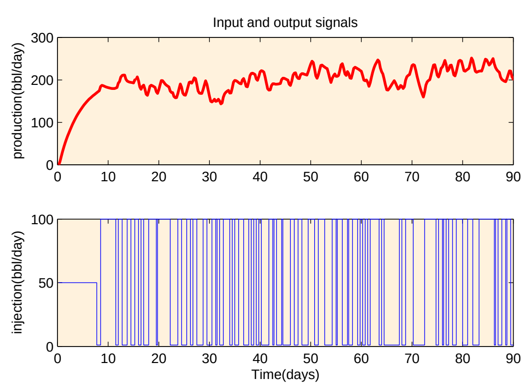

Figure 5-12: RBS Input Signal Applied on Heterogeneous 2D Reservoir

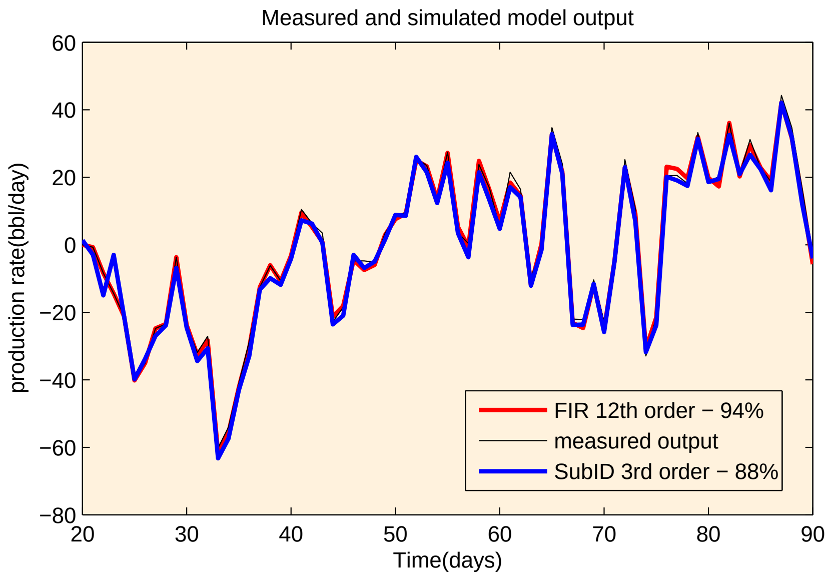

Figure 5-13: Model Identification of Heterogeneous 2D Reservoir

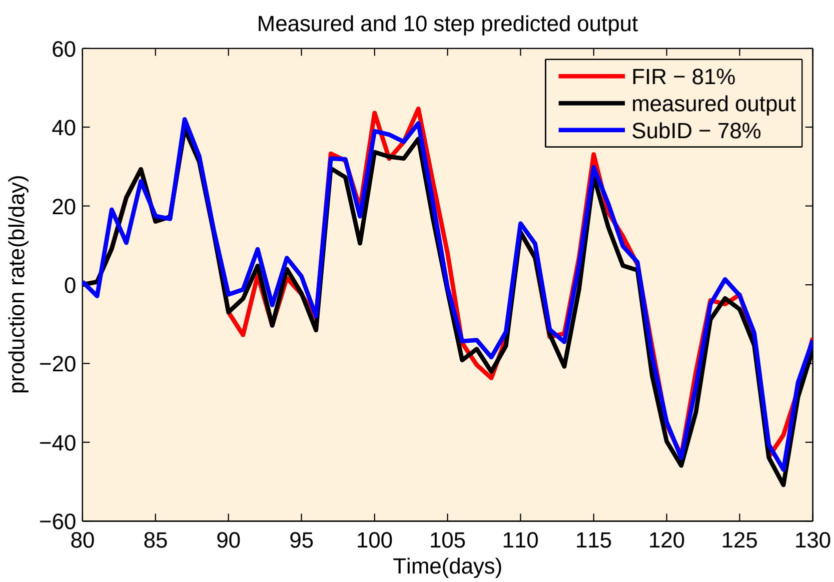

Figure 5-14: Prediction Quality of the Identified Models of Heterogeneous 2D Reservoir (10 step ahead prediction)

5-4 3D Heterogeneous Reservoir

The previous two models are assumed to be 2 dimensional and without an initial condition. In this section, we are going to study the same 5 spot reservoir but with three unlike layers of rock permeability that are intended to add more complexity to the reservoir dynamics. Figure 5-15 shows the model schematics, and permeability pattern of each layer.

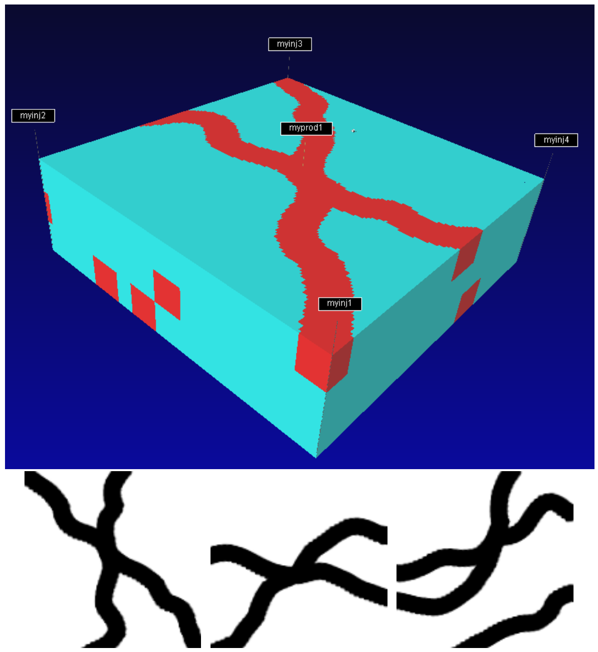

Figure 5-15: 5-spot Heterogeneous 3D Reservoir, with 3 Layers of Different Permeability Map

5-4-1 Step Response Analysis

As we mentioned before, the reservoir does not have an initial condition. This means that we expect to have an instant overshoot in the production well in the beginning. For this reason, we may choose a certain working point, somewhere around 25 days after the injection begins. Figure 5-16 shows the step responses from 1st and 2nd injection wells.

Firstly, it can be seen that there is not much of a difference between the dynamics of various input-output pairs. Secondly, the observed information gathered from this analysis show that the reservoir dynamics are almost the same as the 2D model, except for the linearity range of the system that may affect the signal amplitudes. The input signal for the identification is presented in Figure 5-17 that has the same amplitude as the step experiment.

5-4-2 Model Identification

Figure 5-18 shows the identified models that have the same orders as the "2D Heterogeneous Reservoir", with the more or less the same simulation fit. An important conclusion that can be drawn is that the added complexity in the 3D model does not necessarily increase the order of the linear identified transfer functions, or at least it does not influence the simulation fit.

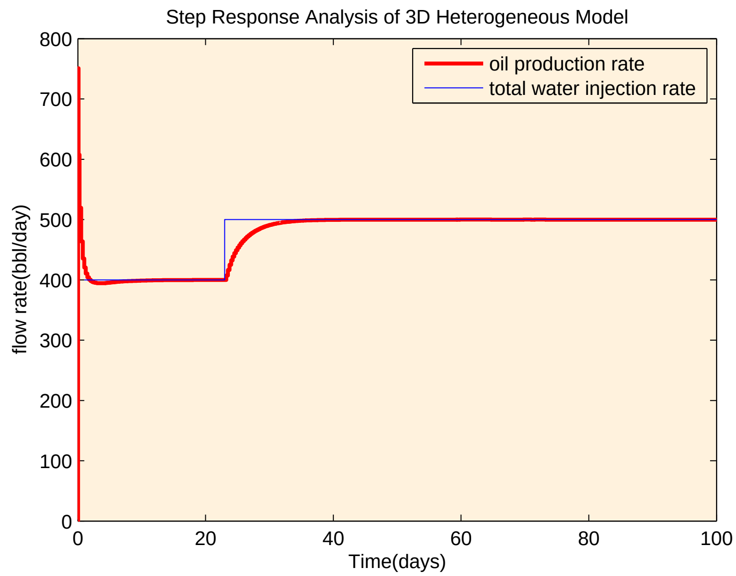

(a) Step Response of Injector1, $100bbl/day$ injection

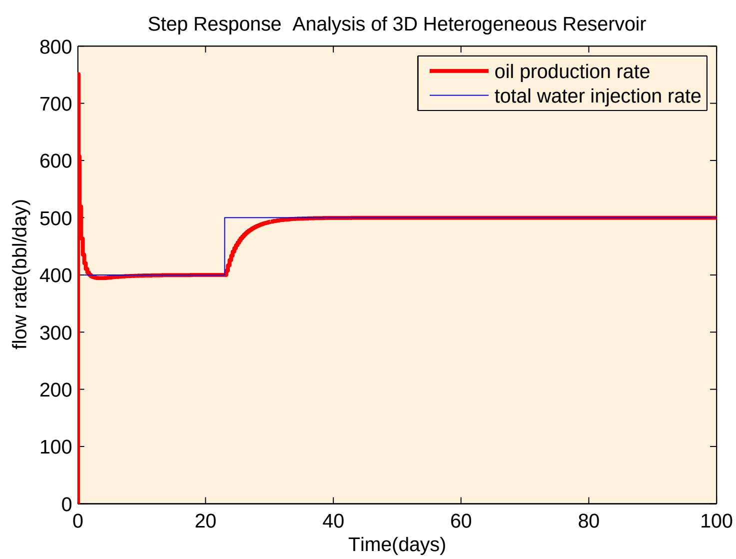

(b) Step Response of Injector2, $100bbl/day$ injection

Figure 5-16: Step Response Analysis of Heterogeneous 3D Reservoir, After 25 Days of Constant Injection Rate of $100bbl/day$ In All Injection Wells

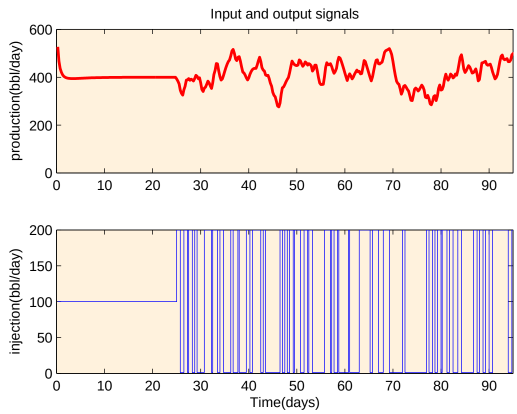

Figure 5-17: RBS Input Signal Applied on Heterogeneous 3D Reservoir

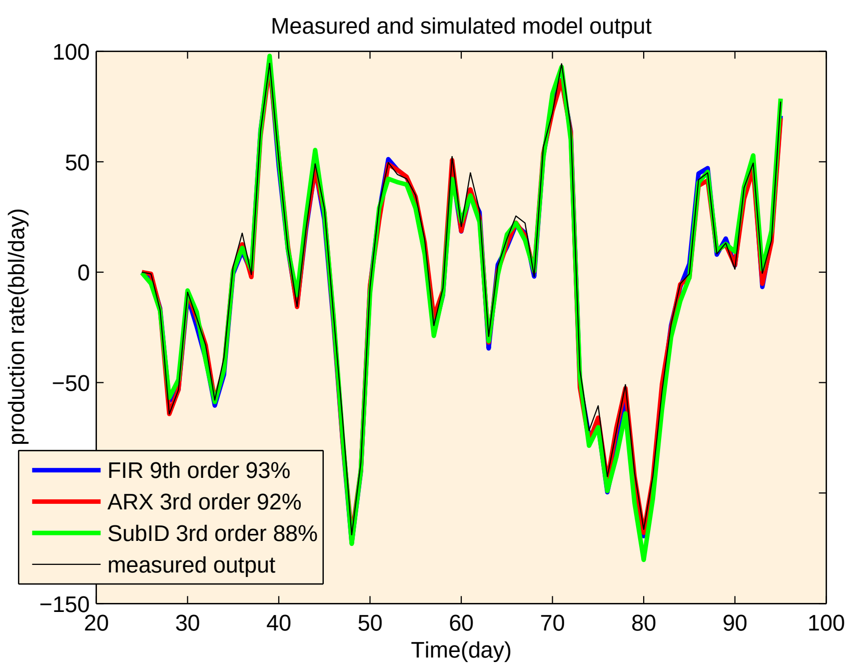

Figure 5-18: Model Identification of Heterogeneous 3D Reservoir

5-5 Reservoir with 6 Wells

The reservoir models that are investigated so far had one production well only. In this section, a 2D reservoir model has been used that has 3 injectors on one side and 3 producers on the other side, as it is depicted in Figure 5-19. This model has also an initial high pressure and thus we expect to see a high production phase in the beginning.

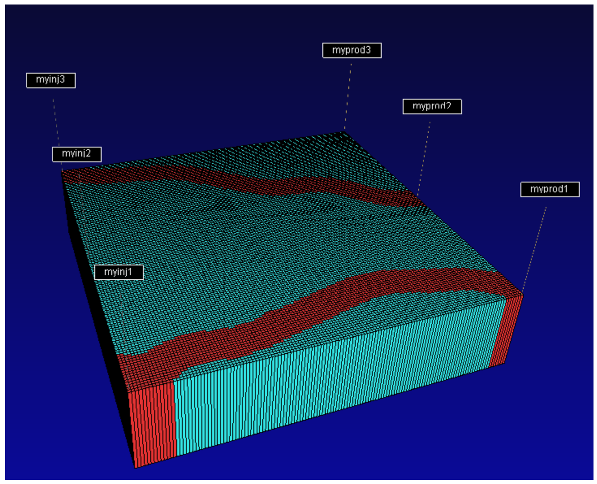

Figure 5-19: 6-Well Heterogeneous 2D Reservoir

5-5-1 Step Response Analysis

Due to the initial condition, a working point of around the day 50 is picked, after which the initial response has almost been died out. In Figure 5-20(a) the output response from the step increase of the injector1 is presented, while the injection rate in all other injectors are kept constant. The responses from the producer3 are zoomed in, since it shows less sensitivity to the inputs changes. The key issue that we should consider here is the odd behavior of the 3rd output. The step responses from the first and second inputs have undershoot and also very nonlinear patterns.

Unlike the previous models, here we can see a few samples delay from the inputs, which might be because of the certain selection of the permeability field. However, since the datasets need to be resampled, this time delay will be disappeared automatically once the resampling factor is larger than the number of the delay samples.

5-5-2 Model Identification

According to the step responses, we can see that the dynamics between different input output pairs are not quite the same. To design an appropriate input signal we should note that since we have a MIMO system , all the modes must be excited at the same time. This means that we need to apply for instance an RBS signal simultaneously in all the inputs. This way, the input signal must have a good margin to satisfy all the requirements based on the step response analysis. Therefore, the extremum values for input signal specifications will be

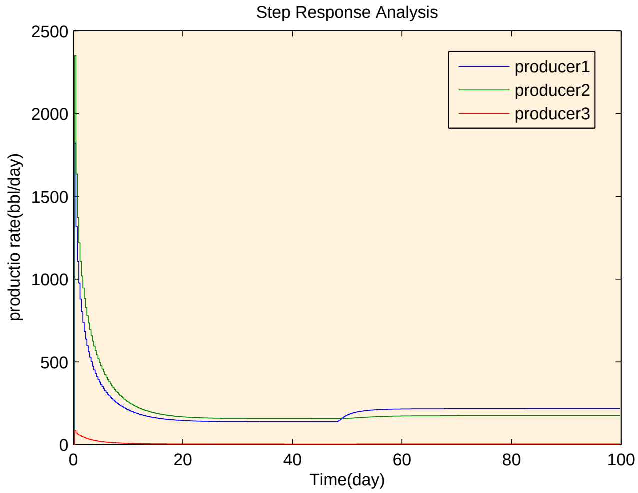

(a) 50 Days of Constant Injection $100 bbl/day$ and Step $200 bbl/day$ in MyInj1

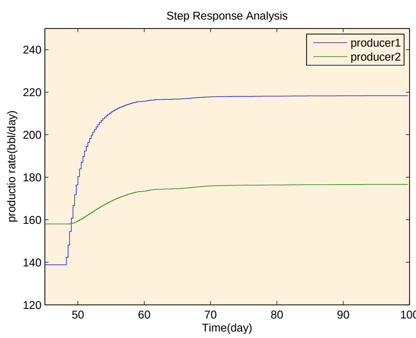

(b) Step Response, Zoomed In for Producers 1 and 2

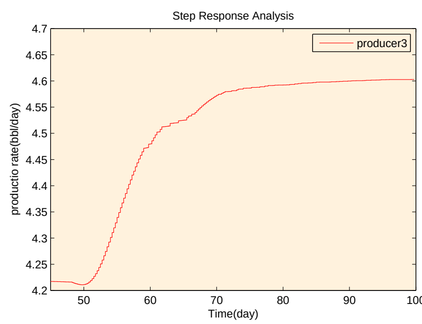

(c) Step Response, Zoomed In for Producer 3

Figure 5-20: Step Response from Injector1 Heterogeneous 2D 6-Well Reservoir

considered, e.g. the longest experiment length. In addition to that, for this model, we ran two different experiments, one with input that has the same power in whole frequency range, and one that has more power in the low frequency, as shown in Figure 5-22.

System Identification toolbox of MATLAB has some limitations for MIMO systems, e.g. the delay samples cannot be selected separately for SubID structure, or it is not possible to have uncommon poles for each input-output pair in ARX structure. Therefore it was not possible to investigate whether changing these values will improve the results or not. In the presented figures however, all the models have no sample delays although there was one sample delay between input 1 and output 3.

It was mentioned earlier that output 3 is less sensitive to the inputs, which makes it harder to identify a model between injectors 1, 2 and 3, and producer 3 with a high simulation fit. Meanwhile referring back to Figure 5-21(b) and 5-20(c) it seems that non-linearities are more pronounced for output 3. Whether this issue stems from numerical hardship in the simulator or it is like this in reality, producer 3 has the least importance among all the outputs. In other words, the role of producer 3 in system equations is not significant at all, and as it can

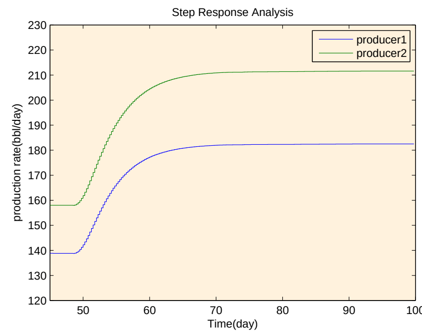

(a) Step Response, Zoomed In for Producers 1 and 2

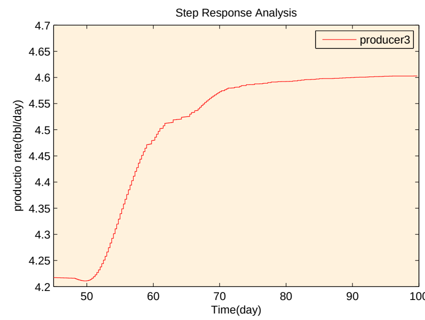

(b) Step Response, Zoomed In for Producer 3

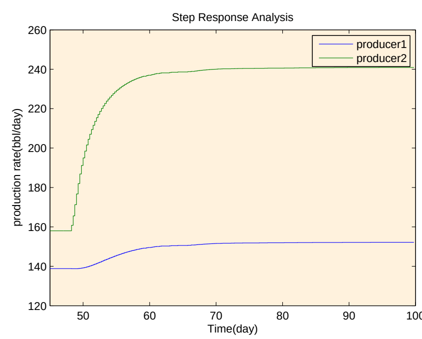

(c) Step Response, Zoomed In for Producers 1 and 2

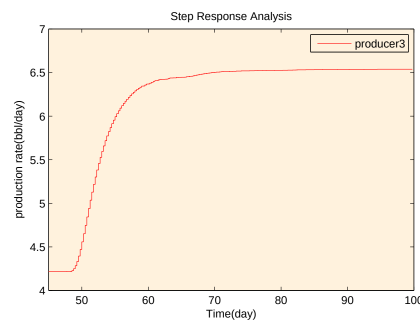

(d) Step Response, Zoomed In for Producer 3

Figure 5-21: 50 Days of Constant Injection $100bbl/day$ and Step $200bbl/day$ in Injector2 5-21(a) & 5-21(b) and in Injector3 5-21(c) & 5-21(d), Heterogeneous 2D 6-Well Reservoir

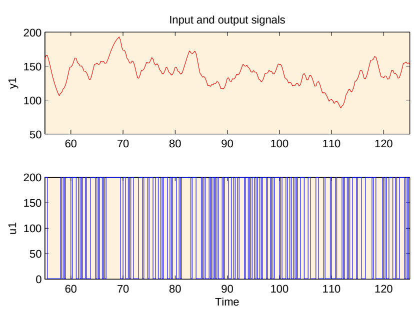

(a) Full Range RBS Signal

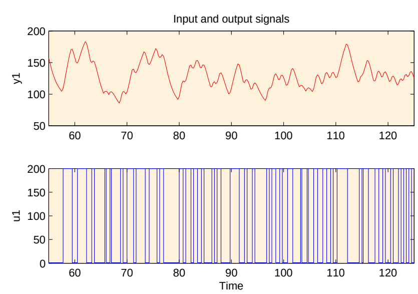

(b) Half Range RBS Signal

Figure 5-22: Input Signal Used in Heterogeneous 2D 6-Well Reservoir

be seen the absolute error we get from the identified model is very small in compare to the relative error. This can be seen from the range of the output values in output 3 in compare to output 1 and 2 in Figure 5-23.

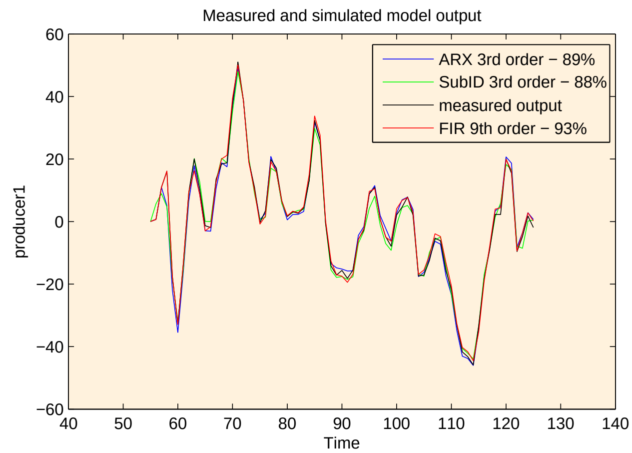

(a) Simulation fit of producer1

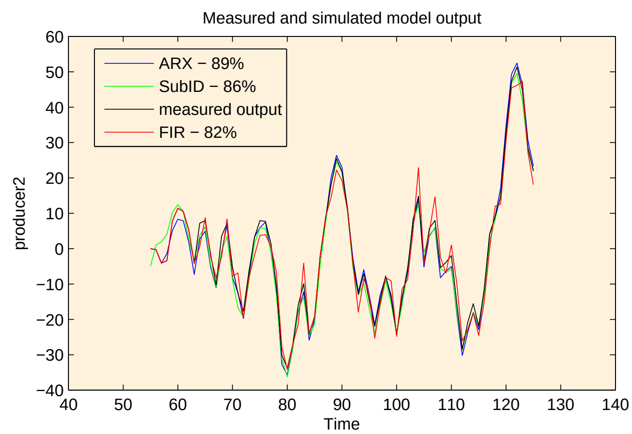

(b) Simulation fit of producer2

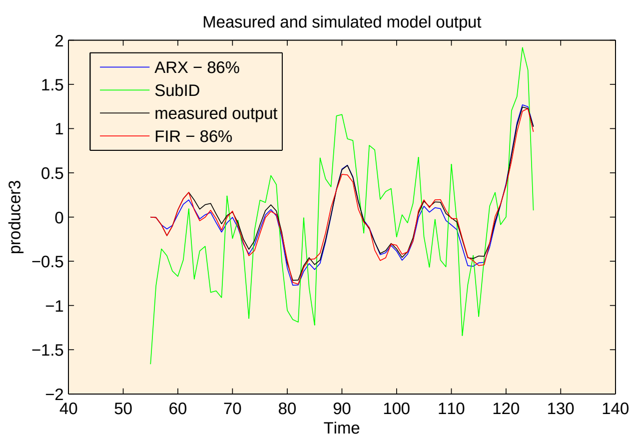

(c) Simulation fit of producer3

Figure 5-23: Simulation Fit With Full Range RBS Signals, in Heterogeneous 2D 6-Well Reservoir

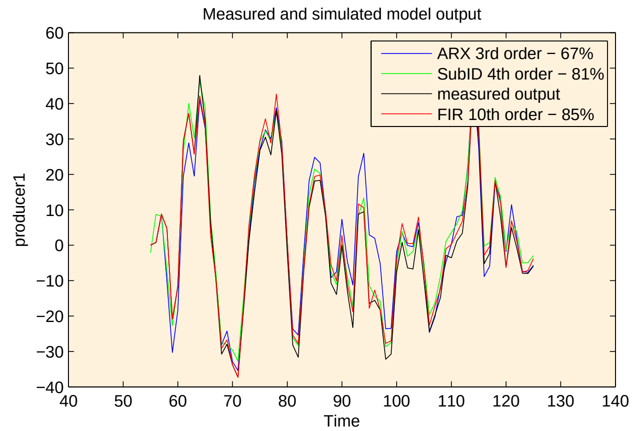

(a) Simulation fit of producer1

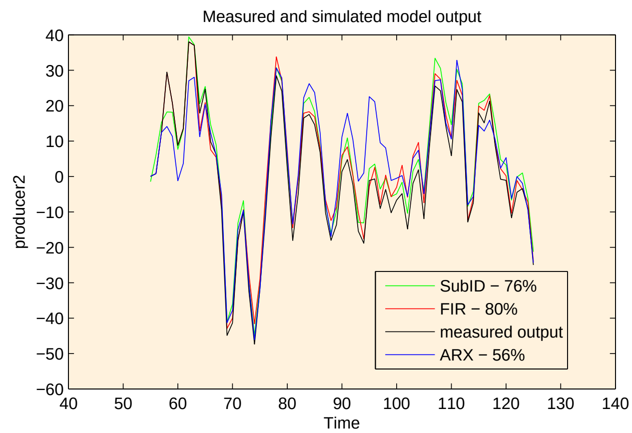

(b) Simulation fit of producer2

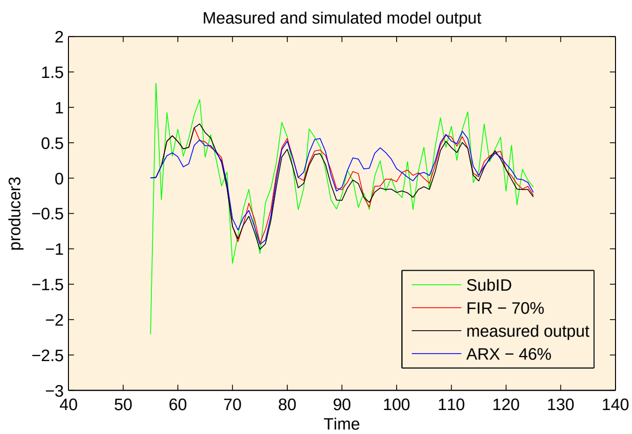

(c) Simulation fit of producer3

Figure 5-24: Simulation Fit With Half Range RBS Signal, in Heterogeneous 2D 6-Well Reservoir

5-6 VanEssen Reservoir Model

5-6-1 Introduction

The final model that we have investigated is a 3D multi layer reservoir, consists of multiple injectors and producers, shown in Figure 5-25. There are 8 injectors and 4 producers, all across the field. In addition there are two permeable streak lines, in which most of the producers are located. Although this field has been synthesized, it is a good example of reality, where we have an uncommon field shape, and well locations are not equally distant. In the mean time, it should be noted that still such a well configuration can be seen as a combination of several five spot models. Moreover, in this model a new set of inputs have been added that have different physical meanings than the injection rates. The production rate of each producer can be manipulated directly by changing BHP [3].

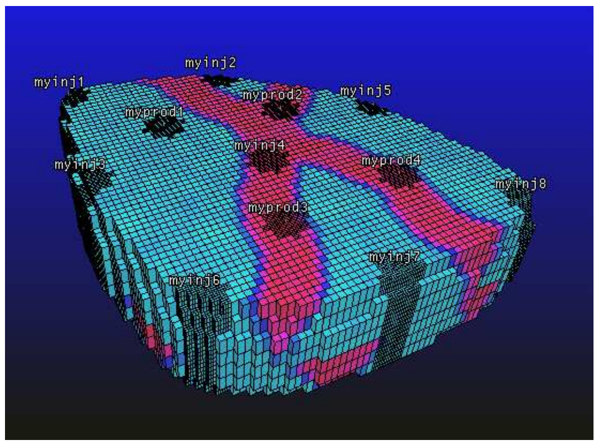

Figure 5-25: 8 Injectors 4 Producer Oil Field of VanEssen Reservoir Model

5-6-2 Model Dynamics

Analyzing all the input output pairs one by one seems almost impossible, since we have 12 inputs and 4 outputs and each test takes quite a lot of time. Alternatively we can select some pairs and assume to have almost similar properties in the vicinity of the neighboring wells. Injector 3 and producer 1, located in the less permeable area and injector 4 and producer 3, located in the more permeable area are selected for the step response analysis. Since the response from changing BHP to the the neighboring producers are almost the same in all the producers, we only present the step response analysis of BHP of the producer1. Figure 5-26 and 5-27 present the steps responses respectively.

We have selected two step amplitude for the injector3 (from 500 to 1000 BBL/day), and for the injector4 (from 500 to 800BBL/day), in order to realize the linearity range as well. Producer1 shows less sensitivity to the injection, perhaps because it is located in a less permeable area. Moreover, in compare to the previous models, we have much slower responses here that may

[3]It must be noted that BHP cannot be changed directly, but instead the desired BHP can be reached by manipulating the valve/choke settings on top of the well.

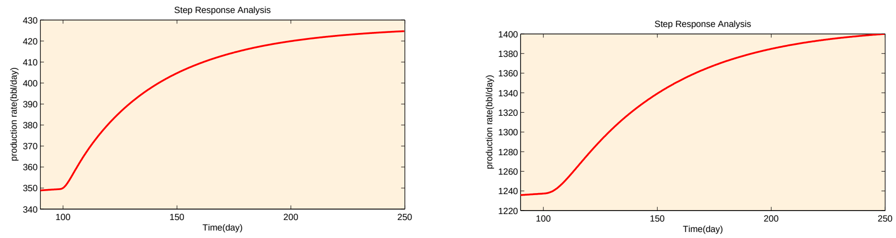

(a) Step Response from Injector3, $500bbl/day$ increase injection, to producer1

(b) Step Response from Injector3, $500bbl/day$ increase injection, to producer3

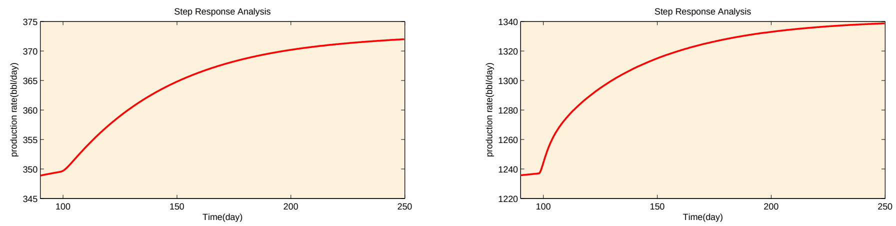

(c) Step Response from Injector4, $300bbl/day$ increase injection, to producer1

(d) Step Response from Injector4, $300bbl/day$ increase injection, to producer3

Figure 5-26: Step Responses From Injectors 3 & 4 to Producers 1 & 3, In VanEssen Reservoir Model

imply longer experiments are needed. However, we will see in the following section that even with data length of five times of the time constant, we can identify reasonably accurate models.

According to Figure 5-27, it can be inferred that decreasing the BHP in producer 1, increases the production rate in the same producer, while it causes less production in other producers. The sudden change of the pressure immediately influences the production rate and as the time goes by, this rate settles down to a new level. In fact this pattern consists of a static (i.e. sudden increase or decrease) and a dynamic (i.e. gradually settling) responses. Since other producers are located in the permeable streaks, we expect a faster response from changes in BHP in other wells.

5-6-3 Model Identification

Since the responses from the two different inputs have different properties, designing an input signal becomes more difficult. Small changes in the BHP cause rapid and magnified changes in the outputs, meanwhile responses from the injection rates cannot be distinguished in the outputs if they are applied in the same time. Figure 5-28(a) shows the production rates in producer1, when only RBS-like BHP with amplitude of $0.2bar$ is applied, and Figure 5-28(b) shows production rates of the same producer, with changes only in the injection rate of amplitude $300bbl/day$. The output from both inputs that are applied simultaneously is shown in Figure 5-28(c), where we can see that BHP response has dominated the injection rate response. Therefore, to have a more detectable output, another set of data is also used in which the amplitude of BHP has been reduced to $0.05bar$ as shown in Figure 5-29.

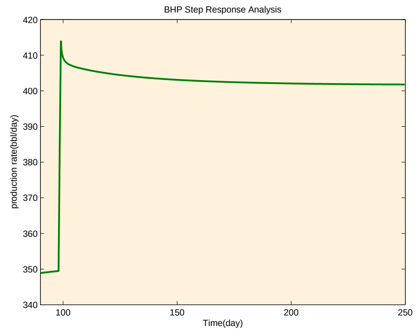

(a) Step Response from BHP of producer1, 1bar increase pressure, to producer1

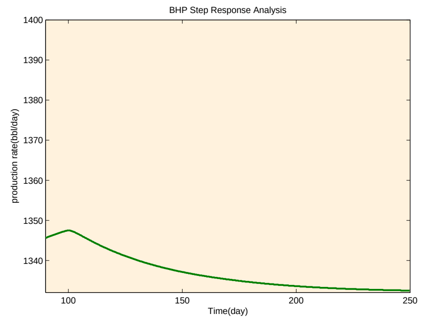

(b) Step Response from BHP of producer1, 1bar increase pressure, to producer2

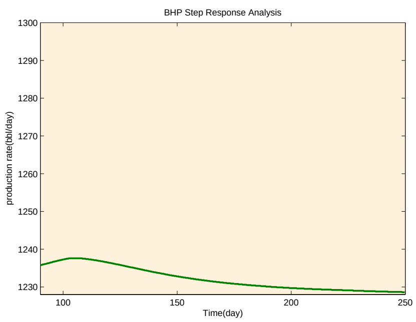

(c) Step Response from BHP of producer1, 1bar increase pressure, to producer3

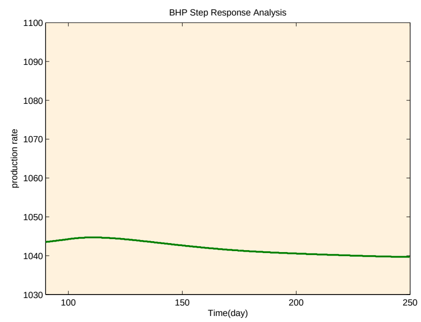

(d) Step Response from BHP of producer1, 1bar increase pressure, to producer4

Figure 5-27: Step Responses From BHP Decrease In Producer1, in VanEssen Reservoir Model

According to Figure 5-30 that presents the simulation fit of the identified models, it can be seen that although the the fits are quite high with either inputs, they are slightly higher when BHP amplitude is higher, which implies that more accurate linear transfer functions can be identified when BHP is more dominant. It was mentioned before that according to the step response analysis, it can be inferred that the response from BHP has faster dynamics and the outputs are more sensitive to the BHP changes rather than to the injection rates and production rates. In this respect, it could be possible that the preprocessing of the dataset corrupts its information in favor of a certain group of the inputs. Moreover, order of the FIR and ARX models that are presented in the figures are limited by computational burden of the PC[4] that has been used. Identifying higher order models were possible, but unfortunately covariance computation of the simulation was ended up with software crash.

5-7 Chapter Conclusion

System identification procedure has been applied to 5 different synthetic reservoirs. The choice of these models has been motivated in the introduction section of this chapter. Model identification of each reservoir model has been preceded by running a number of experiments such as step response analysis and staircase experiment. Obtainable knowledge from the step

[4]Intel Core 2 Duo CPU T7500 @2.20 GHz, 3GB Memory

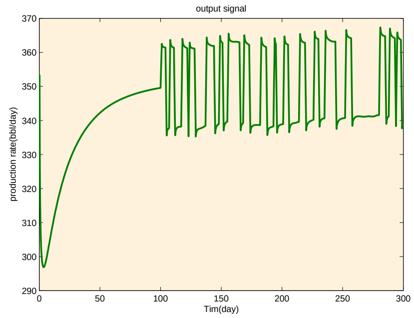

(a) RBS signal on BHP of Amplitude $0.2bar$ in Producer1

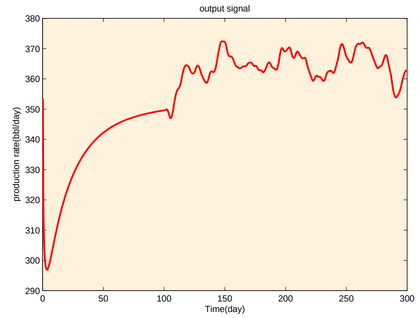

(b) RBS signal on injectors of Amplitude $300bbl/day$ in Producer1

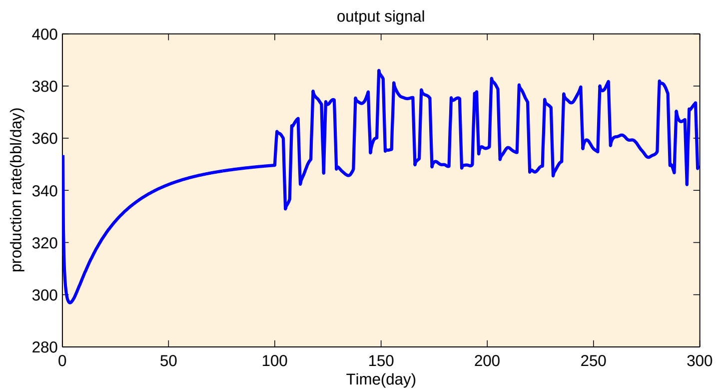

(c) RBS signal on All Inputs in Producer1

Figure 5-28: RBS Signal, with $0.2bar$ Amplitude for BHP, Applied on VanEssen Reservoir Model

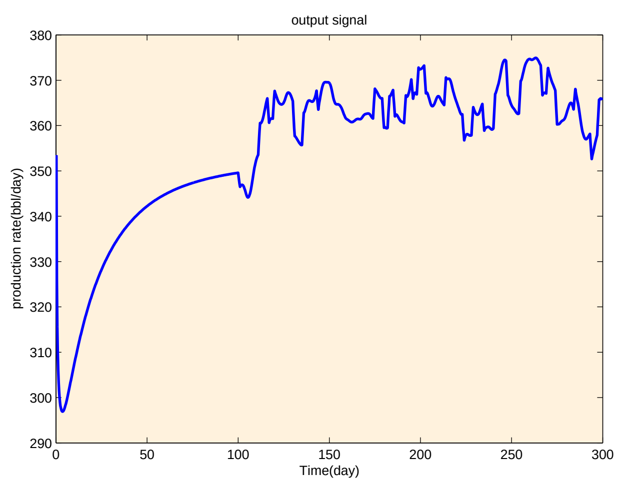

Figure 5-29: RBS Signal, with $0.05bar$ Amplitude for BHP, Applied on VanEssen Reservoir Model

response analysis shows that with an appropriate design of the input signal, identification can be done in a few steps with an acceptable accuracy. However, according to slow changes of the dynamics in the models that we studied, it is not necessary to repeat the step analysis very often. The of the step response must be decided based on the type of the reservoir and the identification purpose.

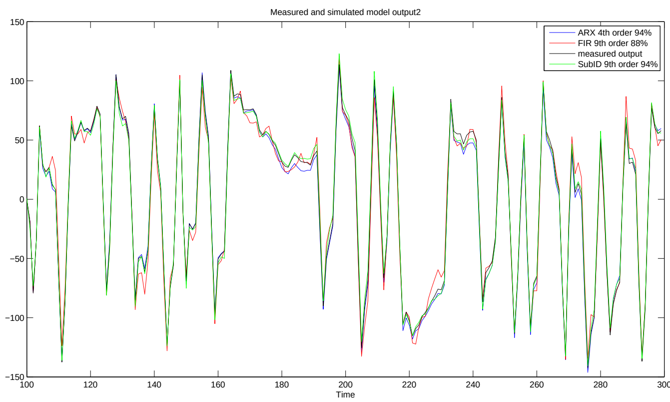

(a) Simulation Fit with BHP Amplitude of $0.2bar$

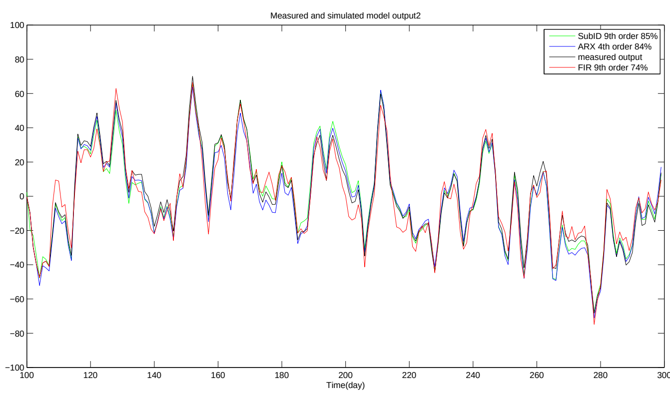

(b) Simulation Fit with BHP Amplitude of $0.05bar$

Figure 5-30: Simulation Fit with Two Sets of Data with Different BHP Amplitude, in VanEssen Reservoir Model

Model structures that are used in this chapter were all linear with limited order. Although the simulation fit and prediction quality were acceptable, unfortunately these models could only be validated against the simulator measurements and also against each other. Moreover, we noticed that in order to identify a reasonably accurate model with high simulation fit for more complex reservoir models, it is not necessary to choose higher order transfer functions. Adding several layers of rock and having different rock properties across the field only causes the simulator to run more slowly. In fact it is possible to reach the same level of accuracy if the identification is done attentively. Therefore it can be concluded that the important dynamics of the system lies in a lower dimension space than what it is expected in the reality.

There are of course a lot more issues to investigate pertaining to model identification, which may cause strategic differences to the final project goal. For instance here we only used RBS like input signals for injection rates to excite the system, while the optimal input signal may not have that much freedom, or may not be even feasible at all due to the production limitations. Therefore the input design must be investigated more thoroughly when the optimal inputs are fixed.

Another troublesome issue is due to the limitations of the available software packages for the MIMO system identification. MATLAB toolbox of System Identification has indeed some limitations when MIMO datasets are used, in terms of model structure selection and their properties. For instance it is not possible to identify a model in OE, ARMAX or BJ structure directly, nor it is possible to have uncommon poles for each input-output pair in ARX structure. Therefore, an exclusive software development might be considered when the number of the inputs and outputs are increased.

Additionally, the benefits of using different inputs, e.g. injection rates, manipulating valve openness and BHP, must be evaluated in terms of controllability and tracking trajectories. The identified models in this chapter had injection rates and BHP as the inputs and production rates as the outputs, while it must be investigated whether using valve openness as the inputs, or having cumulative production rates as the outputs will influence the model accuracy or not.

The working point around which a model is identified is very important, e.g. all the above analysis has been done before the water break through, where the fluid flow in the production wells have only the oil phase. As soon as water front reaches the producers, nonlinearity effects caused by the relative permeability will rise up, and makes it harder to approximate the system with linear models. Therefore, the difficulties pertaining to the different working points are as important as adding more complexities to the models. This specific issue, as well as other issues that have been mentioned previously, are very important and can be further investigated, preferably in a situation that the model is used for control purposes.

Chapter 6

Waterflooding Using Model Predictive Control

6-1 Introduction

The focus of Chapter 5 was basically on the identification of the linear models of the reservoir. The issues that were not treated in the previous chapter, such as identification around various working points or the limitations of the input signal, as well as implementation of the MPC controller will be treated. In MPC design about 80% of the job is to find a proper model, and therefore system identification will be the focus of this chapter too. However, here it will be easier to validate and compare the results, since the quality of the models can be evaluated according to the MPC performance.

The benefits of implementing MPC will be compared only with the open loop control of the waterflooding. It means that optimal trajectories are primarily introduced for the whole life of the reservoir, and then the total reachable Net Present Value (NPV) from the oil production with and without using MPC are calculated, using the simulator. For more detailed information about the methodology please refer to Chapter 2.

The experimental reservoir models that are used in this chapter are, a 2D homogeneous 5-spot reservoir because of its extreme simplicity, and a 3D heterogeneous reservoir of VanEssen model, that has more complex structure.

6-2 2D Homogeneous Reservoir

The model is the same as the one that was used in Chapter 5, except that it has 4 producers in the corners and only one injector in the middle. In addition to that, unlike the previous chapter, the BHP in each producer can be manipulated, i.e. there are 5 inputs and 4 outputs. This model contains $18,225$ grid blocks of dimension $3m \times 3m \times 90m$ in only one layer.

Symbol	Value	Unit
ϕ	0.20	$[-]$
$\rho_o(400bar)$	800	$[kg/m^3]$
$\rho_w(400bar)$	1000	$[kg/m^3]$
c_o	15×10^{-5}	$[1/bar]$
c_w	4×10^{-5}	$[1/bar]$
μ_o	4×10^{-3}	$[Pa.s]$
μ_w	10^{-3}	$[Pa.s]$
p_{bh}^j	$300 - 550$	$[bar]$
$\bar{P}_0$	400	$[bar]$
$\bar{S}_0$	$0.1, \cdots, 0.1$	$[-]$

Table 6-1: Values of Geological and Fluid Properties in Inverted 5-Spot Reservoir Model

The rock permeability is constant and equal to $300mDarcy$, an other geological and fluid properties are given in Table 6-1.

Assuming the reservoir life of 2500 days, the optimal input strategy can be obtained through a gradient based optimization procedure, introduced in [Brouwer and Jansen, 2004]. In this algorithm, the oil price is fixed on $9\$/BBL$ and the separation of oil and water costs $1\$/BBL$, while it is assumed that injection water does not cost at all. The input scheme seems trivial since the configuration has a perfect symmetry, and of course they will be all constant up until the end of the life. It must be reminded that the objective function of this optimization is the maximization of NPV, which means that the production continues until it is profitable to produce oil, and it does not necessarily imply the maximum recovery factor. For this model however, the discounting factor is selected to be zero, which means that the amount of recovered oil is maximized. The end of the production life is then determined by reaching to a certain time when the water-cut in the producers exceeds a certain value.

Figure 6-1 presents oil and water production rates of homogeneous reservoir during its life, which are also the reference trajectories that must be followed. A constant injection rate of $5329BBL/day$ is applied while all the BHP are kept constant and equal to $395bar$. Simulation sampling time is 1 day which will also be the sampling time of collecting the data. It is expected to have a profit of $79.6Million\$$ by the end of this period. Water front reaches the producers after 1500 days, and according to the figure around day 2500 water cut hits 90% during which all wells will be shut down.

Next, this optimal inputs should be applied on the real reservoir which is expected to be different from the model that has been used for optimization (the model-model). As it was mentioned before, we can simulate the reality by using the same homogeneous model with an added permeable streak line (the real-model) as it is shown in Figure 6-2. This channel is 8 times more permeable than the rest of the reservoir.

Naturally because of the existence of such a channel, injected water tends to choose the path with the lowest resistance. As it is shown in Figure 6-3, oil production rate of producer3 increases dramatically and it decreases in other producers in the real-model. Consequently, producer3 starts producing water soon after 250 days, and in the end the amount of produced oil is indeed less than expected. By calculation, the actual profit will be $64.3Million$ which is 19% less than the expected value, *in* $2500day$ *period*.

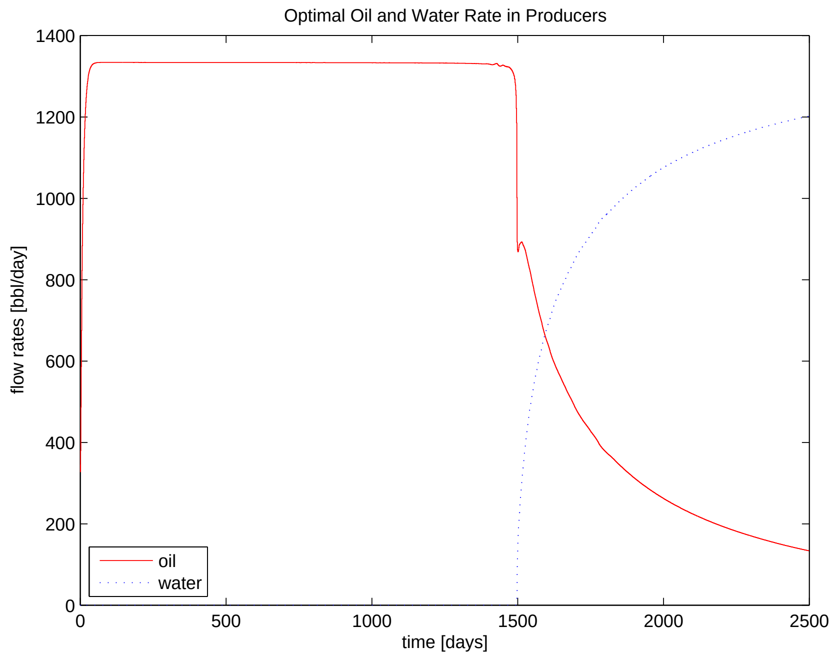

Figure 6-1: Homogeneous 2D Reservoir Model, Optimal Trajectories

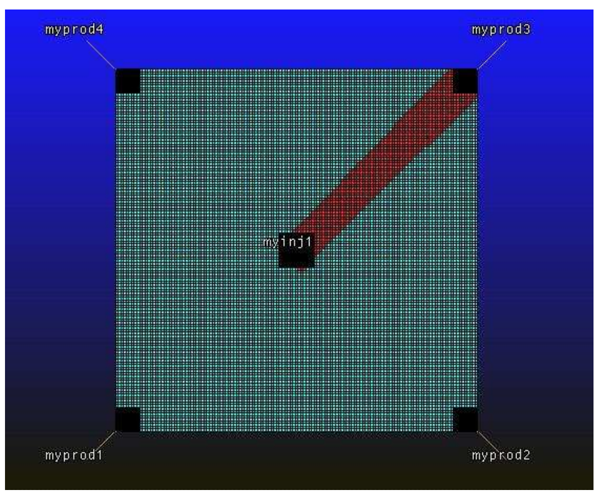

Figure 6-2: Homogeneous 2D Reservoir - Reality - Differences from Optimization Model in Shape of a Streak Permeable Channel

In the remainder of this section we will show how this profit loss can be compensated using the MPC controller. To this end a linear down scaled model must be identified first.

6-2-1 Model Identification

As the system properties are more or less the same as the one that was studied in Chapter5, the preparatory experiments are skipped in this section. Knowing the fact that the optimal

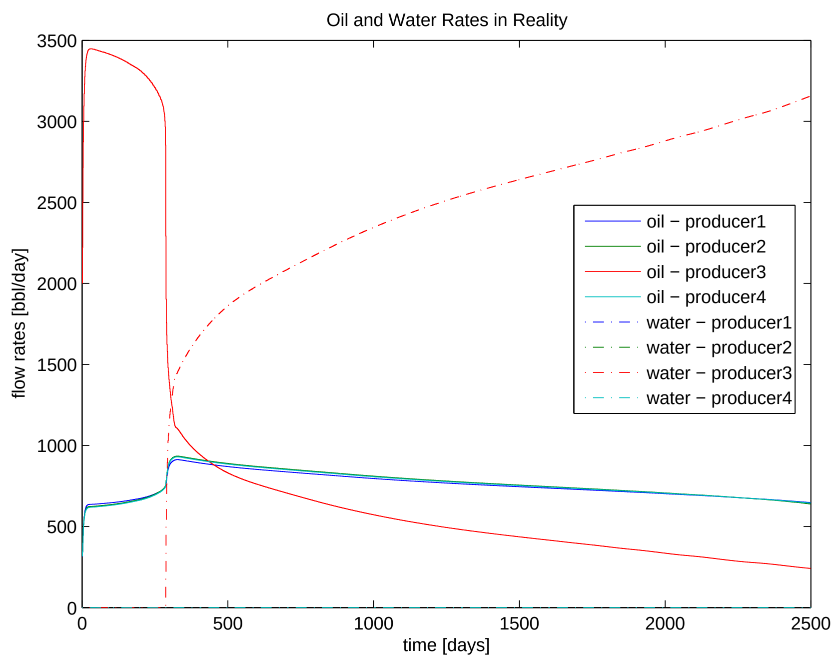

Figure 6-3: Homogeneous 2D Reservoir, Reality Production Rates

input sequence is going to be constant during the whole time, it is not expected to get any information about the system dynamics from the data set, i.e. the constant input signals are not persistently exciting at all. Therefore, some RBS-like variation must be added on top of the inputs. Additionally, the quality of the identified models will be evaluated based on their prediction quality.

-	BHP amp	BHP freq range (normalized)	Injection amp	Injection freq range (normalized)	Profit (J)
optimal	$390bar$	-	$5329bbl/day$	-	4.656x10^6
input1	[394.95 395.05]	[0 0.3]	[4829 5829]	[0 0.7]	4.651x10^6
input2	[394.9 395.1]	[0 0.3]	[4829 5829]	[0 0.7]	4.648x10^6

Table 6-2: Input Signal Specifications

Input Signal Design

Once again it must be noted that the better design of the input signal not only results in more accurate models but also saves much time. Issues like sampling time, length of experiment and frequency range of the excitations are important to notice. We assume that the optimal inputs are supposed to be applied on the system for the first $100days$, with the sampling of one day for the measurements. Also, there is no need to have excitations of high frequency, since the system is very slow (referring to the step response Figures in Chapter 5, the time constant is in order of ten days).

In this reservoir we have one input of injection rate, and four of pressure in the production wells. This means that the amplitudes must be determined in a proper way, in order not to mask each others effect. Figure 6-4 shows two types of input of length 100 days, while the first 20$days$ are kept constant to their nominal value. The input specifications are presented in Table 6-2;

From Figure 6-4(b) it is inferred that before each decrease of BHP in producer 3, the production well 3 shuts in. Since it only happens in one of the producers and during increase of BHP, it might be a numerical problem in the simulator that can be avoided. Moreover, by the end of the period 100 days, the obtained profit *"J"* is closer to the expected value in input1.

Data Pre-Processing

Input and output signals of this system have different range of values since they have different physical dimensions. Therefore, signals must be normalized such that they all have similar power before they can be used for identification, otherwise the injection rates which have higher values would have higher weighting in the prediction error criterion [Van den Hof, 2006]. It should be noted that in order to have real values of the predicted output with the identified models, the predicted output values must be *up-scaled*. Not to mention that the time unit of day is assumed to be scaled into seconds, just the same as previous chapter.

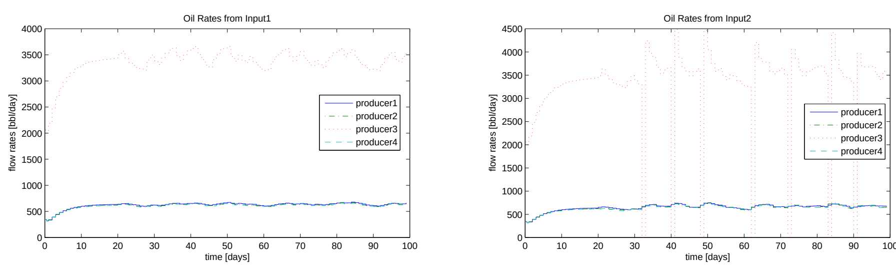

(a) Input1 (b) Input2

Figure 6-4: RBS Signal Added On Top of Optimal Inputs in 2D Homogeneous Reservoir

Figure 6-5 shows the power spectrum of the signals before and after scaling. Note that since data is not going to be resampled and there is no drift stem from the internal noise in the system, identification will be done with non-zero mean signals. Scaling factor is determined in the way that all the inputs and outputs have nominal value equal to BHP.

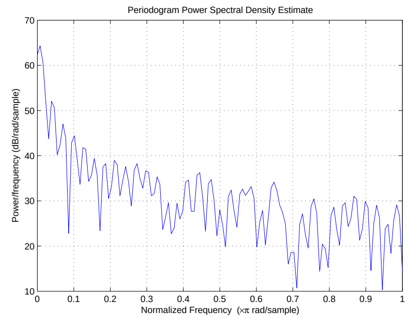

(a) Injector1 Before Scaling

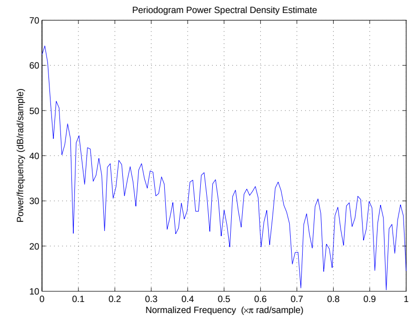

(b) Injector1 After Scaling

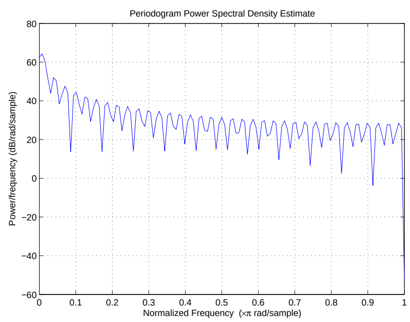

(c) BHP Before Scaling

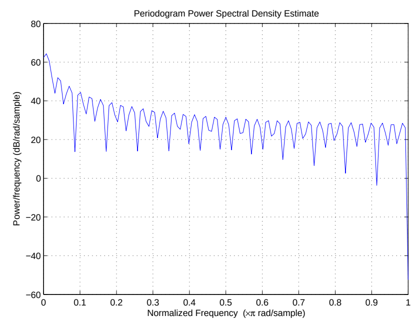

(d) BHP After Scaling

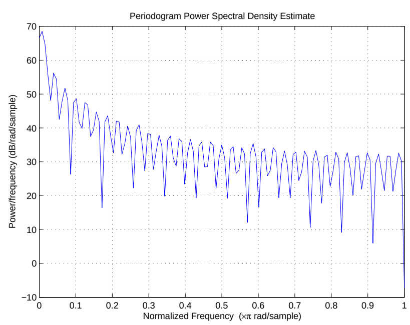

(e) Producer1, 2 and 4 Before Scaling

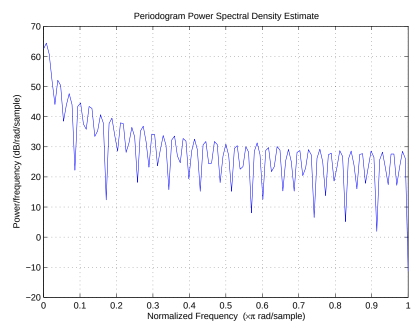

(f) Producer1, 2 and 4 After Scaling

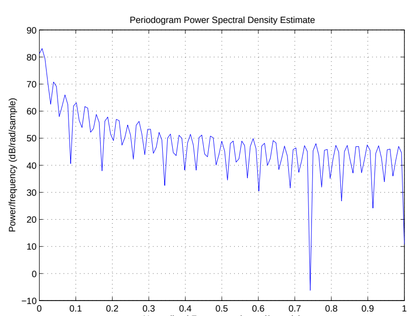

(g) Producer3 Before Scaling

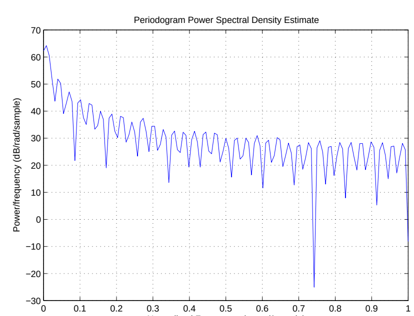

(h) Producer3 After Scaling

Figure 6-5: Power Density of Input/Output Signals Before and After Scaling in 2D Homogeneous Reservoir

Model Quality

SubID and FIR model structures are good candidates for the identifications. SubID is suitable for multivariable systems and FIR has a simple linear structure. Figure 6-6 presents the simulation fit of the two identified models. Due to the simple underlying dynamics, we can see that a very good simulation fit can be reached with low order models.

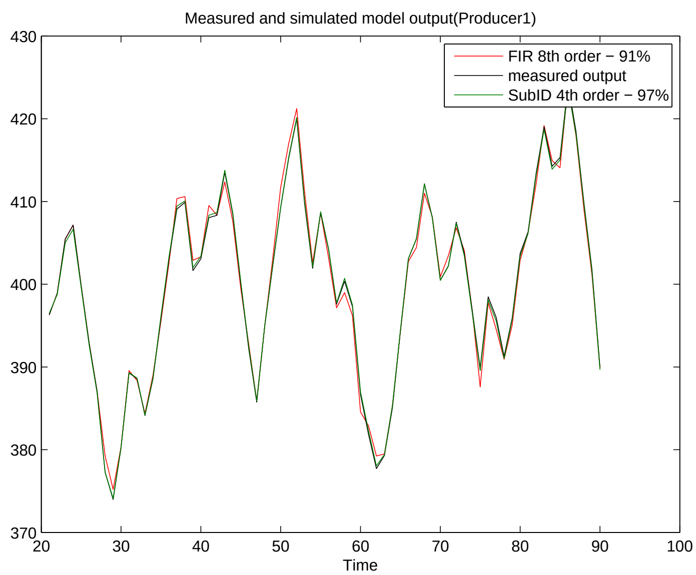

Figure 6-6: Homogeneous 2D Reservoir, Model Identification Fit

SubID model can be validated against real-model reservoir to check its prediction quality. In Figure 6-7 we present the first 200 days of production rates, in addition to the output from $4th$ order SubID model, from day 20. In the period between day 20 and 90 model output and reality measured values are very close (more than 95% fit) as it is the same period for identification. Surprisingly the model predicts accurately enough the next 100 days, that even a production rate drop in producer3 and a bit of increase in the rest of producers can be detected.

6-2-2 Model Predictive Control

The identified model can now be implemented in the MPC controller. The strategy would be to find an optimal control law for a *period of time*, that can steer the outputs to the optimal trajectories found before. Choice of this period may be analyzed under different circumstances. Regardless of time period, identification must be done with the data set most recent to the corresponding end time (i.e. working point). Here we also need to be concerned about enough excitation in the input signals.

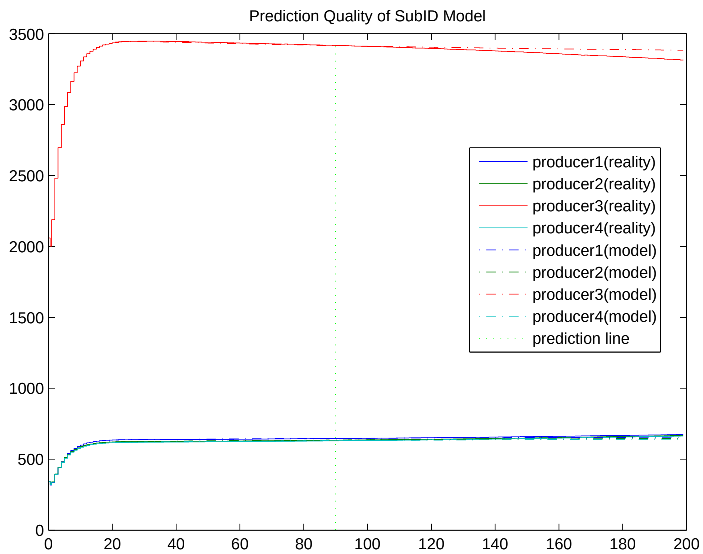

Figure 6-7: Homogeneous 2D Reservoir, SubID Model Prediction Quality

Formulation

For ease of the notation we transform both models into state space form. Then the system can be represented by;

$$\begin{aligned} x_r(k+1) &= A_r x_r(k) + B_{r1} e(k) + B_{r2} u(k) \\ y_r(k) &= C_r x_r(k) + D_{r1} e(k) + D_{r2} u(k) \end{aligned} \tag{6-1}$$

Although the discrete time transfer functions have at least one step delay, the models that have been identified have a feed through term from the inputs. Possible delay from the injection is less than one sample time in the model, and response from BHP has a static term that should not be removed. D_2 however must be eliminated to be able to formulate the predictive control problem. Filtering the output y_r with a delay operator q^{-1} will just do it.

$$\begin{aligned} x_p(k+1) &= A_p x_p(k) + B_p y_r(k) \\ y(k) &= C_p x_p(k) + D_p y_r(k) \end{aligned} \tag{6-2}$$

Where $A_p = D_p = 0$ and $B_p = C_p = I_{pxp}$ with p is the number of outputs. Combining equations above, we have a new system of equations presented in Equation 6-3.

$$\begin{aligned} x(k+1) = \begin{bmatrix} x_r(k+1) \\ y_r(k) \end{bmatrix} &= \begin{bmatrix} A_r & 0 \\ C_r & 0 \end{bmatrix} \begin{bmatrix} x_r(k) \\ y_r(k-1) \end{bmatrix} + \begin{bmatrix} B_{r1} \\ D_{r1} \end{bmatrix} e(k) + \begin{bmatrix} B_{r2} \\ D_{r2} \end{bmatrix} u(k) \\ y(k) &= \begin{bmatrix} 0 & I \end{bmatrix} \begin{bmatrix} x_r(k) \\ y_r(k-1) \end{bmatrix} \end{aligned} \tag{6-3}$$

Choosing the performance signal $z(k) = \begin{bmatrix} \hat{y}(k+1|k) - r(k+1) \\ R^{1/2}u(k) \end{bmatrix}$, the standard predictive control performance index can be written as;

$$J(\upsilon, k) = \sum_{j=0}^{N-1} \hat{z}^T(k+j|k)\hat{z}(k+j|k) \tag{6-4}$$

With N be the simulation horizon and equal to prediction horizon and $\hat{z}(k+j|k)$ is the prediction of $z(k+j)$ at time k. The relation between the state signal x, input signal υ, output signal y, external signal w and performance signal z is given by

$$\begin{aligned} x(k+1) &= Ax(k) + B_1e(k) + B_2w(k) + B_3\upsilon(k) \\ y(k) &= C_1x(k) + D_{11}e(k) + D_{12}w(k) \\ z(k) &= C_2x(k) + D_{21}e(k) + D_{22}w(k) + D_{23}\upsilon(k) \end{aligned} \tag{6-5}$$

With the following substitutions;

$$x(k) = \begin{bmatrix} x_r(k) \\ y_r(k-1) \end{bmatrix},\ y(k) = y_r(k-1),\ w(k) = r(k+1),\ \upsilon(k) = u(k)$$
$$A = \begin{bmatrix} A_r & 0 \\ C_r & 0 \end{bmatrix},\ B_1 = \begin{bmatrix} B_{r1} \\ D_{r1} \end{bmatrix},\ B_2 = \begin{bmatrix} 0 \\ 0 \end{bmatrix},\ B_3 = \begin{bmatrix} B_{r2} \\ D_{r2} \end{bmatrix}$$
$$C_1 = \begin{bmatrix} 0 & I \end{bmatrix},\ D_{11} = 0,\ D_{12} = 0,\ D_{13} = 0$$
$$C_2 = \begin{bmatrix} C_r & 0 \\ 0 & 0 \end{bmatrix},\ D_{21} = \begin{bmatrix} D_{r1} \\ 0 \end{bmatrix},\ D_{22} = \begin{bmatrix} -I \\ 0 \end{bmatrix},\ D_{23} = \begin{bmatrix} D_{r2} \\ R^{1/2} \end{bmatrix}$$

$R^{1/2}$ could be selected as σI in the simplest form, where σ is weight factor that signifies the control effort versus tracking error in Equation 6-4.

It must be noted that the reference $w(k) = r(k+1)$ must be chosen in a proper way in order not to have any conflict with $y(k) = y_r(k-1)$. Moreover note that there is no *equality constraint* in this formulation, but one can define upper and lower bands for the input signals to satisfy the signal limitations.

Primary Results

Figure 6-8 shows the reservoir behavior after applying the suggested control action by MPC, with two identified models of FIR and SubID. Optimal inputs are also presented in Figure 6-9. It can be seen that SubID shows better performance as we can see that all four outputs are closer to the optimal trajectories. FIR model on the other hand does not seem to perform well, although it had a good simulation fit. One reason could be the different range of signals suggested by the MPC controller than the simulation range. In fact the FIR models have been identified with normalized data set, i.e. all the inputs and outputs were downscaled to have the mean value of 400, while the suggested MPC input values must be upscaled before being implemented on the real model.

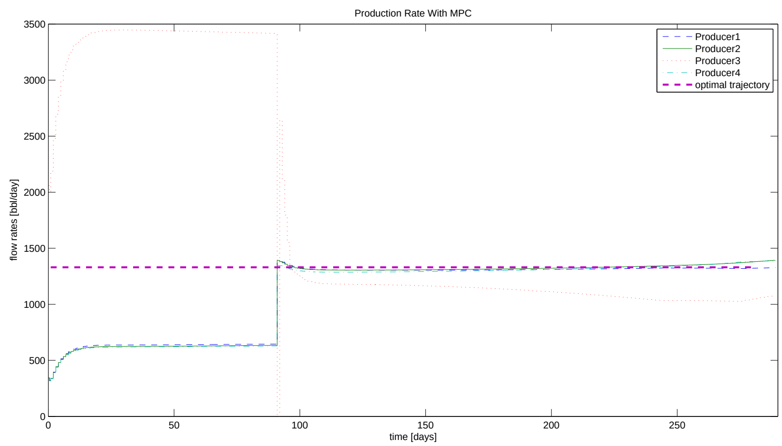

(a) Production Rates, SubID

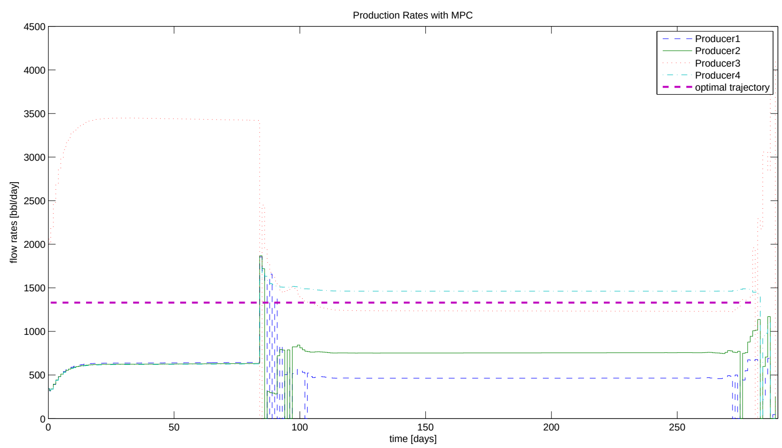

(b) Production Rates, FIR

Figure 6-8: Production Rates Before and After Applying MPC Using SubID and FIR Models, in 2D Homogeneous Reservoir

At the end of this period, a new model can be identified using the last $70days$ of production data. RBS signal with same properties could be added on top of the input. The fit of the new models is shown in Figure 6-11. It is interesting to note that, although the reservoir has reached to a new working point, still a $4th$ order SubID model shows better prediction quality, in compare to lower order (i.e. $2nd$ or $3rd$ order SubID) and also higher order models.

Figure 6-12(a) shows the corrective control laws and production rates after applying MPC in the second period. And production rates including the exciting signal for identification in the same period is presented in Figure 6-12(b). Referring back to the Figure 6-3, an important achievement can be detected here. Without applying an MPC, producer3 was supposed to start producing water from day 250, but thanks to the corrective control action there is no sign of water until day 490. We will see in the remainder of this section that water breakthrough happens after day 500, which is not the expected day according to the real-model shown in Figure 6-2.

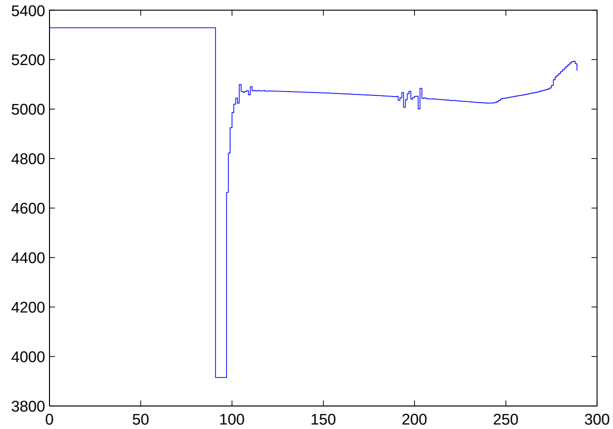

(a) Water Injection Rate, SubID

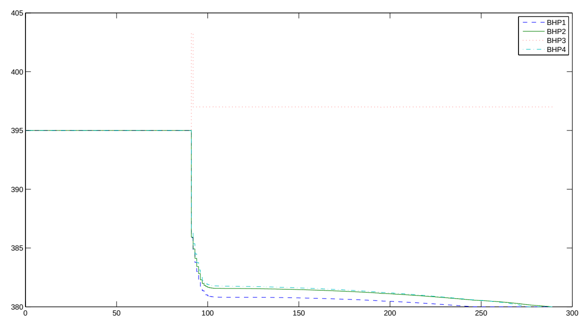

(b) BHP Settings, SubID

Figure 6-9: Optimal Control Laws Suggested by MPC Controller Using SubID Model, in 2D Homogeneous Reservoir

Results After Water Break-Through

Figure 6-13 shows production rates during 1750$days$ with optimal inputs suggested by MPC. As it can be seen water has reached the production wells only in producer3. Referring to grid block saturation, presented in Figure 6-14, other three wells will begin to produce water shortly. As a matter of fact, during the period that the reservoir starts producing water in production wells, nonlinearities are pronounced more than other times. These nonlinearities stem from relative permeability effects, explained in more detailed in [Jansen et al., 2008]. This can also be seen in Figure 6-13 around day 500, where we have water breakthrough in producer3. It is obvious that although the optimal control action could keep producers 1, 2 and 4 on track, production rate of producer3 had a some offset. This offset of course has been corrected in the next period, where we identified a new model. Additionally, we see that after day 1000, the controller could only perform well in half a period as it used to. It implies that the prediction quality of models for producer3 has been reduced.

Updating the models by the end of this period verifies the discussion above. Obtainable simulation fits are lower than previous periods, except the models for producer3 (which has

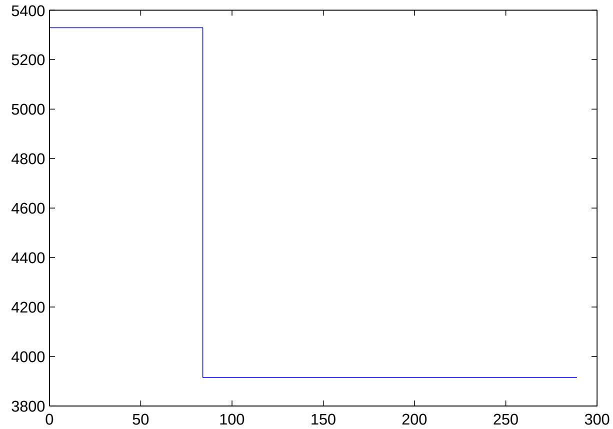

(a) Water Injection Rate, FIR

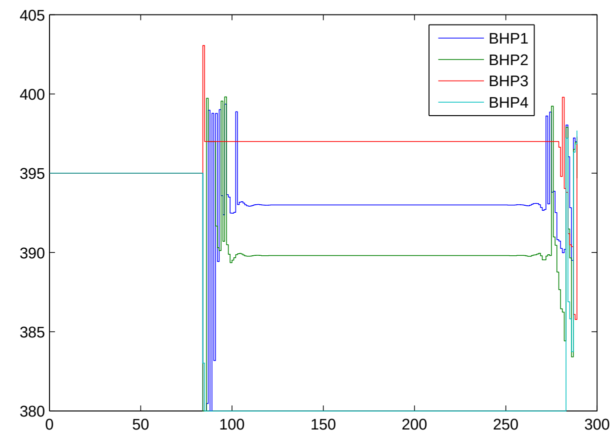

(b) BHP Settings, FIR

Figure 6-10: Optimal Control Laws Suggested by MPC Controller Using FIR Model, in 2D Homogeneous Reservoir

started producing oil and water quite long time ago). Specially the stability of the models become an important issue, if we want to use them for MPC. Figure 6-15 provides model identification results for $4th$ order SubID models.

Experiments using other input signals show that simulation fit of linear models cannot be improved further, regardless of input properties. Therefore, employing linear data driven models for MPC in this period has some limitations. First of all, using unstable models gives erratic and unacceptable results, because of ill-conditioned optimization problem. Second of all, we need to shrink the prediction horizon of MPC, since the models do not remain accurate for long periods. On the other hand, having shorter horizons takes much of freedom from the controller. Therefore we should make a trade off between these two, as it has been shown in Figure 6-16 for 100 days. Liquid rates in this Figure show that, although the optimal BHP values of producer3 are high (i.e. limited by upper constraint for BHP), it still produces in

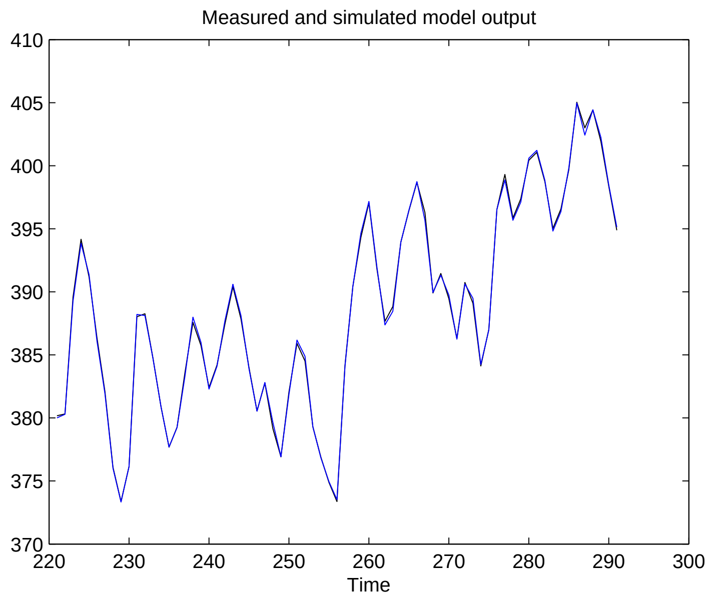

Figure 6-11: Simulation Fit of 97% for 4th Order SubID Model of Producer2 in 2nd period, in Homogeneous 2D Reservoir (second period in lifecycle)

a rather high rate. It is because of the fact that at this point keeping BHP high, causes a pressure increase in neighboring blocks and consequently production rate reaches the same value. Also at the moment producers 2 and 4 starts producing water, two boosts in production rate of producer3 can be detected. By the time we pass this phase, the rates become steady but not close to trajectories at all.

To reduce the production rate after reservoir pressure increases, BHP must be increased too. Figure 6-17 shows production rates when inputs have looser constraints, i.e. upper band of BHP of producer3 is $600bar$ and lower band of BHP of other producers are $300bar$. We can see that input3 is increasing gradually which causes producer3 to produce less at the end of the period. However, the other production rates have not been improved noticeably. As a matter of fact system dynamics around this working point of reservoir are too much complicated to be captured by a linear model, and we should not expect to have a perfect control here. This means that the method has a significant limitation in this period, although it worked reasonably well in past.

This section can be concluded by doing a lifecycle MPC controlled input scheme. Figure 6-18 shows production rates and corresponding inputs of the whole life of the reservoir. The obtained profit is $76.2Million$, which is 18% more than reality without MPC.

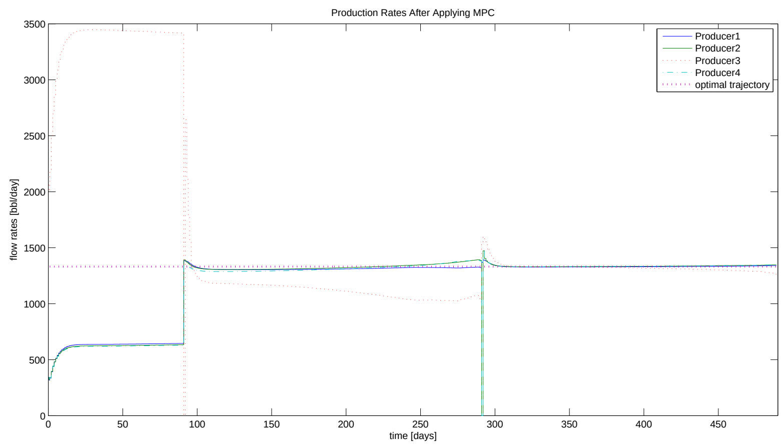

(a) Without The Exciting Inputs

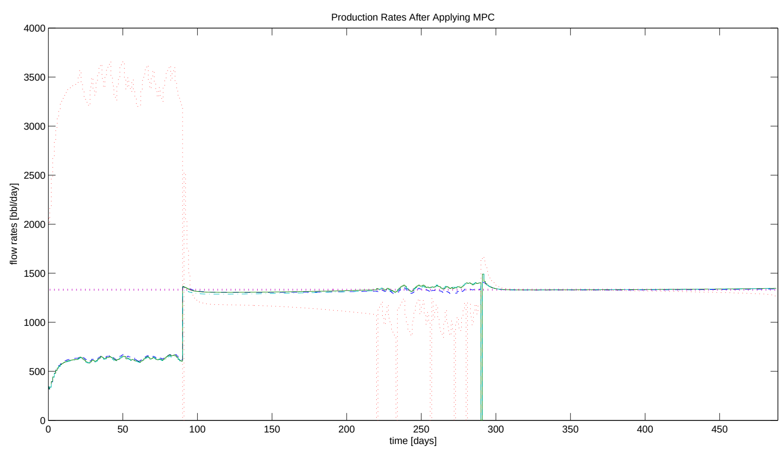

(b) With Exciting Inputs

Figure 6-12: Optimal Trajectory Following In $500days$ Using SubID Model, in 2D Homogeneous Reservoir

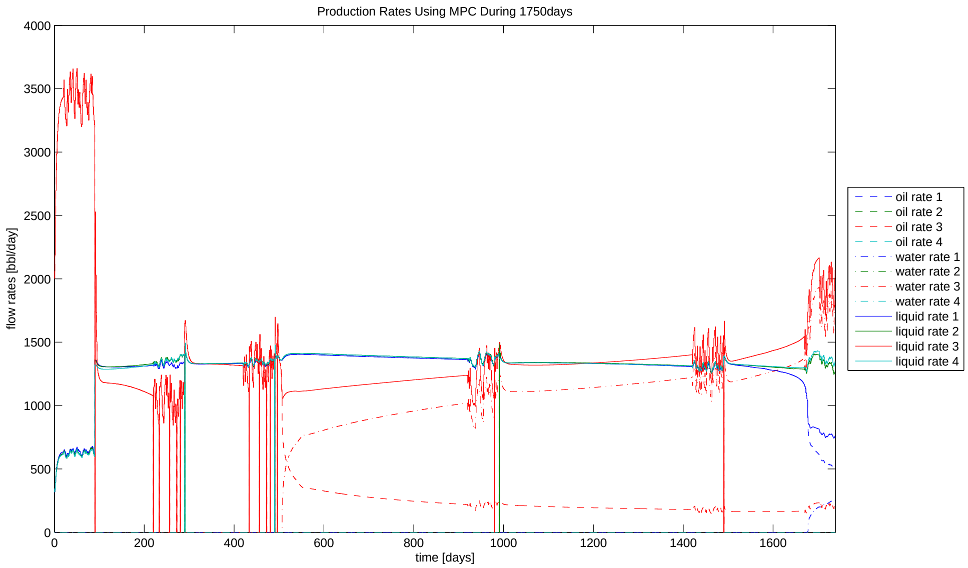

Figure 6-13: Optimal Trajectory Following In $1750 days$ Using SubID Model, in 2D Homogeneous Reservoir

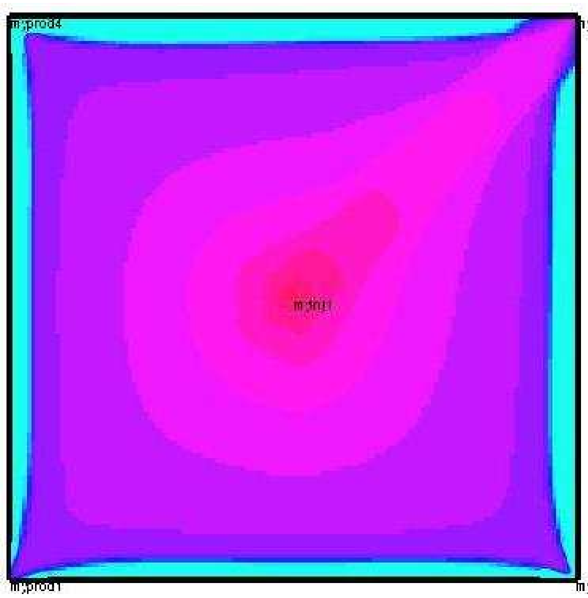

Figure 6-14: Grid Block Saturation Map After $1750 days$, in 2D Homogeneous Reservoir

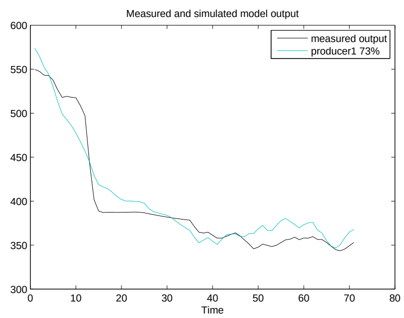

(a) Producer 1

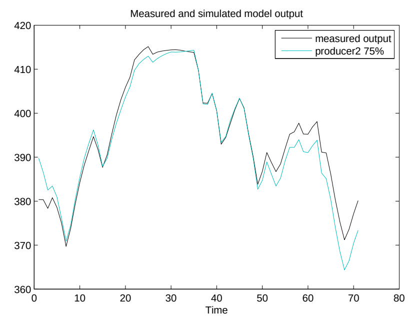

(b) Producer 2

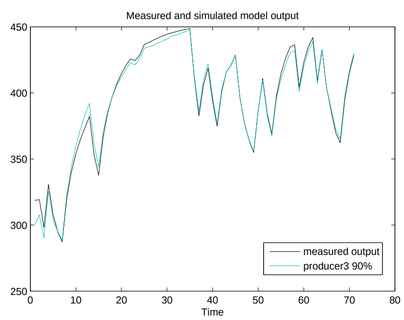

(c) Producer 3

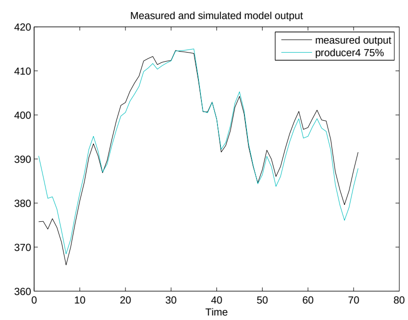

(d) Producer 4

Figure 6-15: Simulation Fit of SubID Models after Water Break Through, in 2D Homogeneous Reservoir

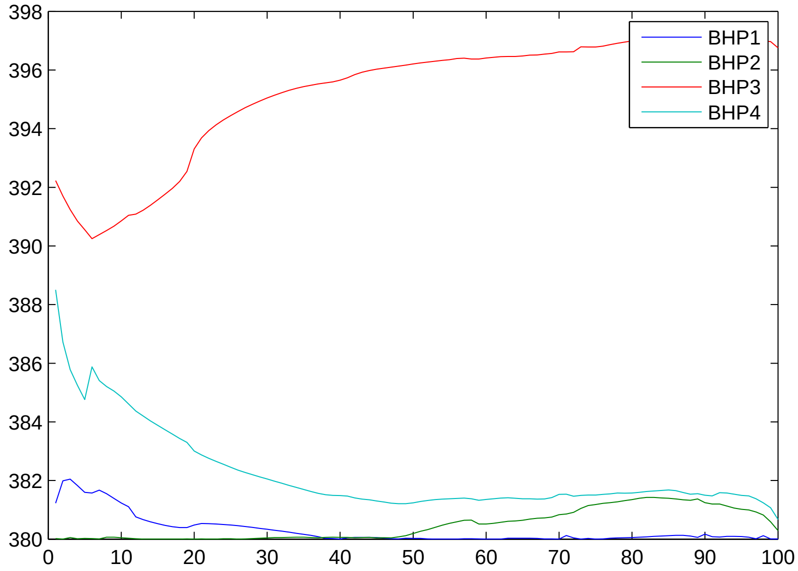

(a) Optimal Inputs

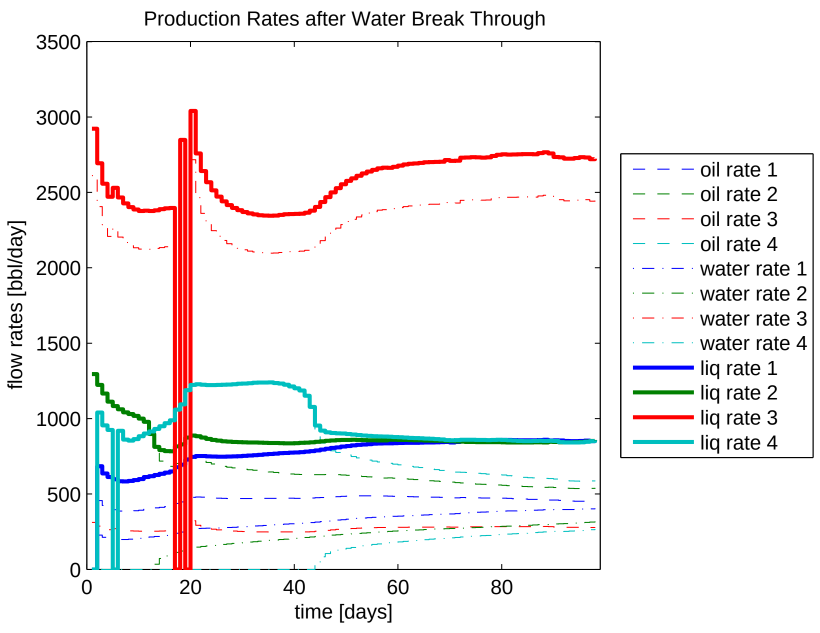

(b) Production Rates

Figure 6-16: Production Rates After Water Break Through Using MPC, in 2D Homogeneous Reservoir

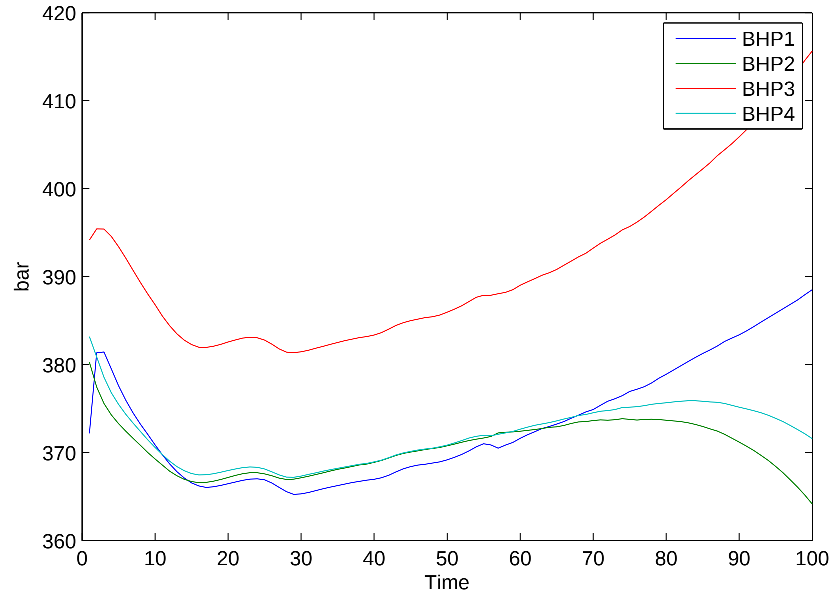

(a) Optimal Inputs

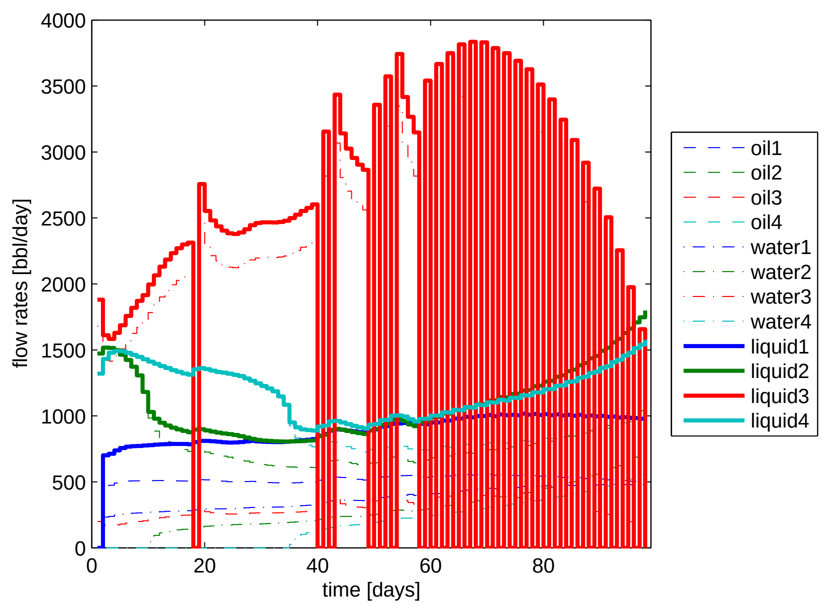

(b) Production Rates

Figure 6-17: Production Rates After Water Break Through Using MPC with Loose BHP Bands, in 2D Homogeneous Reservoir

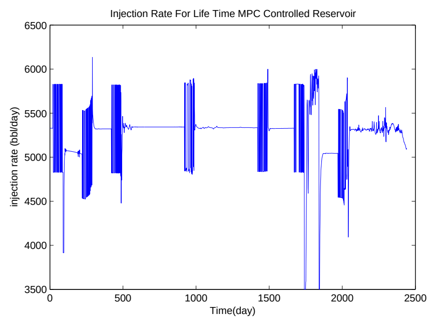

(a) Optimal Injection Rate

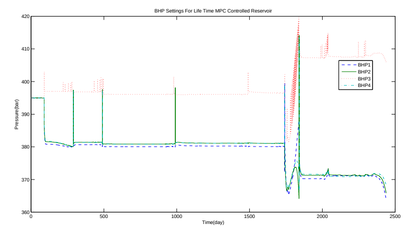

(b) Optimal BHP

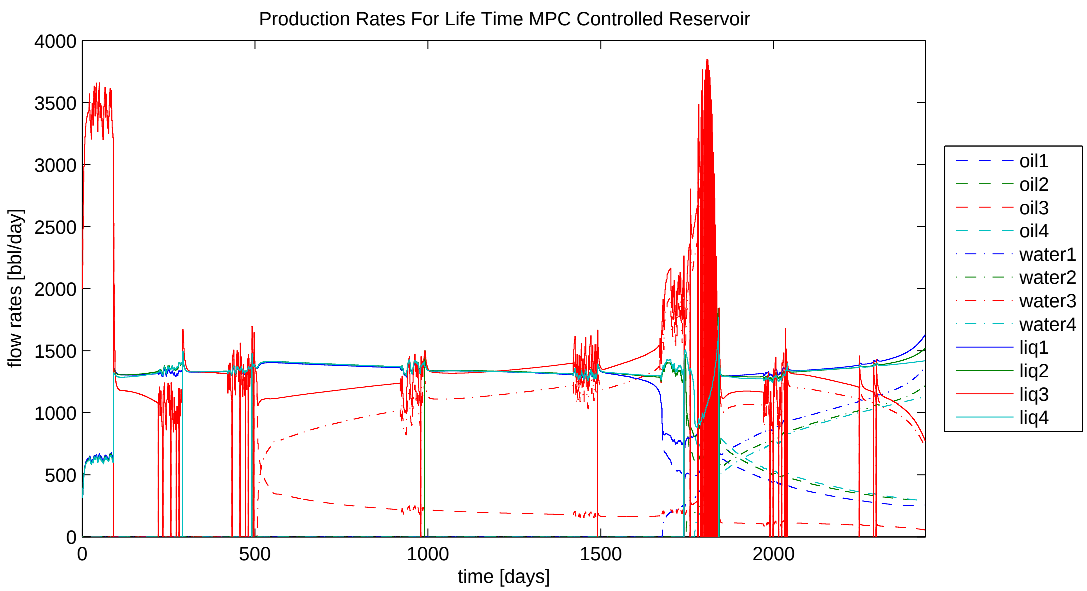

(c) Production Rates

Figure 6-18: Life Cycle MPC Controlled Waterflooding of 2D Homogeneous Reservoir

6-3 Heterogeneous Reservoir, VanEssen Model

VanEssen model used in this section has also the same properties as Chapter 5. Permeability map of the reservoir is presented in Figure 6-19, with 8 injectors and 4 producers. This model has $25,200$ grid blocks of size $40m \times 40m \times 5m$ in 7 vertical layers. Geological and fluid properties are presented in Table 6-3.

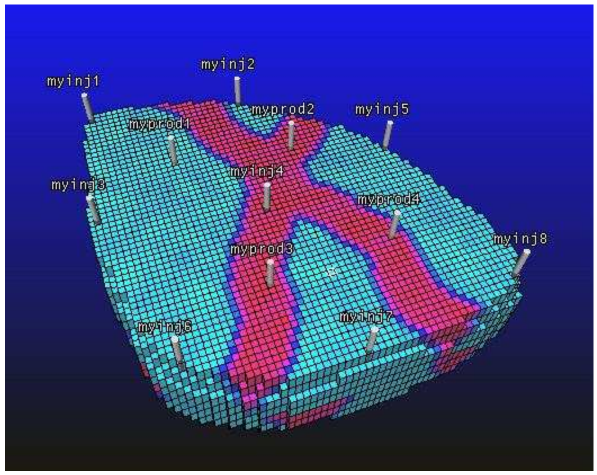

Figure 6-19: Permeability Map of 3D Heterogeneous Reservoir, Used as Model

Symbol	Value	Unit
ϕ	0.20	$[-]$
$\rho_o(400bar)$	800	$[kg/m^3]$
$\rho_w(400bar)$	1000	$[kg/m^3]$
c_o	15×10^{-5}	$[1/bar]$
c_w	4×10^{-5}	$[1/bar]$
μ_o	4×10^{-3}	$[Pa.s]$
μ_w	10^{-3}	$[Pa.s]$
p_{bh}^j	$300 - 550$	$[bar]$
$\bar{P}_0$	$Hydrostaticat4000m$	$[bar]$
$\bar{S}_0$	$0.1, \cdots, 0.1$	$[-]$

Table 6-3: Values of Geological and Fluid Properties in VanEssen Reservoir Model

Lifetime optimization control scheme for the injectors and BHP, and the corresponding production rates are shown in Figure 6-22. Optimization time step is 30 days, for the whole period of 4200 days.

In this section we take into account a discounting factor of 10% to calculate the profit J. This means that the sooner we produce more oil, the more money we can make. Discounting is about taking into account the fact that money loses its value during the course of a project. The discounted value of cash flow during the reservoir life can be calculated by

$$J_{disc}(k) = J(k) \times \frac{1}{(1+d)^n} \tag{6-6}$$

Where n is the number of years since the start of production, and d is discount factor defined in percentage. For oil price of $9\$/bbl$, separation cost of $1\$/bbl$, and zero cost for injection, the discounted predicted J is $600.22 Million\$$. Same oil field with same well locations but with slightly different geological properties is used in place of reality (real-model), depicted in Figure 6-20. Here we have a grid block refinement around the wells to improve the simulation results.

Because the reality model has a different permeability pattern, the waterfront location is slightly different than it is expected from the model-model. Therefore, the production rates would diverge from the optimal values. For instance, as it is shown in Figure 6-21 producer4 has much lower rates and starts producing water almost 500 days after the predicted day. Discounted cost function J of reality model is $555.27 Million\$$, that is 7.5% less than it was anticipated.

Based on what model suggest about water front position, we divide the life of reservoir into three stages; one before water break through, i.e. from beginning to day 500. Second period is during the start of the water production in all producers where nonlinearities are more pronounced, i.e. between day 500 and 1500. And a final stage, where we have two phases of oil and water in production wells, from the day 1500 until the end. The early stage is so short in compare to the other two and contains the effects of the initial condition of the reservoir, specifically the high pressure. In the final stage, it is possible to predict longer with the linear models, since the reservoir has reached to a steady state.

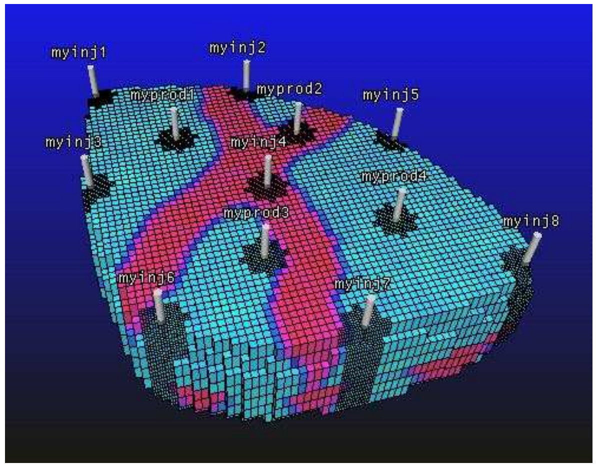

Figure 6-20: Permeability Map of 3D Heterogeneous Reservoir, Used as Reality

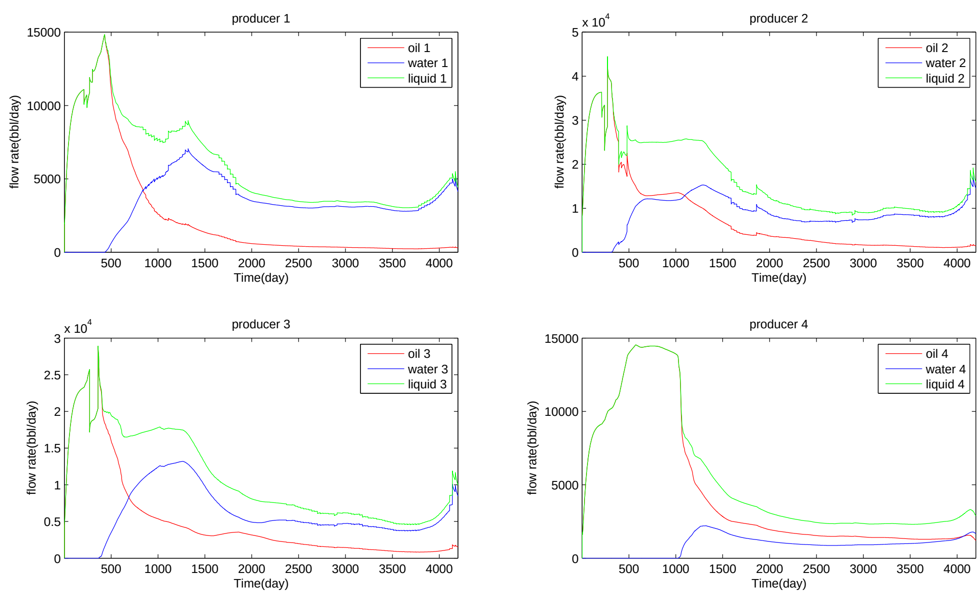

Figure 6-21: VanEssen Model, Reality Production Rates

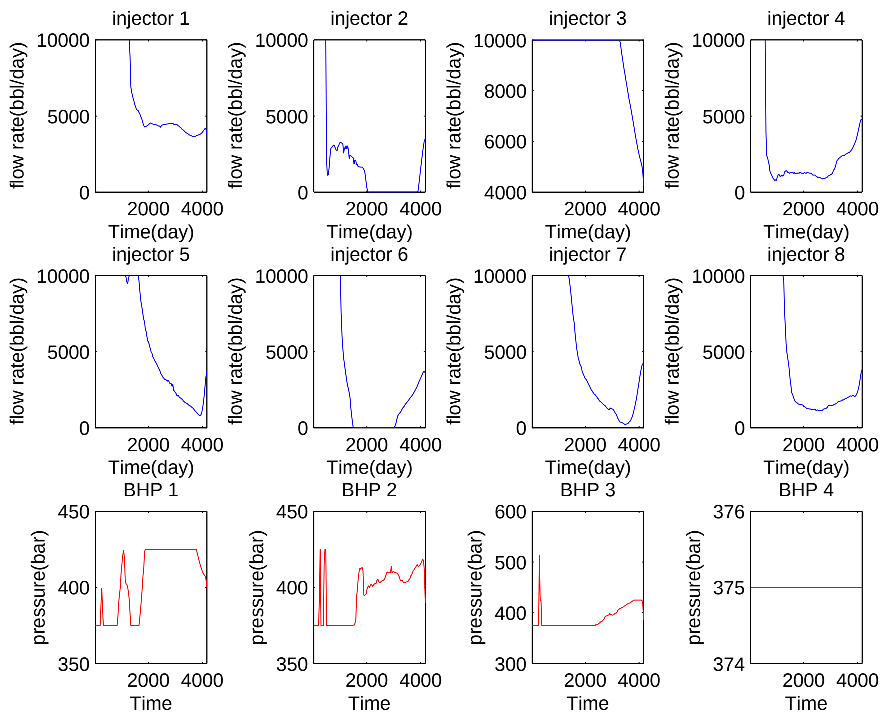

(a) Optimal Inputs

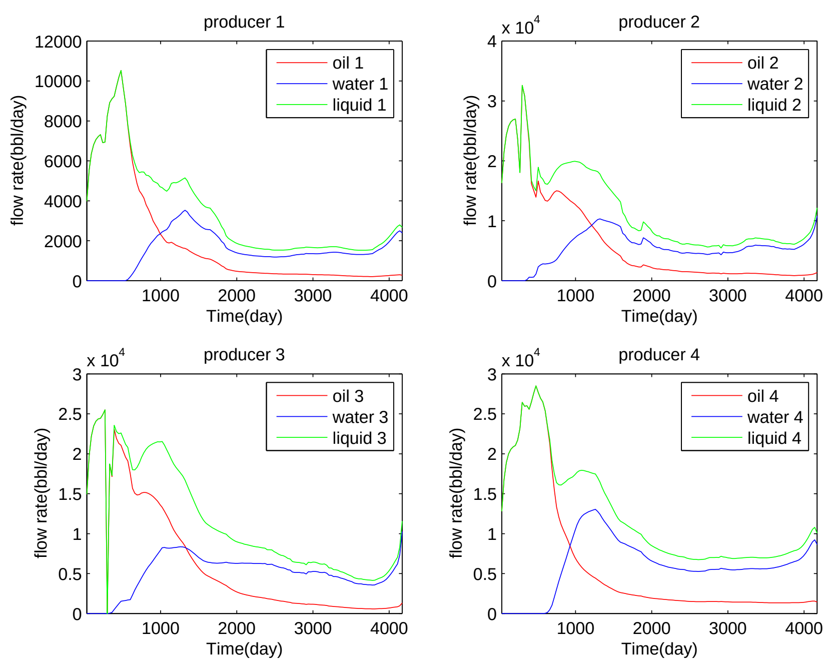

(b) Optimal Outputs

Figure 6-22: VanEssen Model, Optimal Trajectories

6-3-1 Early Production Stage

Unlike the previous section, for this model we assume that the injector rates are fixed to the optimal values and we are only interested in manipulating BHP in the producers. This is of course easier from system identification point of view, but takes the freedom from the MPC controller since the number of inputs is reduced. In the very early production phase the production rates are extremely high, not only because of injecting water, but also from reservoir initial pressure. From the step response analysis in Chapter 5, the input requires to have a length of at least 70 days. Therefore, an RBS signal is added on top of optimal BHP from day 130 until day 200. Same length of 100 days could be picked for the second period of identification and prediction. Results are presented in Figure 6-23 until day 500.

Although the identified SubID models of order 4 to 7 show high simulation fit, according to the results in Figure above, prediction quality of them are not good enough (the model order used for the MPC controller that is presented presented in Figure 6-23 is 6). For periods $200-300$ and $300-400$ the reference tracking quality is better, but naturally for the last period $400-500$ MPC controller doesn't perform well due to nonlinearity effects of the water breakthrough.

Unfortunately the linear models are not able to capture all the effects, specially when the optimal patterns contains sudden drastic changes of values. Since the life cycle optimization has input update frequency of 30 days, which is of course shorter than the reservoir's settling time, MPC controller with linear models fail to provide an appropriate control action to compensate these sharp changes. This means that while it takes some time for the system to be adjusted to the optimal outputs(as expected according to identified models), the real reservoir has reached to a different working point with a different dynamic (and perhaps with a totally different reference). E.g. in producer3 at time instant 380, while it is expected to see an increase in the production rate, just because water reaches this producer the whole production rate decreases suddenly. Such anomalies could be the result of a large time step for the optimization and simulations, and *might* be diminished by more frequent update of the models.

6-3-2 Mid Production Stage

This stage includes early water production of all producing wells, and according to previous section the nonlinear effects are much more pronounced in the dynamics of the system. Therefore, the identified linear models may not be a good substitute for the systems. The production rates for this period between day 500 and 1500 are presented in Figure 6-24 .

In Figure 6-24 we can see that in some periods, reference tracking error is awfully high, although the models that are used for MPC are of $6th$ order SubID with high simulation fits. It must be noted that unlike the early production stage, in this period the injection rates are not constant anymore. Fixing the injection rates to optimal inputs, causes some dynamic changes that has not been captured in the identification data set. For example injector6 has a sudden drop of injection rate at time 600, and consequently it affects the production rate of the closest producer. Looking to the tracking error of period 600 to 800 of producer3, we can see the result of this effect. Also in producer4 we have divergence from the optimal output right after the water breakthrough. Yet in some periods we have good performance by MPC, and the rates are very close to the optimal outputs.

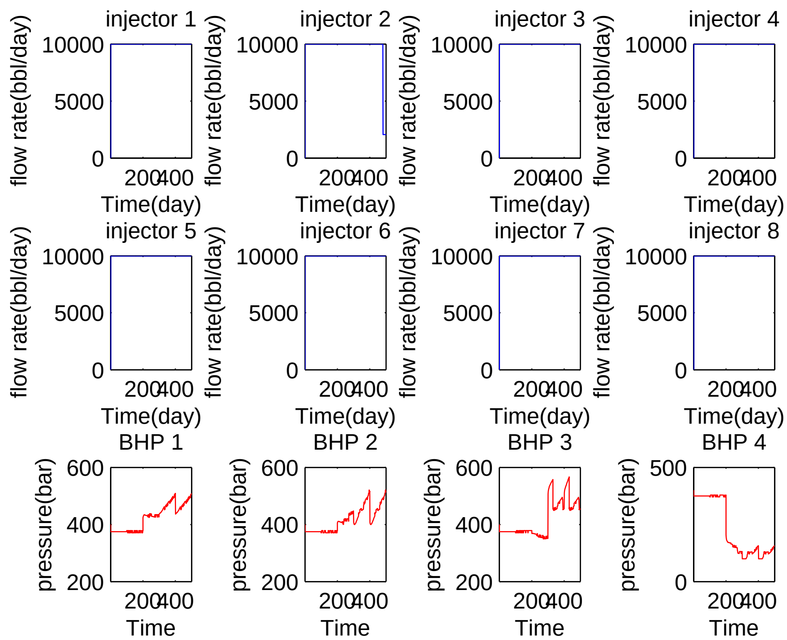

(a) MPC Inputs

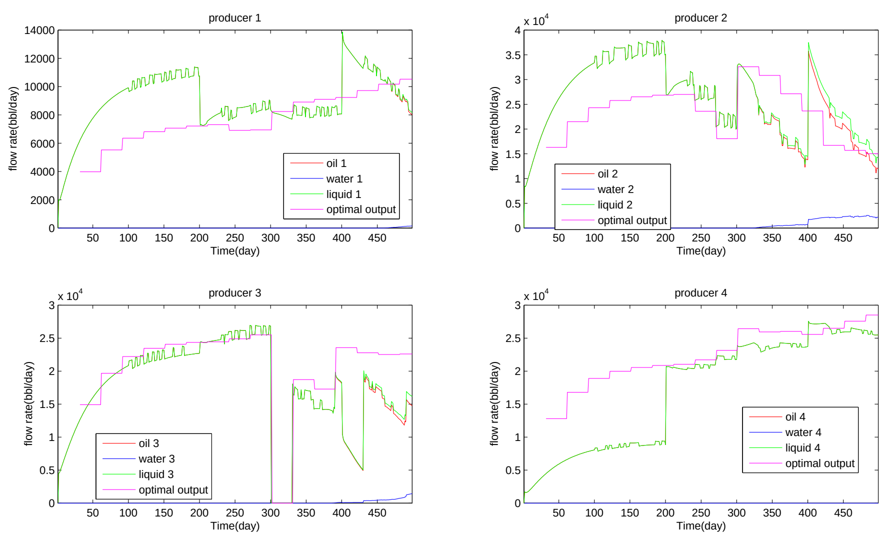

(b) Production Rates

Figure 6-23: Early Production Stage(before water break through) Controlled By MPC and Optimal Trajectories, In VanEssen Model

6-3-3 Final Production Stage

In this stage reservoir dynamics are changing very smoothly in compare to the previous stages. As a matter of fact the reservoir has reached to a quasi steady state point, and the

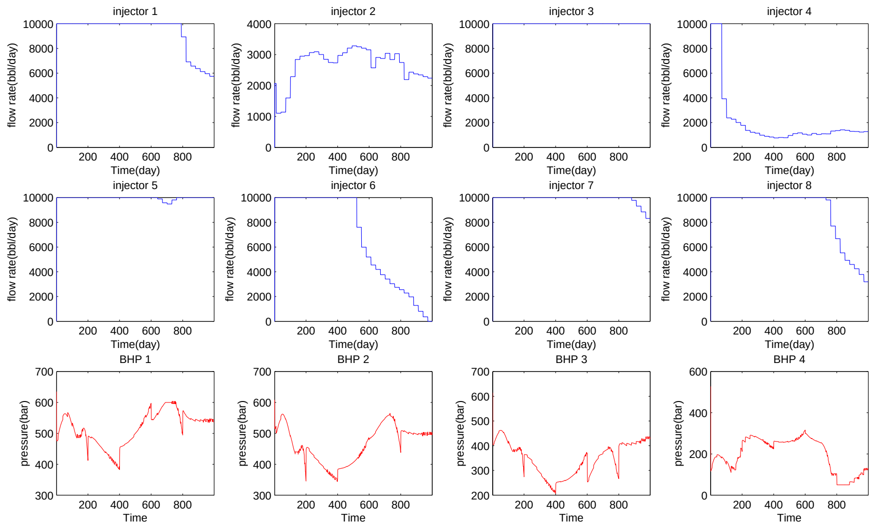

(a) MPC Inputs

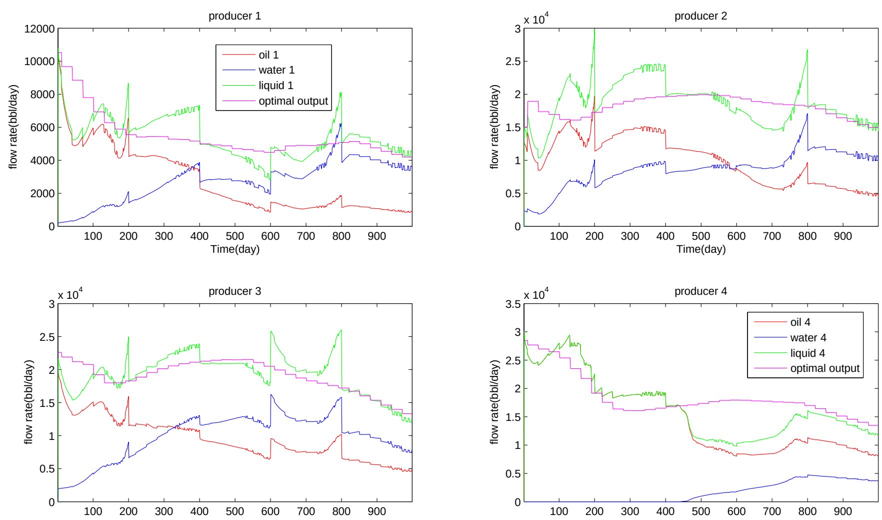

(b) Production Rates

Figure 6-24: Mid Production Stage (between day 500 and 1500, during water break through) Controlled By MPC and Optimal Trajectories, In VanEssen Model

optimal output doesn't contain erratic changes anymore. However, looking into the optimal *injection* rates (that are fixed already), still we see significant changes in the inputs that causes considerable tracking error, e.g. in producer1 around time step 1500 that is presented in Figure 6-25. In fact the effect of changing injection rates was not captured in the identification period, and therefore models cannot predict the correct outputs. Unfortunately the inputs are not reoptimized during this period and the tracking error cannot be compensated until the next working point, where the identified model is uptadet.

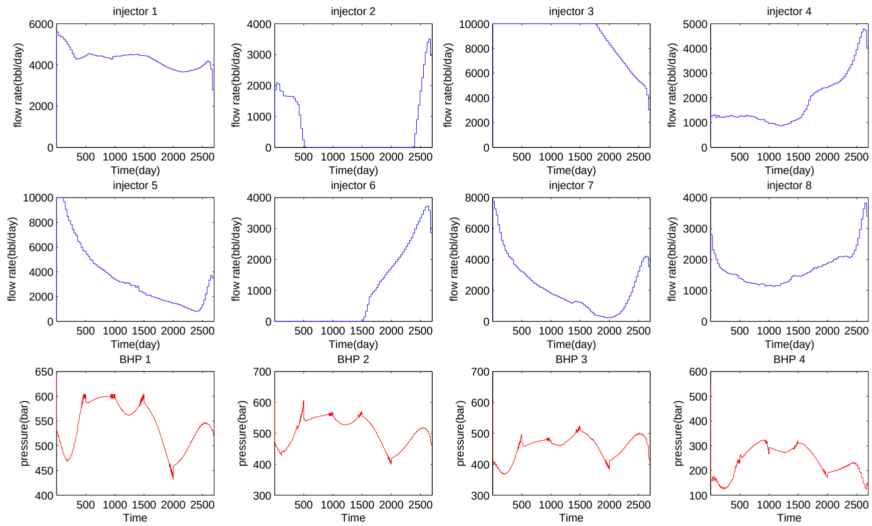

(a) MPC Inputs

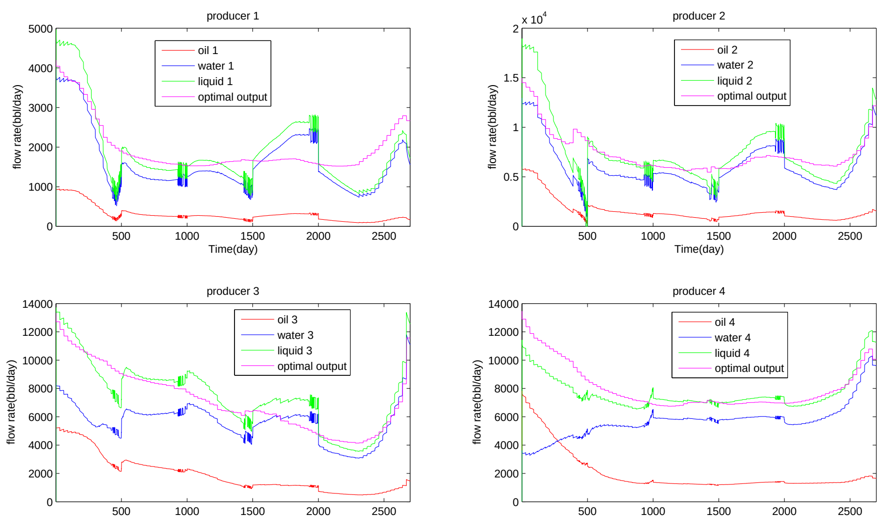

(b) Production Rates

Figure 6-25: Final Production Stage(between day 1500 and 4200, after water break through) Controlled By MPC and Optimal Trajectories, In VanEssen Model

6-3-4 Life Cycle MPC Controlled VanEssen Model

Figure 6-26 presents the reservoir production rates during the whole life of reservoir. In the same Figure uncontrolled production rates are presented to see the benefits of the MPC controller. Looking back at Figures 6-19 and 6-20, we can see that producer4 is located in a permeable channel in the model-model, and is located in less permeable rock in the real-model. Therefore, it will have lower production rates unless it is controlled with updated inputs. Such differences between model and reality indeed causes less profit. We have shown that it is possible to steer the reservoir to the expected manner, using linear models and MPC. The obtained NPV at the end of the reservoir life is 590.60$Million\$$, which is 6.3% higher than uncontrolled reservoir.

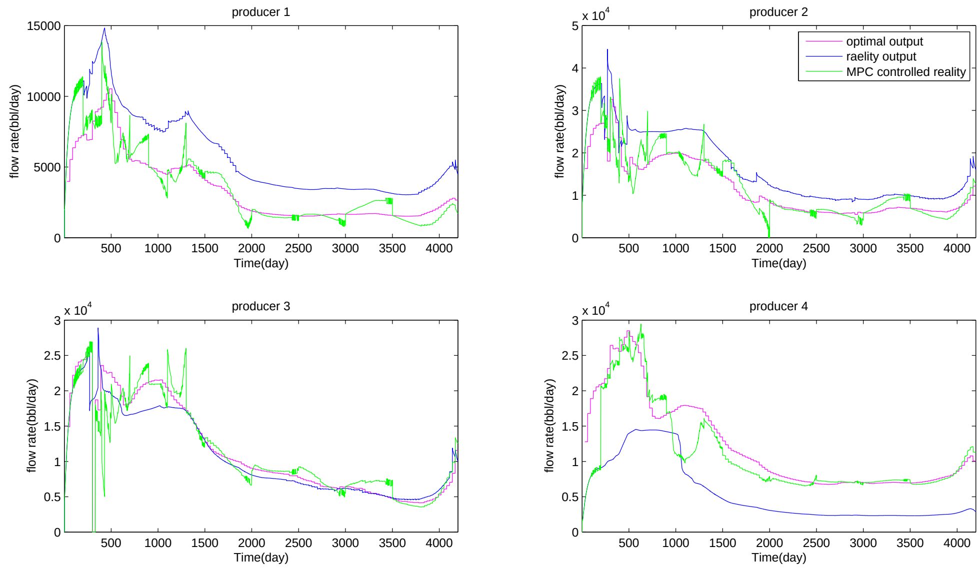

Figure 6-26: Life Cycle MPC Controlled Waterflooding of 3D Heterogeneous Reservoir, VanEssen Model

6-4 Chapter Conclusion

In this chapter we studied the identifying of the linear down scaled models of two synthetic reservoirs, to be implemented later in a MPC controller. According to the results, we see that the dynamics of the reservoir lies in a lower dimension subspace, since we were able to identify accurate models with very low orders. However, the dynamics do not remain in a fixed subspace, as the reservoir condition changes during its life. In order to approximate the dynamics with LTI models, certain working points in the life of the reservoir must be chosen. The required model order to have an acceptable simulation fit and an acceptable prediction horizon, is highly dependant on the system complexity and waterflooding stage of the selected working point. During the period close to the time that water front reaches the producers, linear models fail to predict well. Additionally, in the early stage of the production, when reservoir's initial pressure plays a major role, models are not always trusted. On the other hand, models are reasonably accurate when the reservoir is in other working points.

The focus of this chapter was more on the homogeneous model, where we have shown how differently models perform in terms of their predictability, after they are implemented in a MPC. SubID models outperform the FIR models, although they had more or less the same simulation fit. Simple FIR models must be of high orders to have good fit, and transforming them to subspace representation results in an even higher order models. Therefore, it is not computationally efficient to use FIR for complex models with large number of inputs and outputs.

The quality of the MPC controller was highly dependent on the prediction quality of the model. As a result, the tracking error of the outputs are lower wherever the models are updated. During, and to some extent after the water breakthrough in each production well, the performance of the MPC is rubbish, and it must be studied in more details whether updating the references can improve the control quality or not.

In these two reservoir models, the constraints are assumed to be very relaxed in order to observe the performance of the MPC controller. However, the validity of this issue must be investigated further in more details.

For the heterogeneous VanEssen model, the controller was confined to reoptimize the BHP only, while the injection rates were fixed. This of course causes some trouble, specially when the production rates are influenced by significant changes of the injection rates. However, still the results were improved in compare to the open loop (uncontrolled reservoir). Based on the pattern suggested by the model-model, we divided the whole production life into three stages. In early stage of first 500 days, the working points were chosen every 100 days. In the second stage (between day 500 to 1500) and the third stage (between day 1500 to 4200) the working points were spread in even periods of 200 and 500 days respectively. The input signals for the identification had the same properties in every period. In fact we determined these inputs based on the analysis of the same reservoir in Chapter 5. Yet, for the heterogeneous reservoir, it is interesting to see how much improvement can be gained if the injection could also be manipulated with the MPC controller.

Although the current results are promising, there is a room for improvement if the models are updated more frequently. Since the model simulation fits are already too high, we cannot say whether different input signals can improve model qualities or not. It seems that as long as inputs have certain properties, we can be sure about the amount of information captured in the data set. As a matter of fact, these models have a certain limit that cannot be surpassed by changing the inputs. Perhaps more frequent updates increase the performance of the MPC controller.

Finally it must be reminded that all the experiments above have been done using a simulator. This means that there are still some effects that might have been disregarded when it cannot be verified with a real production data, e.g. noise or disturbance effects that are very common in reality were not taken into account in our experiments.

Chapter 7

Conclusions and Recommendations

As the outlook of the world energy consumption suggests, demand for hydrocarbon is rising constantly in the future. With 70% of the oil production coming from fields that are very old, the optimal management of a reservoir to maximize the recovery factor is an important topic. Despite many advances in reservoir simulation and management, reservoir engineers still struggle in setting optimal injection/production target rates for such fields [1].

CloReM is a model based optimization algorithm to increase reservoir profitability using systems & control techniques. Reservoir models are nonlinear and of very large scales, and there are several factors that must be taken into account in optimization. Limited by computers computational capability, the time scale of the CloReM is large. As a result, responses to several disturbances and undesired effects of uncertainties are very slow.

This thesis presents a MPC methodology to improve CloReM performance. The idea aims at the contribution of developing low order data driven linear models of "injection-production rates", and "BHP-production rates" pairs, using system identification methods. Having a faster update rate, these models are able to account for undermodeling issues of large scale nonlinear models. Besides, these undesirable effects of disturbances and model uncertainties can be circumvented more effectively.

A two level control strategy is proposed to keep the system outputs on the optimal trajectories (in the lower level), that have been optimized for the production life of the reservoir (in the upper level). MPC framework with locally identified low order linear models, is a proper choice for the control level for two major reasons; firstly because MPC can be easily implemented and well tuned for MIMO systems, and is able to handle any signal constraints, and secondly because models can be updated rapidly using injection/production data. Although these models are not based on physics principals (and thus do not have long prediction horizon), they are a good replacement to predict system outputs locally and describe short term reservoir behavior.

[1] Quoted from the website of "The Smart Oilfield Consortium", at the Department of Energy Resources Engineering, Stanford University

7-1 Review of Results

Assuming that certain assumptions are hold around a working point, system identification methods can provide linear low order models directly. Since the quality of the model is dependent on the data set, a proper input signal must be designed based on system dynamics. Properties of the input signal for identification purpose, is in fact limited due to the existing production limitations, and also more importantly, because of fixed optimal system inputs (i.e. MPC controller output and also lifecycle optimization). Therefore, the advantages of applying a persistently exciting input must be analyzed and motivated before implementation.

Usually different identification methods are combined to get the most confident results. It was motivated in Chapter 3 that PEI and SubID are good candidates, regarding the system properties. PEI can provide a disturbance model and also there are useful software packages available for both identification and validation. On the other hand, SubID has a simple structure that is well suited for the MIMO systems, and more importantly it is computationally efficient.

Reservoir Modeling with System Identification

In Chapter 5, system identification procedure has been applied to 5 different synthetic reservoirs. It has been shown that step response experiment between each input/output (i.e. injection rate/production rate) pair, can provide rudimentary information about the underlying dynamics, e.g. possible sample delays and the largest time constant. The latter is important in the sense that the properties of the input signal such as length and frequency range, can be determined based on it. Moreover, staircase experiment can be used to verify the linearity range of the system around the working point, in order to keep the signal amplitudes in that interval. However, it was concluded that repeating such experiments frequently do not seem necessary, as long as reservoir dynamics do not change dramatically (this was the case specially for homogeneous reservoir models that have less complexities). More specifically, step response experiment must be highly motivated (in reality), as it requires a long time for a complete test results. We should mention that, in this thesis properties of the experiments and their repetitiveness, have been determined based on trial and error and rules of thumb.

For the most simple example of a 2D homogeneous reservoir, all the three model structures of FIR, ARX and SubID have more or less the same simulation fit. ARX and SubID could provide good approximation with first or second order models. FIR on the other hand, requires higher order for better fit and since the data must have been resampled before identification, model order was in fact limited by the number of the samples. In the same section, we have shown that, resampling a non zero mean data-set causes numerical issues if they are used for identification. Therefore, a proper sampling frequency of data acquisition must be employed, or otherwise, the mean of the data should be removed beforehand. In the latter case, the model outputs (specifically the predicted output) must be treated with extra care, since they may show some drift from the real output.

In the next three reservoir models, more complexities were introduced by adding heterogeneities and more layers. Still we showed that with a proper design of the input and having sufficiently informative data sets, reservoir dynamics can be captured with low order linear models. Simulation fits were more or less the same, while model orders were naturally higher. In the 6well reservoir model, it has been shown that, although identified models of the output that has less sensitivity to the input changes do not provide good fit, the absolute mismatch error between model and reality is in fact extremely small in compare to the other outputs, and therefore can be neglected.

In the most realistic reservoir model, VanEssen model, BHPs were also employed as the inputs. The input signal design was a little more complicated in compare to previous models, due to the large number of input/output pairs and having inputs of two different natures (i.e. injection rate, and pressure). However, since all the inputs must be applied simultaneously, marginal values are selected to satisfy both inputs requirements. Furthermore, we have shown that BHP have more dominant effects on the outputs (production rates), and a higher simulation fit can be reached with a higher BHP amplitude. On the other hand, with very high BHP amplitude, the response from injection rates on the production rates are not clearly detectable. Therefore, depending on the model purpose and the model inputs, one should make a trade off between the specifications of the BHP and injection rates input design.

Waterflooding Using Model Predictive Control

In Chapter 6 we introduced the MPC framework, applied on two reservoir models. The quality of the identified models in terms of prediction horizon depends on the production phase of the reservoir. In the early stages, when the initial pressure plays a major role on production rates, the models are not reliable for long horizons and must be updated more frequently, specially for more complex reservoirs. Thereafter, when water reaches the producers, nonlinearity effects are more pronounced and linear models fail to provide even good approximation for short horizons. During other times, a well identified model can remain valid for rather a long time. According to the results, it seems that the model orders are not varying in different stages, and only parameters need to be updated.

As it was expected, SubID has outperformed FIR for one reason because we implemented MPC with Subspace representation. This means that FIR models must be transformed into subspace, and since the FIR model have generally high order, the transferred models have extremely higher orders. This issue naturally reduce the performance of FIR in the optimization algorithm. Moreover, we should address that all the inputs and outputs were normalized to have a certain signal power before identification. In this respect, it should be further investigated whether it influences low performance of the MPC controller with FIR models or not. Due to the poor results from the FIR models, for VanEssen model only SubID structure has been studied.

The performance of the proposed MPC is only investigated against uncontrolled life cycle optimization, i.e. the injection and production rates are only optimized once for the whole life of the reservoir, based on the large-scale nonlinear model (Model model). The parameter uncertainties and model discrepancies have been introduced by using a slightly different model with unlike geological properties (Real model).

For homogeneous 2D model, where both injection rates and BHP are controlled, the NPV is increased 16%. In 3D heterogeneous VanEssen model though, we fixed the injection rates and only BHP were manipulated. In some periods, where injection rates have significant variations, this issue reduced the performance of the MPC controller considerably. Yet with all the complexity and controlling only BHP, we showed that MPC can increase NPV up to almost 6.3%.

7-2 Recommendations for Future Work

Although the results of this thesis as described in previous section are promising, still there are some areas that need further investigations. Some suggestions for further study in different levels are given.

Input Design

In this thesis preparatory experiments and input design is according to a knowledge base that is created with some rules of thumb and trial and error. Indeed more structured way with more intuition can increase the efficiency and quality of the identified models. Moreover, it is useful to be further investigated the benefits of applying step responses in different stages of production.

Additionally, the effects of adding persistently (or sufficiently) exciting, RBS-like signals to the inputs, on the amount of produced oil (i.e. from economical point of view), and on the reservoir and field equipments (i.e. from feasibility point of view), need to be studied in more details.

Model Structure

According to the model complexities and the number of inputs and output, we were limited to few model structures for system identification. Although the results were satisfying, still if extra noise or disturbances are introduced (i.e. in reality) other PEI structures such as ARMAX and BJ may provide better approximations. Therefore, it is suggested that for complex reservoir models, more dedicated study of different model structures is included.

Inputs and Outputs

The inputs of the models were selected from the most influential elements of the system, i.e. injection rates and BHP. Valve settings could also be used for inputs instead of BHP, and it is interesting to see if any advantage can be gained with that.

Furthermore, the production rates were optimized for the life of the reservoir and inevitably they were the system outputs. However, it is very important to investigate the obtainable benefits by using fractional flow rates. In practice, fractional flow meters are extremely expensive and it must be highly motivated to implement them on every producer well.

On the other hand, in the reference trajectory level, cumulative rates can be tracked instead of instantaneous rates. This issue is in fact more useful when we want to look into longer production life. In the early stages, the production rates are governed by reservoir initial pressure, and it is not easy to manipulate the rates, specially in wells with very high or very low production rates. More precisely it means that in the early stage, some producers may have higher (or lower) rates in compare to the references, that can be compensated more easily later on by producing lesser (or higher).

Validating Models

From validation point of view, there are quite a few criteria that the models can be compared to. In this thesis we only validated the models against each other, and sometimes their prediction quality were compared with the simulator. However, this step must be regarded more discreetly in more structured way. For instance, it is suggested that the outputs of the linear low order models are compared with *nonlinear models*, *linearized models* and *different identification methods* and if possible with *real measurements*. Also it is useful to have a mathematical measure of reliability range of such models.

Moving Horizon MPC

Due to the hardship of implementation of moving horizon MPC, in this thesis we had fixed the control windows, and corrective control action suggested by MPC controller were applied all together. In the future it is strongly recommended to integrate the MPC framework with simulator, and designing an state estimator (e.g. kalman filtering), to update the inputs step by step.

Adding Measurement Noise and Disturbances

For the sake of clarity, it was assumed that the measurements are not contaminated with noise and also the only source of disturbance is due to the model discrepancies. It is useful to see the performance of linear models in the presence of more noise and disturbances.

Integrating with CloReM

It was mentioned in Chapter 2 that since dynamic (re)optimization is very time consuming (i.e. in the upper level), the performance of the MPC in the lower level is only compared to the open loop dynamic optimization. More clearly, the optimal trajectories are determined by a single life cycle optimization. However, it is interesting to investigate the performance of the proposed secondary loop, when it is fully integrated with CloReM. This issue is in fact considered as the final goal and requires more dedicated research.

Bibliography

[Albertoni and Lake, 2003] Albertoni, A. and Lake, L. (2003). Inferring interwell connectivity only from well rate fluctuations in waterfloods. *SPE 83381*.

[Allgower et al., 2000] Allgower, F., Findeisen, R., Nagy, Z., Diehl, M., Bock, H., and Schloder, J. (2000). Efficient nonlinear model predictive control for large scale constrained processes. *Proceedings of the Sixth International Conference on Methods and Models in Automation and Robotics, Miedzyzdroje, Poland, 2000, pp. 43-54.*

[Awashti et al., 2008] Awashti, A., Sankaran, S., Nikolaou, M., Saputelli, L., Saputelli, L., and Mijares, G. (2008). Meeting the challenges of real time production optimization- a parametric model based approach. *SPE 111853*.

[BP, 2009] BP (2009). Bp statistical review of world energy. *bp.com/statisticalreview*.

[Brouwer and Jansen, 2004] Brouwer, D. R. and Jansen, J. D. (2004). Dynamic optimization of waterflooding with smart wells using optimal control theory. *SPE Journal(SPE78278) 9(4). 391-402*.

[Demiryurek et al., 2008] Demiryurek, U., Banaei-Kashani, F., Shahabi, C., and Wilkinson, F. (2008). Neural network based sensitivity analysis for injector-producer relationship identification. *SPE 112124*.

[Hubbert, 1956] Hubbert, M. K. (1956). Nuclear energy and the fossil fuels. *Drilling and Production Practice (1956) American Petroleum Institute and Shell Development Co. Publication No. 95, See pp 9-11, 21-22.*

[IEA-WEO, 2008] IEA-WEO (2008). International energy agency. *IEA World Energy Outlook 2008*.

[Jansen et al., 2008] Jansen, J., Bosgra, O., and den Hof, P. V. (2008). Model-based control of multiple flow in subsurface oil reservoir. *Journal of Process Control*.

[Jansen and Currie, 2008] Jansen, J. and Currie, P. (2008). *Modeling and Optimization of Oil and Gas Production Systems (Lecture Notes)*. TU Delft.

[Jansen, 2007] Jansen, J. D. (2007). Model based control of subsurface flow. *8th International Symposium on Dynamics and Control of Process Systems (DYCOPS), Cancun*.

[Jansen, 2008] Jansen, J. D. (Nov 2008). *System Theory for Reservoir Management*. Lecture Note for course AES 1490, TU Delft.

[Kadam and Marquardt, 2007] Kadam, J. V. and Marquardt, W. (2007). Integration of economical optimization and control for intentionally transient process operation. *Assessment and Future Directions, LNCIS 358, pp. 419434.*

[Kadam et al., 2003] Kadam, J. V., Marquardt, W., Schlegel, M., Backx, T., Bosgra, O. H., Brouwer, P., Dnnebier, G., van Hessem, D., Tiagounov, A., and de Wolf, S. (2003). Towards integrated dynamic real time optimization and control of industerial processes. *Precedings Foundations of Computer Aided Process Operations(FOCAPO2003).*

[Kuchuk et al., 2005] Kuchuk, F., Hollaender, F., and Onur, I. G. M. (2005). Decline curves from deconvolution of pressure and flow rate measurements for production optimization and prediction. *SPE 96002*.

[Lee et al., 2008] Lee, K.-H., Ortega, A., Nejad, A. M., and Ershaghi, I. (2008). A method for characetrization of flow units between injection-production wells using performance data. *SPE 11422*.

[Liang et al., 2007] Liang, X., Hunan, C., Weber, D., Lake, L., Sayarpour, M., and Al-Yousef, A. (2007). Optimization of oil production based on capacitance model of production and injection rates. *SPE 107713*.

[Liu and Mendel, 2007] Liu, F. and Mendel, J. M. (2007). Forecasting injector-producer relationships from production and injection rates using and extended kalman filter. *SPE 110520*.

[Meum et al., 2008] Meum, P., P. Tøndel, J. G., and Aamo, O. (2008). Optimization of smart well production through nonlinear model predictive control. *SPE 112100*.

[Renard et al., 1998] Renard, G., Dembele, D., Lessi, J., and Mari, J. (1998). System identification approach applied to watercut analysis in waterflood layered reservoirs. *SPE 39606*.

[Saputelli et al., 2003] Saputelli, L., Nikolaou, M., and Economides, M. (2003). Self learning resrvoir management. *SPE 2003, Annual Technical Conference and Exhibition, Denver, SPE 84064*.

[Sayarpour et al., 2007] Sayarpour, M., Zuluaga, E., Kabir, C., and Lake, L. (2007). The use of capacitance resistive models for rapid estimation of waterflood performance and optimization. *SPE 110081*.

[T.Heijn et al., 2004] T.Heijn, Markovinovic, R., and Jansen, J. (2004). Generation of low order reservoir models using system theoretical concepts. *SPE 88361*.

[Tyagunov, 2004] Tyagunov, A. A. (2004). *High Performance Model Predictive Control for Process Industry*. PhD thesis.

[van den Boom and Backs, 2007] van den Boom, T. and Backs, T. (Nov 2007). *Model Predictive Control*. Lecture Note for course SC4060, TU Delft.

[Van den Hof, 2006] Van den Hof, P. (2006). *System Identification (Lecture Notes)*. TU Delft.

[van Doren et al., 2005] van Doren, J. F. M., Markovinovic, R., and Jansen, J. D. (2005). Reduced-order optimal control of water flooding using proper orthogonal decomposition. *Computational Geoscience*.

[Verhaegen, 2007] Verhaegen, M. (2007). *Filtering and system identification : a least squares approach*. Cambridge, UK : Cambridge University Press.

[Yousef, 2005] Yousef, A. A. (2005). *Investigating Statistical Techniques to Infer Interwell Connectivity from Production and Injection Rate Fluctuations*. PhD thesis, University of Texas, Austin.

[Yousef et al., 2006a] Yousef, A. A., Gentil, P., Jensen, J. L., and Lake, L. W. (2006a). Capacitance model to infer interwell connectivity from production- and injection-rate fluctuations. *SPE 95322*.

[Yousef et al., 2006b] Yousef, A. A., Lake, L. W., and Jensen, J. L. (2006b). Analysis and interpretation of interwell connectivity from production and injection rate fluctuations using a capacitance model. *SPE 99998*.

[Zandvliet, 2008] Zandvliet, M. (2008). *Model-based Lifecycle Optimization of Well Locations and Production Settings in Petroleum Reservoirs*. PhD thesis, 3ME - TU Delft.

[Zhu, 2001] Zhu, Y. (2001). *Multivariable system identification for process control*. Springer - Amsterdam.

Appendix A

Discrete Time Signals and Systems

A-1 Discrete Time Signals

The reason one might be interested in discrete time representation of the model is due to the use of computers for signal processing. Therefore almost in all situations for signal analysis and signal processing *sampled signals* are treated. Consider the finite sequence of input $u(k)$, $k = 1, 2, \ldots, N$. The frequency domain representation of this signal is defined by the function $U_N(\omega)$, as

$$U_N(\omega) = \frac{1}{\sqrt{N}} \sum_{k=1}^{N} u(k) e^{-j\omega k} \tag{A-1}$$

The values at $\omega = 2\pi k/N, k = 1, 2, \ldots, N$ form the Discrete Fourier Transform (DFT) of the sequence. Thus the time domain signal can be obtained by the inverse DFT. The DFT decomposes the time domain signal into its frequency domain component; the value of $U_N(2\pi k/N)$ is the weight at $\omega = 2\pi k/N$. The $U_N(\omega)$ is called periodogram of the signal $u(k)$ and $|U_N(2\pi k/N)|^2$ is a measure of the energy contribution of the signal at frequency $\omega = 2\pi k/N$.

Talking about the signals, one is generally interested in the frequency content of the signal and power distribution of it over the frequency range. The power spectrum of a discrete signal $u(k)$ is defined as the DFT of the autocorrelation function of $u(k)$;

$$\Phi_u(\omega) \triangleq \sum_{\tau=-\infty}^{+\infty} R_u(\tau) e^{-j\omega\tau} \tag{A-2}$$

With

$$R_u(\tau) \triangleq \bar{E}(u(k)u(k-\tau)) \tag{A-3}$$

The expected value $\bar{E}$ for either stationary stochastic or deterministic signal $u(k)$ or a combination of them (quasi stationary) is defined as

$$\bar{E}u(k) \triangleq \lim_{N\to\infty} \frac{1}{N} \sum_{k=1}^{N} Eu(k) \tag{A-4}$$

Note that for stationary stochastic signals, mean value and the auto correlation function are constant in time. From equations above one can define the total power of the signal $u(k)$ as

$$\mathcal{P} = R_u(0) = \frac{1}{2\pi}\int_{-\pi}^{\pi} \Phi_u(\omega)d\omega \tag{A-5}$$

Due to the fact that in practice $N < \infty$ measurements of the $u(k)$, it is needed to approximate R_u and Φ_u. By replacing the expected value operator $\bar{E}$ by time average in Equation A-3, for autocorrelation function it yields

$$\hat{R}_u^N(\tau) = \begin{cases} \frac{1}{N}\sum_{k=0}^{N-1} u(k)u(k-\tau) & \text{if } |\tau| < N-1 \\ 0 & \text{if } |\tau| > N-1 \end{cases} \tag{A-6}$$

Then the spectrum can be calculated as (with scaled Fourier transform)

$$\hat{\Phi}_u N(\omega) = \sum_{\tau=-\tau_m}^{+\tau_m} \hat{R}_u^N(\tau)e^{-j\omega\tau} \tag{A-7}$$

With a suitable τ_m, e.g. $\tau_m = N/10$. It can be shown that when $N \to \infty$ these two estimates will converge with probability one to R_u and Φ_u , provided that $u(k)$ is ergodic. This implies that when the number of samples N is large these estimates will be accurate.

A-2 Discrete Time SISO Systems

In most of the computer controlled systems, the process input $u(t)$ is kept constant during the sampling interval using a Zero Order Hold (ZOH)(note that by selecting sampling time equal to one time unit, $u(t)$ is used instead of $u(k)$ in which t means sampling instants). For a linear time invariant single input single output (SISO) process with impulse response g_k in each instant of $k = 1, 2, \ldots$ we have

$$y(t) = \sum_{k=1}^{\infty} g_k u(t-k) \quad t = 1, 2, \ldots \tag{A-8}$$

The impulse response g_k, is the response $y(t) = G(q)u(t)$ when $u(t)$ is a discrete pulse $\delta(t)$. By incorporating the unit forward shift operator q, the *transfer operator* of the process in equation above will be defined as

$$G(q) = \sum_{k=1}^{\infty} g_k q^{-k} \tag{A-9}$$

It can be shown that the sampled n-th order LTI process using a ZOH results in an n-th order difference equation as follows

$$y(t) + a_1 y(t-1) + \ldots + a_n y(t-n) = b_1 u(t-1) + \ldots + b_n u(t-n) \tag{A-10}$$

If q get replaced by the z-transform variable z then as it is shown in equation (A-11) the transfer function $G(z)$ will be obtained. Note that an arbitrary time delay of d samples is also incorporate in this equation

$$G(z) = \frac{b_1 z^{-1} + \ldots + b_n z^{-n}}{1 + a_1 z^{-1} + \ldots + a_n z^{-n}} z^{-d} \tag{A-11}$$

In this point, one can realize the reason why the models in the form of impulse response in equation (A-8) are called *non-parametric models*, while the ones in the form of difference equation as in equation (A-10) are considered as *parametric models*.

The equations above were deduced for the linear systems; however we know that the problem that we face in this thesis is about the reservoir modeling which is in fact non-linear. To handle this issue it is required to adopt a linear framework to define the relation between the $u(t)$ and $y(t)$. Therefore the behavior of the system should be analyzed around one particular set-point (an equilibrium point or during a limited time interval less than the largest time constant). In the situation that the system needs to work around multiple set-points, a model must be identified for each of them.

A-3 Discrete Time MIMO Systems

Another aspect of our problem is that it has indeed multi inputs and multi outputs (MIMO). The SISO formulation can be extended for MIMO systems with m inputs and ℓ outputs. Now the transfer operator in equation (A-9) could be replaced by

$$G(q) = \sum_{k=1}^{\infty} G_k q^{-k} \tag{A-12}$$

For a MIMO process, G_k is a sequence of $\ell \times m$ matrices which form the discrete time impulse response. For the purpose of identification, a suitable description of a MIMO process is a set of difference equations as follows

$$y(t) + A_1 y(t-1) + \ldots + A_n y(t-n) = B_1 u(t-1) + \ldots + B_n u(t-n) \tag{A-13}$$

Where A_i are $\ell \times \ell$ and B_i are $m \times \ell$ and constant matrices. Therefore the input/output relation will be

$$A(q)y(t) = B(q)u(t) \tag{A-14}$$

Where $A(q)$ and $B(q)$ are polynomial matrices. The canonical representation of $A(q)$ and $B(q)$ in diagonal form of Matrix Fraction Description (MFD) is

$$A(q) = \begin{bmatrix} A_{11}(q) & 0 & \ldots & 0 \\ 0 & A_{22} & & \vdots \\ \vdots & & \ddots & 0 \\ 0 & \ldots & 0 & A_{\ell\ell}(q) \end{bmatrix}, \quad B(q) = \begin{bmatrix} B_{11}(q) & \ldots & B_{1m}(q) \\ \vdots & \ddots & \vdots \\ B_{\ell 1}(q) & \ldots & B_{\ell m}(q) \end{bmatrix} \tag{A-15}$$

Where $A_{11}(q), \ldots, A_{\ell\ell}(q)$ are all monic polynomials with relevant degrees, and the degrees of $B_{i1}(q), \ldots, B_{im}(q)$ are equal to or less than that of $A_{ii}(q)$. Under this arrangement, a m-input, ℓ-output process is decoupled into ℓ, m-input single output sub processes.

Substituting q with z, the transfer function of the process could be reached as

$$G(z) = A(z)^{-1} B(z) \tag{A-16}$$

Provided that $A(q)$ is invertible.

The canonical form introduced above has advantages; a) It is simple. b) All the SISO processes identification algorithms that have been found previously, can be generalized for MIMO. c) Delay correction can be done for each single transfer function. However there is one disadvantage with this diagonal form MFD and that is the transfer function is not always minimal. This means that the order of its direct state space realization can be higher than the McMillan degree of the process. This problem can be solved using model reduction techniques.

In that sense, the Hankel matrix $\mathcal{H}$ of a discrete time process $G(z)$ is introduced, which is a double infinite matrix

$$\mathcal{H} \triangleq \begin{bmatrix} G_1 & G_2 & G_3 & \dots \\ G_2 & G_3 & G_4 & \dots \\ G_3 & G_4 & G_4 & \dots \\ \vdots & \vdots & \vdots & \end{bmatrix} \tag{A-17}$$

Where $G_k, k = 1, \dots, \infty$ is the impulse response of $G(e^{j\omega})$. The rank of the Hankel matrix is equal to δ , the minimal order (McMillan degree) of $G(z)$. The δ singular values of $\mathcal{H}$, $h_1, \dots, h_\delta$ are called Hankel singular values of the process $G(z)$, and the largest singular value is also called the Hankel norm of $G(z)$.

A-4 Linear Process with Disturbances

In the modeling of industrial processes, there are always measurement noises and unmeasurable disturbances which cannot be controlled and in the meantime their effects on the outputs cannot be neglected.

$$y(k) = G(z)u(k) + v(k) \tag{A-18}$$

The input signal $u(k)$ can be considered as noise free because it is often the test signal. The disturbance vector $v(k)$ is typically not measurable, but as it was mentioned before in the advantages of the system identification, one can find a model for the disturbances. The reconstructed output is

$$y(k) = G(z)u(k) + \underbrace{H(z)e(k)}_{v(k)} \tag{A-19}$$

Here the measurement noise $v(k)$ is modeled by a filtered white noise $e(k)$ as $H(z)e(k)$. $H(z)$ is assumed to be stable, inversely stable and monic. It should be noted that $v(k)$ is independent of the input signal $u(k)$ (for any open loop system).

Appendix B

Prediction Error Identification Methods

B-1 Least Squares Methods

The following two sections are mainly extracted from [Zhu, 2001] and [Van den Hof, 2006].

These methods are used widely for system identification since they are very easy to comprehend and implement and they have a closed solution. The idea is to find unknown parameters of mathematical relation in a way that the sum of the squares of some chosen error criteria is minimized. It should be noted that these methods can be used to estimate models of linear dynamics processes (depending on the model parametrization). This section discusses two procedures called Finite Impulse Response (FIR) and Auto Regressive with eXogenous input (ARX).

B-1-1 Finite Impulse Response

FIR representation of a LTI dynamic system is

$$y(k) = g_1 u(k-1) + g_2 u(k-2) + \ldots + g_n u(k-n) + \varepsilon(k), \tag{B-1}$$

With parameters of FIR structure being equivalent to value of system impulse response in different time steps. The input/output relation according to the model that is shown in Equation A-19 is

$$y(k) = B(z,\theta)u(k) + \varepsilon(k), \tag{B-2}$$

Where θ is the vector that contains the parameters and ε is *fitting error* that in LS it is referred to as *equation error* (minimizing criterion of parameter estimation algorithm). B is a polynomial of order n which is also called the order of the FIR model.

B-1-2 ARX Models

ARX algorithm finds the rational transfer function between the input and output data using least square procedure. ARX structure is

$$A(z,\theta)y(k) = B(z,\theta)u(k) + \varepsilon(k). \tag{B-3}$$

The same as FIR, parameters estimate can be found by minimizing the $\sum \varepsilon(k)^2$. The order of polynomial $A(z,\theta)$ is n which is the same as the order of the estimated transfer function $G(z) = B(z,\theta)/A(z,\theta)$. It can be shown that the number of the to be estimated parameters are $2n$, which implies that the order of the persistence of the input should be at least $2n$.

However, to select a model order n that brings reasonable simulation fit, *output error* is used instead of equation error as

$$V_{OE} = \frac{1}{N}\sum_{k=1}^{N} \hat{\varepsilon}_{OE}(k)^2, \tag{B-4}$$

where

$$\hat{\varepsilon}_{OE}(k) = y(k) - \hat{y}(k) = y(k) - \frac{\hat{B}(z,\theta)}{\hat{A}(z,\theta)}u(k). \tag{B-5}$$

Output error ε_{OE} consists of the model misfit and the output disturbance. Putting $A(z,\theta) = I$, obviously it becomes the equation error as mentioned in FIR model. Generally the loss function decreases as the order n increases, and model has proper order when V_{OE} stops decreasing significantly. Increasing the order of the system, reduces the output error, while the model quality can be poor due to large variance. For the finite dimensional processes, when the level of the disturbance is high, the true order may not be found using this model, then the order determined by ARX can be higher than the true model.

In contrary to FIR model, that delivers an unbiased and consistent estimate in open loop identification (i.e. input and disturbance are not correlated), in ARX it is not valid unless the $\varepsilon(k)$ is considered as white noise, which is quite restrictive. Therefore to solve this bias problem, again one needs higher order models or alternatively other methods need to be applied.

B-2 Extension of Least Squares Methods

The discussed structures above don't give much freedom in modeling the existing noise and disturbances. On the other hand a good advantage of LS methods is that the predictor is linear in θ. That mean the minimization problem is easier to solve and a global minimum is guaranteed, since there exist an analytical solution. In this section deeper attention is paid for extended LS procedures.

B-2-1 Output Error Methods

In Section B-1 equation error was used as the criterion for model estimation. The motivation of doing so is the simplicity of computation of the parameters θ. As it can be inferred by the name, in OE the chosen criterion is the output error ε_{OE} because it is closer to model applications requirements such as accuracy of the simulation. The process model is simply as the form of Equation A-18, with process noise $v(k)$ assumed to be zero mean white noise $e(k)$ and

$$G(z,\theta) = \frac{B(z,\theta)}{A(z,\theta)}. \tag{B-6}$$

The output error and corresponding cost function is calculated with Equations B-4 and B-5. It should be noted that the ε_{OE} is nonlinear in the parameters of polynomial $A(z)$ (and consequently nonlinear in θ). Therefore no analytical solution exists to this minimization problem and numerical algorithms are needed for finding the minimum. This is indeed much more time consuming than the ARX method.

OE gives a consistent estimate of parameter vector θ only when the order of the model is correct in open loop identification. If the model order is lower than the true one, the error of the transfer function is weighted by the input spectrum, i.e. the model is biased and the fit is not accurate. This somehow can be seen as an advantage of this method in the sense that the bias error of transfer function can be manipulated by the input design. These properties are guaranteed only if the numerical minimization algorithm succeeded to converge to global minimum. To this matter Söderström and Stoica (1982) have shown that if the test input $u(t)$ is white noise, then the output error method will converge to the global minimum of cost function, otherwise local minima may exist.

B-2-2 Prediction Error Methods

The consistency of the results that are concluded by means of the methods introduced above, was under the condition of open loop system identification. Also there is still no model is proposed for the disturbances. PEI methods are developed to handle these issues in addition to that they give the most efficient estimate of the parameters, i.e. minimum variance in the cost of a nonlinear estimator.

B-2-3 (1)ARMAX

The true process model is assumed to be

$$A_0(z,\theta)y(k) = B_0(z,\theta)u(k) + C_0(z,\theta)e(k), \tag{B-7}$$

Where A_0 and C_0 are monic polynomials of order n and B_0 is of order n and not monic. The real values of output $y(k)$ cannot be reproduced since the exact values of the white noise $e(k)$ don't exist, and also it varies in each experiment. Instead one can find a way to accurately predict y. The chosen predictor $\hat{y}$ should have a property that can enable us to find the parameters θ by minimizing the error between $y(k)$ and $\hat{y}(k)$. That is

$$\hat{y}(k,\theta) \triangleq \frac{B(z,\theta)}{C(z,\theta)}u(k) + [1 - \frac{A(z,\theta)}{C(z,\theta)}]y(k). \tag{B-8}$$

Since it is assumed that A and C are monic, the fraction of A/C is also monic. Therefore the second term in Equation B-8 is not monic anymore, and as a subsequent this term is only contributed to the values of y until one step before the present time k, i.e. $k-1, k-2, \dots$. The interpretation of naming this methods as prediction error should be clear by now, as the current value of the output $\hat{y}(k)$ is predicted by help of the input values up to present time and the output values until previous step $k-1$. Figure B-1 shows the idea of constructing the prediction error, which is conferred by use of Equation B-7.

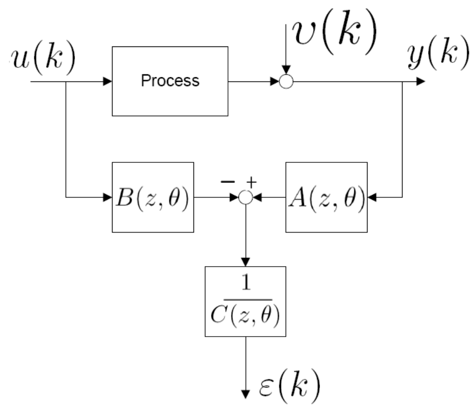

Figure B-1: Error generation of ARMAX model

The cost function for the ARMAX model to minimize is

$$V_{ARMAX} = \frac{1}{N}\sum_{k=1}^{N}(\frac{1}{C(z,\theta)}[A(z,\theta)y(k) - B(z,\theta)u(k)])^2. \tag{B-9}$$

Again, this function is not linear in estimator θ so one needs to use numerical optimization algorithms to get the answer. An advantage of ARMAX model is that it is very suitable for some controller design techniques. Yet the idea of having a model for disturbance $v(k)$ is not satisfied thoroughly by ARMAX since the process model and output disturbance model share the same denominator $A(z)$(not independent).

B-2-4 (2)Box-Jenkins

Box-Jenkins method is in fact an OE developed by introducing an extra model for output disturbance $v(k)$. The true process is assumed to be

$$y(k) = \underbrace{\frac{B_0(z,\theta)}{A_0(z,\theta)}}_{G_0}u(k) + \underbrace{\frac{C_0(z,\theta)}{D_0(z,\theta)}}_{H_0}e(k), \tag{B-10}$$

With $D(z,\theta)$ is monic polynomial of order n. Figure B-2 shows a block diagram of how to produce the prediction error in general. Due to the Equation B-10, the estimator of Box-Jenkins is defined as

$$\hat{y}(k,\theta) \triangleq \frac{D(z,\theta)B(z,\theta)}{C(z,\theta)A(z,\theta)}u(k) + [1 - \frac{D(z,\theta)}{C(z,\theta)}]y(k), \tag{B-11}$$

And parameters of this model are determined by minimizing

$$V_{BJ} = \frac{1}{N}\sum_{k=1}^{N}(\frac{D(z,\theta)}{C(z,\theta)}[y(k) - \frac{B(z,\theta)}{A(z,\theta)}u(k)])^2. \tag{B-12}$$

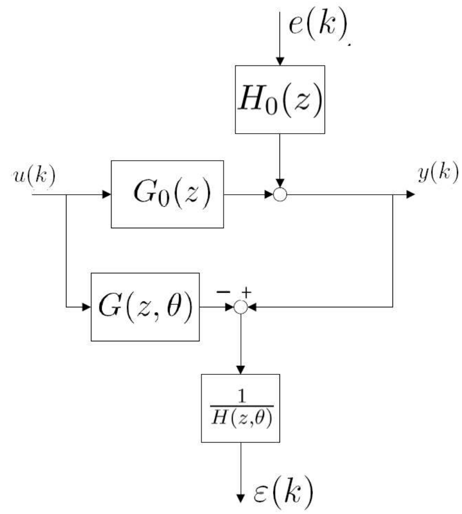

Figure B-2: Error generation of PEI model

The BJ model has the advantage of being consistent even in closed loop identification, this implies that one can expect more accurate model of the process with BJ than OE. However, the complexity of the structure makes it hard to implement and requires costly numerical optimization techniques.

It can be shown that by proper selection of $A(z)$, $B(z)$, $C(z)$ and $D(z)$ in Equation B-10 all the introduced models so far, can be regarded as PEI. One can interpret the difference between the BJ and OE as the introduced model $H(z)$ for the disturbance. That is true, in addition to that the OE is not a minimum variance estimator unless the disturbance $v(k)$ is a white noise. Hence

$$cov(\hat{\theta}_{BJ}) < cov(\hat{\theta}_{OE}) \tag{B-13}$$

B-2-5 Output Error vs. Prediction Error

Choosing the best method among all these identification models, is something that highly dependant on the use of the model, application environment and computational limitations.

Situations in which the model is expected to be used for control purposes, often the model that minimizes the output error is desirable, since the accurate input/output relationship $G(z)$ is an important issue. When downscaled models are needed, due to numerical complication, it is advantageous to first estimate a high order model and then perform a model reduction, Zhu(1998). In addition, results of recent research show that in this way the variance of the model reduces in compare of using direct estimation of low order model, Tjärnström and Ljung (1999). In this prospect, ARX is preferred over OE for high order model estimation, since it is particularly unbiased. But in the situation where low order is imposed, experiences show that the OE is more accurate.

In practice, modeling a process with order lower than the true one, consists of both *bias error* and *variance error*. Gou and Ljung (1994) showed that the bias error is dominated by variance error for increasing model order. This implies that according to Equation B-13, for direct low order estimation, it is wise to choose PEI methods like BJ and ARMAX. For a noise free case, where bias error is the only source of the error, the OE is optimal since the noise free criterion is minimized directly. For the open loop processes where the output disturbance is nearly white noise, OE is recommended whenever the transfer function G, is more of interest. PEI methods indeed result in models with higher accuracy.

Appendix C

Subspace Identification

The following section is mainly extracted from [Verhaegen, 2007]

The system identification methods that are introduced in Appendix B, are based on running an iterative optimization algorithm to find the parameterized input/output relationship. From this point of view, subspace identification (SubID) is considered as a completely different approach. The idea is that it is possible to retrieve certain subspaces which are related to the system state space matrices, according to block-Hankel matrices, structured from input and output data. It makes the use of two important linear algebra concepts, SVD and RQ factorization, instead of nonlinear optimization used in OE and PEI methods, which makes it more attractive. However, the statistical analysis of SubID is much more complicated than the other two. This is because SubID doesn't explicitly minimize a cost function to obtain the system matrices. In the following, to have an easily understanding of the method, first we consider a system without any noise (deterministic system), and then dive into the formulation of a system with colored process and measurement noise.

C-1 Subspace Identification for Deterministic Systems

An LTI system with m input, ℓ output and n states (order of the system) can be represented in state space form as

$$\begin{aligned} x(k+1) &= Ax(k) + Bu(k) \\ y(k) &= Cx(k) + Du(k) \end{aligned} \tag{C-1}$$

The goal is to find system matrices A, B, C and D and initial state vector $x(0)$ from the given finite number of N samples of a minimal process. For an arbitrary positive integer s, which is $N >> s > n$, one can write the *data equation* in compact matrix form

$$Y_{0,s,N} = \mathcal{O}_s X_{0,N} + \mathcal{T}_s U_{0,s,N} \tag{C-2}$$

Where $U_{0,s,N}$ and $Y_{0,s,N}$ are input and output block Hankel matrices respectively, and are defined as

$$U_{0,s,N} = \begin{bmatrix} u(0) & u(1) & \dots & u(N-1) \\ u(1) & u(2) & \dots & u(N) \\ \vdots & \vdots & \ddots & \vdots \\ u(s-1) & u(s) & & u(N+s-2) \end{bmatrix} \tag{C-3}$$

$$Y_{0,s,N} = \begin{bmatrix} y(0) & y(1) & \dots & y(N-1) \\ y(1) & y(2) & \dots & y(N) \\ \vdots & \vdots & \ddots & \vdots \\ y(s-1) & y(s) & & y(N+s-2) \end{bmatrix}$$

And $\mathcal{O}_s$, the *extended observability matrix*, $X_{0,N}$ and $\mathcal{T}_s$ are

$$\mathcal{O}_s = \begin{bmatrix} C & CA & CA^2 & \cdots & CA^{s-1} \end{bmatrix}^T \tag{C-4}$$

$$X_{0,N} = \begin{bmatrix} x(0) & x(1) & x(2) & \cdots & x(N-1) \end{bmatrix}$$

$$\mathcal{T}_s = \begin{bmatrix} D & 0 & 0 & \cdots & 0 \\ CB & D & 0 & \cdots & 0 \\ CAB & CB & D & \cdots & 0 \\ \vdots & & & \ddots & \\ CA^{s-2}B & CA^{s-3}B & \dots & CB & D \end{bmatrix}$$

The Equation C-2 relates matrices constructed from data to matrices constructed from system matrices. In search for system matrices, one should be very interested in finding first two entries of the extended observability matrix $\mathcal{O}_s$. Assuming the matrix $\mathcal{T}_s$ is known in Equation C-4, if $\mathcal{T}_s U_{0,s,N}$ is subtracted from $Y_{0,s,N}$, it can be seen that each column of $Y_{0,s,N} - \mathcal{T}_s U_{0,s,N}$ is a linear combination of the matrix $\mathcal{O}_s$, which means that the column space of the matrix $Y_{0,s,N} - \mathcal{T}_s U_{0,s,N}$ is contained in that of $\mathcal{O}_s$, that is $range(Y_{0,s,N} - \mathcal{T}_s U_{0,s,N}) \subseteq range(\mathcal{O}_s)$. It is important to show the two column spaces of $Y_{0,s,N} - \mathcal{T}_s U_{0,s,N}$ and $\mathcal{O}_s$ are equal, since system matrices A_T and C_T can be reached under an unknown similarity transformation T by calculating SVD of $Y_{0,s,N} - \mathcal{T}_s U_{0,s,N}$. Further discussion will be followed.

Although $\mathcal{T}_s$ is indeed unknown, one can approximate it by using the least square of estimate of $\hat{\mathcal{T}}_s$ in

$$\min_{\mathcal{T}_s} \| Y_{0,s,N} - \mathcal{T}_s U_{0,s,N} \|_F^2 \tag{C-5}$$

When the input is selected such that the matrix $U_{0,s,N}$ has full row rank (persistently exciting of degree s for each input and total degree of sm for m inputs), the solution to the above least square problem is

$$\hat{\mathcal{T}}_s = Y_{0,s,N} U_{0,s,N}^T (U_{0,s,N} U_{0,s,N}^T)^{-1} \tag{C-6}$$

Therefore it complies

$$Y_{0,s,N} - \hat{\mathcal{T}}_s U_{0,s,N} = Y_{0,s,N} \underbrace{\left(I_N - U_{0,s,N}^T (U_{0,s,N} U_{0,s,N}^T)^{-1} U_{0,s,N}\right)}_{\Pi^{\perp}_{U_{0,s,N}}} \tag{C-7}$$

Here matrix $\Pi^{\perp}_{U_{0,s,N}}$ is the orthogonal projection onto the column space of $U_{0,s,N}$ because it has the property $U_{0,s,N}\Pi^{\perp}_{U_{0,s,N}} = 0$. By multiplying $\Pi^{\perp}_{U_{0,s,N}}$ to both sides of Equation C-2, it yields

$$Y_{0,s,N}\Pi^{\perp}_{U_{0,s,N}} = \mathcal{O}_s X_{0,N}\Pi^{\perp}_{U_{0,s,N}} \tag{C-8}$$

Under the assumption that the system is minimal, one can conclude that, $range(\mathcal{O}_s) = n$. Also as it has been shown by Verhaegen(2007), with the same condition on the degree of persistency of the input, the $range(Y_{0,s,N}\Pi^{\perp}_{U_{0,s,N}})$ is equal to n. Therefore with this condition, the column space of the extended observability matrix can be recovered by using the SVD of the matrix $Y_{0,s,N}\Pi^{\perp}_{U_{0,s,N}}$.

C-2 RQ Factorization to Improve Numerical Efficiency

Instead of computing $Y_{0,s,N}\Pi^{\perp}_{U_{0,s,N}}$ which is very large, and needs to calculate $\Pi^{\perp}_{U_{0,s,N}}$ that involves computation of matrix inverse, one can choose a more efficient way by using the following RQ factorization

$$\begin{bmatrix} U_{0,s,N} \\ Y_{0,s,N} \end{bmatrix} = \begin{bmatrix} R_{11} & 0 & 0 \\ R_{21} & R_{22} & 0 \end{bmatrix} \begin{bmatrix} Q_1 \\ Q_2 \\ Q_3 \end{bmatrix} \tag{C-9}$$

It is not difficult to show that the matrix $Y_{0,s,N}\Pi^{\perp}_{U_{0,s,N}}$ is equal to $R_{22}Q_2$. Moreover, by use of the Sylvester's inequality, one can see that the rank of the matrix $R_{22} \in \mathbb{R}^{s\ell \times s\ell}$ is also n.

The SVD of the matrix R_{22} is given by

$$R_{22} = U_n \Sigma_n V_n^T \tag{C-10}$$

With $\Sigma_n \in \mathbb{R}^{s\ell \times s\ell}$ and $rank(\Sigma_n) = n$, then U_n can be denoted by

$$U_n = \mathcal{O}_s T = \begin{bmatrix} CT \\ CT(T_{-1}AT) \\ \vdots \\ CT(T_{-1}AT)^{s-1} \end{bmatrix} = \begin{bmatrix} C_T \\ C_T A_T \\ \vdots \\ C_T A_T^{s-1} \end{bmatrix} \tag{C-11}$$

Hence the matrix C_T equals the first ℓ rows of U_n and matrix A_T can be calculated by solving the equation below under the condition that $s > n$

$$U_n(1:(s-1)\ell,:)A_T = U_n(\ell+1:end,:) \tag{C-12}$$

Having the matrices A_T and C_T, matrices B_T, D_T and initial condition $x_T(0)$ can be computed by solving a least squares problem, defined as specific representation of Equation C-1 which is linear in entries of $x_T(0)$, B_T and D_T (Verhaegen (2007)).

C-3 Subspace Identification with Process and Measurement Noise

Figure C-1 shows the data generation of a process with both process and measurement noises. Here, it is assumed that the $w(k)$ and $v(k)$, process noise and measurement noise respectively, are filtered zero mean white noise, which are uncorrelated with the input $u(k)$.

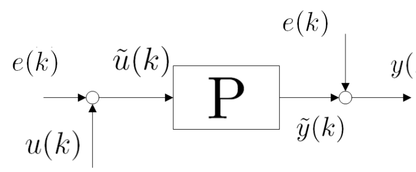

Figure C-1: System with Process and Measurement Noise

The state space representation of the system is

$$\begin{aligned} \tilde{x}(k+1) &= A\tilde{x}(k) + Bu(k) + w(k) \\ y(k) &= C\tilde{x}(k) + Du(k) + v(k) \end{aligned} \tag{C-13}$$

The above signal generating system can be shown in more explicit way such as

$$\begin{aligned} \bar{x}(k+1) &= A\bar{x}(k) + Bu(k) \\ y(k) &= C\bar{x}(k) + Du(k) + \bar{v}(k) \end{aligned} \tag{C-14}$$

Where $\bar{v}(k)$ is given by

$$\begin{aligned} \xi(k+1) &= A\xi(k) + w(k) \\ \bar{v}(k) &= C\xi(k) + v(k) \end{aligned} \tag{C-15}$$

With $\xi(k) = \tilde{x}(k) - \bar{x}(k)$. This equation shows that $\bar{v}(k)$ is a colored noise and independent of input $u(t)$. Therefore

$$\bar{v}(k) = CA^k(\tilde{x}(0) - \bar{x}(0)) + \sum_{i=0}^{k-1} CA^{k-i-1}Bw(i) + v(k) \tag{C-16}$$

As it was shown for deterministic system, the block Hankel representation of the system in form of Equation C-14 is

$$Y_{i,s,N}\Pi^{\perp}_{U_{i,s,N}} = \mathcal{O}_s X_{i,N}\Pi^{\perp}_{U_{i,s,N}} + V_{i,s,N}\Pi^{\perp}_{U_{i,s,N}} \tag{C-17}$$

This equation is independent of input $U_{i,s,N}$, since it has been projected onto the column space of $U_{i,s,N}$, by multiplying both sides to $\Pi^{\perp}_{U_{i,s,N}}$ from right. To retrieve the column space of $\mathcal{O}_s$, the last term in Equation C-17 must be eliminated, to remove the influence of noise on the extended observability matrix. This is done in order to have an unbiased estimate of the system matrices. Multiplying sides of the Equation C-17 by a proper *instrumental variable matrix* $Z_N \in \mathbb{R}^{sz\times N}$ can satisfies this providing that $\lim_{N\to\infty}\frac{1}{N}V_{i,s,N}\Pi^{\perp}_{U_{i,s,N}}Z_N^T = 0$ and $rank(\lim_{N\to\infty}\frac{1}{N}V_{i,s,N}\Pi^{\perp}_{U_{i,s,N}}Z_N^T) = n$.

Satisfying the condition of persistency of excitement on the input, it can be shown that

$$range(\lim_{N\to\infty}\frac{1}{\sqrt{N}}R_{32}) = range(\mathcal{O}_s) \tag{C-18}$$

Where $s > n$, and R_{32} is obtained by the RQ factorization of

$$\begin{bmatrix} U_{s,s,N} \\ U_{0,s,N} \\ Y_{s,s,N} \end{bmatrix} = \begin{bmatrix} R_{11} & 0 & 0 \\ R_{21} & R_{22} & 0 \\ R_{31} & R_{32} & R_{33} \end{bmatrix} \begin{bmatrix} Q_1 \\ Q_2 \\ Q_3 \end{bmatrix} \tag{C-19}$$

Consequently, system matrices A_T, C_T can be estimated consistently by SVD of the matrix R_{32} similar to the previous section. The matrices B_T and D_T also initial condition $x_T(0)$ can be calculated by solving a least square problem, which resembles the output error method. The real output $y(k)$ is generated by the parameterized form of

$$y(k) = \phi(k)^T\theta + \upsilon(k) \tag{C-20}$$

Because $\upsilon(K)$ is not correlated with $\phi(k)$, an unbiased estimate of θ can be obtained by solving

$$\min_{\theta}\frac{1}{N}\sum_{k=0}^{N-1}\|y(k) - \phi(k)^T\theta\|_2^2 \tag{C-21}$$

The identification method presented here is called Past Inputs Multivariable Output Error State sPace (PI-MOESP), since it uses past input data matrix $U_{0,s,N}$ as Z_N.

When only the input-output transfer function is investigated, Equation C-13 can be written in innovation form as in Equation C-22, where $e(k)$ is a zero mean white noise and K is the Kalman gain:

$$\begin{aligned} x(k+1) &= Ax(k) + Bu(k) + Ke(k) \\ y(k) &= Cx(k) + Du(k) + e(k) \end{aligned} \tag{C-22}$$

Now the block Hankel matrix relation of the system is shown by

$$Y_{i,s,N}\Pi^{\perp}_{U_{i,s,N}} = \mathcal{O}_s X_{i,N}\Pi^{\perp}_{U_{i,s,N}} + \mathcal{S}_s E_{i,s,N}\Pi^{\perp}_{U_{i,s,N}} \tag{C-23}$$

In which the influence of the input is removed. Here, $E_{i,s,N}$ is a block Hankel matrix constructed from the sequence $e(k)$, and $\mathcal{S}_s$ describes the weighting matrix of the $E_{i,s,N}$.

$$\mathcal{S}_s = \begin{bmatrix} I_\ell & 0 & 0 & \cdots & 0 \\ CK & I_\ell & 0 & \cdots & 0 \\ CAK & CK & I_\ell & \cdots & 0 \\ \vdots & & & \ddots & \\ CA^{s-2}K & CA^{s-3}K & \dots & CK & I_\ell \end{bmatrix} \tag{C-24}$$

Like the PI-MOESP method, the effect of the noise should be removed by multiplying both sides of Equation C-23 to an instrumental variable sequence Z_N. This time, instead of only $U_{0,s,N}$, both $U_{0,s,N}$ and $Y_{0,s,N}$ are used, since it gives better estimates for finite number of data. This is the basis of the method called PO-MOESP, where PO stands for Past Outputs. this method implies that the range of the extended observability matrix $\mathcal{O}_s$ can be obtained by Equation C-18 where R_{32} is calculated by the RQ factorization as

$$\begin{bmatrix} U_{s,s,N} \\ \begin{bmatrix} U_{0,s,N} \\ Y_{0,s,N} \end{bmatrix} \\ Y_{s,s,N} \end{bmatrix} = \begin{bmatrix} R_{11} & 0 & 0 \\ R_{21} & R_{22} & 0 \\ R_{31} & R_{32} & R_{33} \end{bmatrix} \begin{bmatrix} Q_1 \\ Q_2 \\ Q_3 \end{bmatrix} \tag{C-25}$$

With the condition that the input signal $u(t)$ satisfies

$$\begin{aligned} rank(\lim_{N\to\infty} \frac{1}{N} \begin{bmatrix} X_{s,N} \\ U_{s,N} \end{bmatrix} \begin{bmatrix} Y^T_{0,s,N} & U^T_{0,s,N} & U^T_{s,s,N} \end{bmatrix}) = n + sm \\ rank(\lim_{N\to\infty} \frac{1}{N} \begin{bmatrix} X_{0,N} \\ U_{0,2s,N} \end{bmatrix} \begin{bmatrix} X^T_{0,N} & U^T_{0,2s,N} \end{bmatrix}) = n + 2sm \end{aligned} \tag{C-26}$$

Therefore, similar to the PI-MOESP, the system matrices A_T, B_T, C_T and D_T and initial condition $x_T(0)$ can be obtained from the SVD of the R_{32}.

Another subspace identification method is proposed called *Numerical Algorithm for Subspace IDentification*, N4SID, which is based on the solutions to least squares problem. Without getting deep into the method, it implies that for a minimal system represented in Equation C-22, with $x(k)$, $u(k)$ and $e(k)$ ergodic stochastic processes such that the white noise sequence $e(k)$ is uncorrelated with $x(j)$ and $u(j)$ for all $k, j \in \mathbb{Z}$, and input sequence $u(k)$ satisfies the conditions Equation C-26, for $N \to \infty$ the column space of the $\mathcal{O}_s$ can be approximated by matrix U_n, the SVD of $R_{32}R_{22}^{-1}\begin{bmatrix} U_{0,s,N} \\ Y_{0,s,N} \end{bmatrix} = U_n\Sigma_n V_n^T$. That is to say for $N \to \infty$

$$\mathcal{O}_s X_{s,N} \approx R_{32}R_{22}^{-1}\begin{bmatrix} U_{0,s,N} \\ Y_{0,s,N} \end{bmatrix} = U_n\Sigma_n V_n^T \tag{C-27}$$

And

$$rank(R_{32}R_{22}^{-1}\begin{bmatrix}U_{0,s,N}\\Y_{0,s,N}\end{bmatrix} = U_n\Sigma_n V_n^T) = n \tag{C-28}$$

N4SID solution enables the approximation of the state sequence of the Kalman filter that is contained in $X_{s,N}$. The row space of the state sequence of Kalman filter can be approximated by

$$\hat{X}_{s,N} = \Sigma_n^{1/2} V_n^T \tag{C-29}$$

The system matrices A_T, B_T, C_T and D_T can now be estimated by solving another least squares problem such as

$$\begin{bmatrix}\hat{A}_T & \hat{B}_T\\ \hat{C}_T & \hat{D}_T\end{bmatrix} = \arg \min_{AT,B_T,C_T,D_T} \| \begin{bmatrix}\hat{X}_{s+1,N}\\ Y_{s,1,N-1}\end{bmatrix} - \begin{bmatrix}A_T & B_T\\ C_T & D_T\end{bmatrix}\begin{bmatrix}\hat{X}_{s,N-1}\\ U_{s,1,N-1}\end{bmatrix} \|_F^2 \tag{C-30}$$

C-4 Estimating the Kalman Gain K_T

Estimates of the covariance matrices related to the innovation form in Equation C-22, can be obtained from the state estimate $\hat{X}_{s,N}$, together with the estimated system matrices from the least squares problem in Equation C-30.

$$\begin{bmatrix}\hat{Q} & \hat{S}\\ \hat{S}^T & \hat{R}\end{bmatrix} = \lim_{N\to\infty}\frac{1}{N}\begin{bmatrix}\hat{W}_{s,1,N}\\ \hat{V}_{s,1,N}\end{bmatrix}\begin{bmatrix}\hat{W}_{s,1,N}^T & \hat{V}_{s,1,N}^T\end{bmatrix} \tag{C-31}$$

Where the residuals of the least squares problem of Equation C-30, $\hat{W}_{s,1,N}$ and $\hat{V}_{s,1,N}$, are given by

$$\begin{bmatrix}\hat{W}_{s,1,N-1}\\ \hat{V}_{s,1,N-1}\end{bmatrix} = \begin{bmatrix}\hat{X}_{s+1,N}\\ Y_{s,1,N-1}\end{bmatrix} - \begin{bmatrix}\hat{A}_T & \hat{B}_T\\ \hat{C}_T & \hat{D}_T\end{bmatrix}\begin{bmatrix}\hat{X}_{s,N-1}\\ U_{s,1,N-1}\end{bmatrix}. \tag{C-32}$$

The estimate of the Kalman gain $\hat{K}_T$ for the system is therefore

$$\hat{K}_T = (\hat{S} + \hat{A}_T\hat{P}\hat{C}_T^T)(\hat{R} + \hat{C}_T\hat{P}\hat{C}_T^T)^{-1}, \tag{C-33}$$

With $\hat{P}$ is the solution of the following Riccati equation

$$\hat{P} = \hat{A}_T\hat{P}\hat{A}_T^T + \hat{Q} - (\hat{S} + \hat{A}_T\hat{P}\hat{C}_T^T)(\hat{R} + \hat{C}_T\hat{P}\hat{C}_T^T)^{-1}(\hat{S} + \hat{A}_T\hat{P}\hat{C}_T^T). \tag{C-34}$$

Appendix D

Relative Permeability Effects on Multiphase Flow

As it was mentioned in Chapter 3, dependency of parameters to states of the system is a major source of non-linearity. Permeability is a measure of the ability of a porous medium to transmit fluids, and is addressed with field unit of *Darcy* or SI unit of m^2. Therefore according to Darcy's law the fluid velocity (and also production rate) in a certain block is determined by permeability. In multi-phase flow through porous media the permeability to each phase is generally a nonlinear, path-dependent, function of the *phase saturations*. The gas, oil and water saturations, S_g, S_o and S_w, are defined as the fraction of the pore space occupied by the corresponding phase, such that, by definition, $S_g + S_o + S_w = 1$. In the case of three-phase gas-oil-water flow, Darcys law is

$$\nu_i = -k\frac{k_{ri}}{\mu_i}\nabla p_i, \quad , i \in \{g, o, w\}. \tag{D-1}$$

where k is the absolute permeability (also known as the homogeneous permeability) governed by rock properties *only*, while $0 < k_{rg} < 1$, $0 < k_{ro} < 1$ and $0 < k_{rw} < 1$ are the relative permeabilities which are nonlinear functions of the phase saturations and represent the reduction of permeability to one phase due to the presence of the other phases. The products $k_g = kk_{rg}$, $k_o = kk_{ro}$ and $k_w = kk_{rw}$ are known as the effective permeabilities to gas, oil and water respectively. More specifically there is a term called *mobility*, λ that is the quotient of viscosity and permeability, which plays a major role in movability of the fluid.

$$\lambda_i \triangleq \frac{kk_{ri}(S)}{\mu_i}, \quad , i \in \{g, o, w\}. \tag{D-2}$$

The physics of the relative permeability effect is related to the the interfacial tension between the phases (which gives rise to capillary pressure), the wettability of the of the rock, and the tortuosity of the pores [Jansen and Currie, 2008]. Figure D-1 depicts a typical set of relative permeability curves for oil and water flow during the saturation of a block. After the formation of oil, it starts to migrate from bottom to the top and replaces the water that has already occupied the pore. At the end of this process some water will always be left in the pore space, known as *connate* water or *interstitial* water. Oil saturation process (that is called *imbibition* by production engineers) therefore starts from a situation with a water saturation S_{wc}, known as the connate water saturation. Because the water can not flow until the water saturation exceeds S_{wc}, it is also referred to as the *critical* water saturation or the *immobile* water saturation. At the end of the drainage process, a certain amount of oil remains trapped in the larger pores from which it cannot be displaced by water. This oil is known as residual oil, and the associated saturation S_{or} as the *residual* oil saturation. At the beginning and the end of the imbibition process, the presence of connate water and residual oil in the pores results in relative permeabilities below the theoretical maximum of one. These values, k^0_{row} and k^0_{rw}, are known as the *end-point relative permeabilities*. The subscripts *row* are used instead of *ro* to distinguish relative oil permeabilities in an oil-water system from those in an oil-gas system.

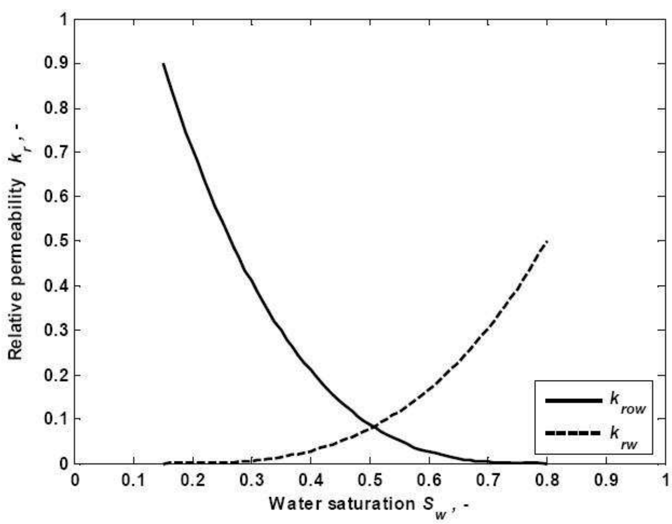

Figure D-1: Relative permeabilities to oil and water during imbibition (i.e. increasing water saturation)

Relation between saturation and permeabilities are often determined with laboratory experiments on core samples, called core flooding. In the absence of measured data, it may be necessary to revert to empirical relationships for the the relative permeabilities. For oil-water flow under imbibition conditions the relationship can be represented by

$$k_{row} = k^0_{row}(1 - S^*_w)^{n_{ow}}, k_{rw} = k^0_{rw}(S^*_w)^{n_w} \quad \text{with} \quad S^* \triangleq \frac{S_w - S_{wc}}{1 - S_{or} - S_{wc}} \tag{D-3}$$

With n_{ow} and n_w are known as the Corey exponents. They are both larger than one with typical values between 2 and 4. Similar relations exist for gas-oil phase. In case of oil-water flow, the total relative permeability to *liquid flow* (the same for both phases) is given by $(k_r)_{ow} = k_{row} + k_{rw}$. In case of gas-oil flow the total relative permeability is given by $(k_r)_{go} = k_{rg} + k_{rog}$, and similarly, for three-phase flow $(k_r)_{gow} = k_{rg} + k_{ro} + k_{rw}$. To help illustrating the effect of relative permeability on production rates in the producer wells, refer to the section 3.4.3 of [Jansen, 2008], also Figure 6-1 in Chapter 6.

Acronyms

ANN Artificial Neural Network

ARMAX AutoRegressive Moving Average with eXogenuous input

ARX AutoRegressive with eXogenuous input

BHP Bottom Hole Pressure

CloReM Closed-loop Reservoir Management

CRM Capacitance Resistive Model

DFT Discrete Fourier Transform

DUT Delft University of Technology

EKF Extended Kalman Filter

EnKF Ensemble Kalman Filter

ETFE Empirical Transfer Function Estimate

FIR Finite Impulse Response

ICV Inflow Control Valves

IPR Inflow Performance Relationship

LS Least Square

LTI Linear Time Invariant

MIMO Multi Input Multi Output

MLR Multiple Linear Regression

MPC Model Predictive Control

MSE	Mean Squared Error
N4SID	Numerical Algorithm for Subspace Identification
NMPC	Nonlinear Model Predictive Control
NPV	Net Present Value
OE	Output Error
PIMOESP	Past Inputs Multivariable Output Error State Space
POD	Proper Orthogonal Decomposition
POMOESP	Past Inputs and Outputs Multivariable Output Error State Space
PEI	Prediction Error Identification
SID	Subspace Identification
SISO	Single Input Single Output
VIF	Variance Inflation Factor
ZMWN	Zero Mean White Noise
ZOH	Zero Order Hold